VYSOKÉ UČENÍ TECHNICKÉ V BRNĚ

BRNO UNIVERSITY OF TECHNOLOGY

FAKULTA CHEMICKÁ
ÚSTAV FYZIKÁLNÍ A SPOTŘEBNÍ CHEMIE

FACULTY OF CHEMISTRY
INSTITUTE OF PHYSICAL AND APPLIED CHEMISTRY

AUTOMATED DETERMINATION OF PHOTOCATALYTIC SELF-CLEANING SURFACE ACTIVITY BY COLOR INDICATOR INKS

DIPLOMOVÁ PRÁCE
MASTER'S THESIS

AUTOR PRÁCE — Bc. JANA BEDNÁRKOVÁ
AUTHOR

BRNO 2015

VYSOKÉ UČENÍ TECHNICKÉ V BRNĚ

BRNO UNIVERSITY OF TECHNOLOGY

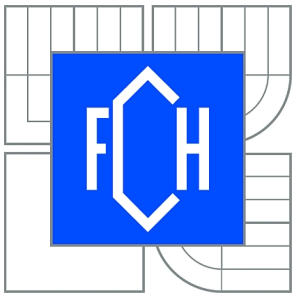

FAKULTA CHEMICKÁ

ÚSTAV FYZIKÁLNÍ A SPOTŘEBNÍ CHEMIE

FACULTY OF CHEMISTRY

INSTITUTE OF PHYSICAL AND APPLIED CHEMISTRY

AUTOMATED DETERMINATION OF PHOTOCATALYTIC SELF-CLEANING SURFACE ACTIVITY BY COLOR INDICATOR INKS

AUTOMATIZOVANÉ STANOVENÍ FOTOKATALYTICKÉ AKTIVITY SAMOČISTICÍCH POVRCHŮ POMOCÍ INDIKÁTOROVÝCH INKOUSTŮ

DIPLOMOVÁ PRÁCE

MASTER'S THESIS

AUTOR PRÁCE — Bc. JANA BEDNÁRKOVÁ

AUTHOR

VEDOUCÍ PRÁCE — Ing. PETR DZIK, Ph.D.

SUPERVISOR

BRNO 2015

Vysoké učení technické v Brně
Fakulta chemická
Purkyňova 464/118, 61200 Brno 12

Zadání diplomové práce

Číslo diplomové práce:	**FCH-DIP0854/2014**	Akademický rok: **2014/2015**
Ústav:	Ústav fyzikální a spotřební chemie	
Student(ka):	**Bc. Jana Bednárková**	
Studijní program:	Spotřební chemie (N2806)	
Studijní obor:	Spotřební chemie (2806T002)	
Vedoucí práce	**Ing. Petr Dzik, Ph.D.**	
Konzultanti:		

Název diplomové práce:

Automatizované stanovení fotokatalytické aktivity samočisticích povrchů pomocí indikátorových inkoustů

Zadání diplomové práce:

1. Prostudujte relevantní literární zdroje a sestavte rešerši shrnující současný stav poznání o využití barevných indikátorových inkoustů pro měření fotokatalytické aktivity.
2. Optimalizujte složení indikátorového inkoustu vhodného pro depozici piezoelektrickým tiskem.
3. Optimalizujte stávající aparaturu pro měření rychlosti odbarvení indikátorového inkoustu.
4. Prostudujte fotokatalytickou aktivitu různých fotokatalytických vrstev s využitím optimalizovaného postupu.

Termín odevzdání diplomové práce: 11.5.2015

Diplomová práce se odevzdává v děkanem stanoveném počtu exemplářů na sekretariát ústavu a v elektronické formě vedoucímu diplomové práce. Toto zadání je přílohou diplomové práce.

Bc. Jana Bednárková	Ing. Petr Dzik, Ph.D.	prof. Ing. Miloslav Pekař, CSc.
Student(ka)	Vedoucí práce	Ředitel ústavu

V Brně, dne 30.1.2015

prof. Ing. Martin Weiter, Ph.D.
Děkan fakulty

ABSTRACT

This diploma thesis deals with testing of suitable indicator ink for photocatalytic evaluation. In the theoretical part I reviewed the indicator inks that are used for photocatalytic assesment and the kinetics that could describe the dye degradation.
In experimental part, several dyes were selected, printed on glass substrate with photocatalytic layer and tested. The apparatus was adjusted for testing of inks of various colors. After selection of the proper indicator inks, I tried to optimize the printing conditions to obtain a better layer structure. Finally I focused on apparatus optimization.

ABSTRAKT

Tato diplomová práce se zabývá testováním vhodných indikátorových inkoustů k ohodnocení fotokatalytické aktivity. V teoretické části jsem studovala literaturu související s možnostmi stanovování fotokatalytické aktivity a zaměřila se také na kinetiku, kterou je zmíněnou fotokatalýzu možné ohodnotit.
V experimentální části jsem mnou vybraná barviva natiskla na skleněný substrát obsahující vrstvu oxidu titaničitého a následně je otestovala. Došlo také k úpravě aparatury, aby bylo možné měřit větší škálu barev. Po otestování a vybrání vhodných barviv jsem se pokusila o optimalizaci podmínek tisku. Nakonec jsem optimalizovala i samotnou aparaturu.

KEYWORDS

Titanium dioxide, photocatalysis, indicator ink, degradation rate

KLÍČOVÁ SLOVA

Oxid titaničitý, fotokatalýza, indikátorový inkoust, rychlost degradace

BEDNÁRKOVÁ, J. *Automatizované stanovení fotokatalytické aktivity samočisticích povrchů pomocí indikátorových inkoustů.* Brno: Vysoké učení technické v Brně, Fakulta chemická, 2015. 82 s. Vedoucí diplomové práce Ing. Petr Dzik, Ph.D.

PROHLÁŠENÍ

I declare that the diploma thesis has been worked out by myself and that all the quotations from the literature sources used, are correct and complete. the content of the diploma thesis is the property of the Faculty of Chemistry, Brno University of Technology and all commercial uses are allowed only when approved by the supervisor and the dean of the Faculty of Chemistry, Brno University of Technology.

……
student's signature

ACKNOWLEDGEMENT

I would like to express huge thanks to my supervisor, Ing. Petr Dzik, Ph.D for what he has taught me during my studies. I especially appreciate his friendliness and willingness when discussing any problem I had faced.
I would also like to show my gratitude to Bc. Alena Pápayová and Bc. Eva Máchová for correction of my English in this thesis.
I appreciate my lab collegues, especially Martina Blašková, Klára Knobová, Ivana Uhrová and Andrea Třešňáková for the great working environment they created.
Last but not least, I do feel grateful for my parents supporting me in anything I have ever decided to do.

CONTENT

“Everything should be made as simple as possible, but not simpler.”
Albert Einstein

1 INTRODUCTION

Photocatalysis is a well discussed and promising field of science. It offers several applications that can be used mostly in environmental studies. Nowadays among the best known are self-cleaning effect, self-sterilizing effect and water and air purification.

Photocatalytic water treatment has shown good results and suggests the future solution for removing of dyes from waste water in textile industry. Self-sterilizing property can easify the hygiene maintanence in hospital. Water and air purification studies need more methods than simple adsorption ones – especially if the photocatalyst is able to decompose the impurity and not only to catch it. These are the main reasons why the photocatalytic research keeps growing in importance.

For photocatalysis occurence, the UV light presence (5% part of the sunlight) is crucial. Even though the UV light content in sunlight is not high, it is sufficient to use TiO_2 for coating of buildings in cities with serious pollution problems. Thanks to titania hydrophilic properties, rain can remove all the impurities adsorbed on the building walls. Among other self-cleaning application examples, I would like to mention covering of tunnel lamps. In this case, TiO_2 protects the lamp from turning dirty and black from vehicle emission.

2 THE CURRENT STATE OF THE TOPIC

2.1 Concept and principles of photocatalysis

Photocatalytic reactions are photochemical processes taking place on the semiconductor surface and leading to the increase of the photoreaction rate. This increase is caused by using of a proper catalyst and its interaction with substrate or molecules in excited state or interaction with the primar product.

The mentioned interaction occures because of the electron-hole pair existence. These are created by the absorption of a quantum of light of given wavelength. The energy of the light absorbed must be bigger than (or equal to) the band gap energy of the catalyst used. Then the electron from valence band can be excited to the conduction band so the electron-hole pair is created. Unless there is an acceptor for electron or hole, the recombination of both species takes place very fast (energy is dissipated as heat).

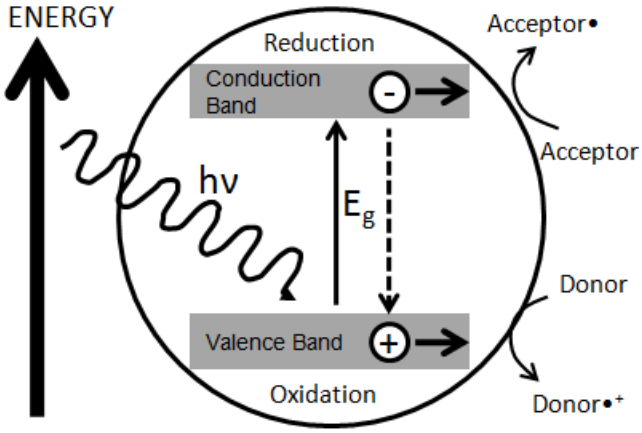

Figure 1 *Mechanism of electron-hole establishment. [1]*

The holes in valence band have strong oxidation properties, while electrons found in conduction band are good reductive agents. If there are more electrons or holes established, we can observe reduction or oxidation processes with adsorbed particles or surface functional groups.

2.1.1 Elementary processes

The following elementary processes play significant role during photocatalysis: [3]

- Adsorption – is a necessary step before the surface reaction. There are two types of adsorption to be considered – physical adsorption and chemisorption.
  In the case of *physical adsorption*, there are only weak forces between the adsorbed components and surface (van der Waals forces) and there is no activation energy needed for this step. The heat of adsorption is low. More layers are possible.
  On the other hand, in the case of *chemisorption*, strong bonds are observed resembling those of covalent bonds. The activation energy is needed for this step, although it is quite low compared to other steps (surface reaction). The heat of reaction corresponds to the chemical reactions. Only monolayer is assumed. [3]
  Chemisorption can be further divided into *associative* and *dissociative*.

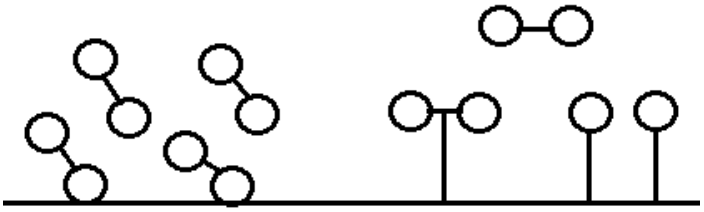

Figure 2 *Physical adsorption (left) and chemisorption (right) – associative and dissociative.*

- Desorption – is the inverse phenomenon to adsorption and often plays an important role in the whole reaction rate. If the desorption step rate is too low, meaning the interaction between product and surface of the catalyst (active site) is too high. Then the surface will be filled with products occupying too much space on it which would lead to decreasing of the rate of surface reaction, as there will be no space for the reactant to be adsorbed and so no reaction will occure.

- Excitation – is an important step for the photocatalysis to take place. Sufficient energy (bigger than the band gap energy) is needed for this step to occure.

- Charge separation – is caused by the excitation of electron from valence band to conduction band. This creates the electron-hole pair representing the charge separation in the system.

- Diffusion – is generally very important. There are two diffusion steps – *inter-particle* and *intra-particle* diffusion. The first one describes the transporting of reactant from the bulk to the catalyst surface. The second one is considered, when using porous catalyst, then the transport in the pores of catalyst is necessary to face up.

- Surface reaction – descibes the reaction of the adsorbed reagents to final adsorbed products.

2.1.2 Reaction rate and yield

Reaction rate is the rate for the formation of a substance in a given reaction. It is a function of composition (concetration), temperature and pressure. *Yield of a product* expresses the ratio of amount of substance created (product) to amount of reagent. The number of created molecules per absorbed photon is called the *quantum yield*. [3]

2.1.2.1 Parameters influencing the photocatalytic rate

Following five parameters are considered to be important for photocatalytic activity of given process: [4]

1. *The mass of catalyst* influences linearly the reaction rate until the point where the full absorption of photons happens. Since this point no matter how much catalyst we add, the reaction rate is constant.
2. *The wavelength* curve provides determination of energy band gap E_G for catalytic measurements – until some wavelengths values the reaction rate is constant. However, when increasing the wavelenght, we get to the rapid rate decrease. This is caused by

non-sufficient energy for titania electron excitation → active sites are not formed so the reaction cannot take place (or only in a small scale).

3. *The concetration* dependence characterizes the basic Langmuir-Hinschelwood kinetics – the reaction rate increases with increasing reactant concentration until all the surface is covered by adsorbed species (assuming monolayer adsorption).
4. *Low temperatures* are favoured for adsorption since it is a spontaneous and exothermic process.
5. The last important factor worth mentioning is *radiant flux*. Until a certain value, the reaction rate grows linearly with radiant flux. After reaching this, there is a square root dependance. If the radiant flux is too high, the recombination of photo-generated electrons and holes takes place. The exothermic recombination reaction could increase the temperature and this could lead to declining adsorption of the reactant.

2.1.3 Heterogenous photocatalysis

Heterogenous catalysis represents a reaction between molecules in gas or solution catalyzed by solid catalyst. It plays an important role in chemical industry and is one of the most topics to be reasearched nowadays because of greater importance of economical and environmental aspects. The main reason for applying the heterogenous catalysis is increasing the reaction rate and gaining the optimal selectivity for given reaction. [2]

If we do not consider the mass transfer limitations, generally heterogenous photocatalysis consists of 5 steps – as seen in the picture. [3]

1. Diffusion of reactant to the surface of catalyst.
2. Adsorption of reactant on the surface.
3. Surface reaction, establishment of photoinduced electrones and holes, electron transfer reaction (creating of radicals).
4. Desorption of the product from the surface.
5. Diffusion of the product from the surface of catalyst.

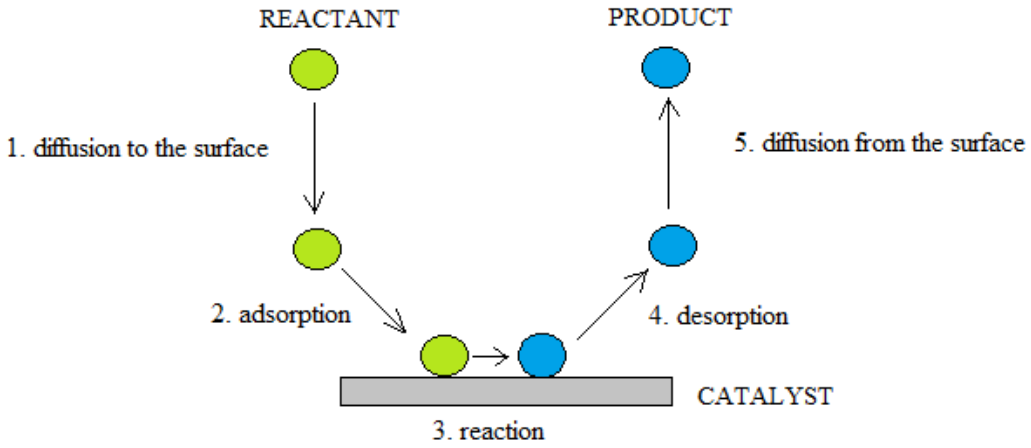

Figure 3 *Five general steps of heterogenous photocatalysis.*

However, the *mass transfer limitations* are usually necessary to face. This means that the *diffusion rate* (movement of reactants in the pore system of the catalyst) is lower than the reaction rate, which causes the formation of concentration gradient in the catalyst

particle. Extreme temperatures can cause higher reaction rate than the diffusion rate suggesting the diffusion rate to be the determing step in the reaction mechanism. [3]

2.1.4 Charge carriers reactive pathways

The photocatalysis mechanism is well described on the example with titania (catalyst) and water. After the absorption of sufficient energy, electrons and holes are established. Vb represents the valence band, cb the conduction band. [4]

$$TiO_2 \xrightarrow{h\nu} e_{cb}(TiO_2) + h^+_{vb}(TiO_2) \tag{1}$$

If there is a suitable acceptor on the surface of catalyst, redox reaction can take place. In the opposite case, new electron-hole pair can recombine while releasing of energy.

Two following equations describe two ways of establishment of OH radical with good oxidative properties.

$$h^+_{vb}(TiO_2) + H_2O \longrightarrow TiO_2 + HO^{\bullet}_{ads} + H^+ \tag{2}$$

$$h^+_{vb}(TiO_2) + HO^-_{ads} \longrightarrow TiO_2 + HO^{\bullet}_{ads} \tag{3}$$

Generally the donor (H_2O) reacts with the holes in the valence band, while acceptor (O_2) reacts with electrons in the conduction band.

$$h^+_{vb}(TiO_2) + D_{ads} \longrightarrow TiO_2 + D^+_{ads} \tag{4}$$

$$e^-_{cb}(TiO_2) + A_{ads} \longrightarrow TiO_2 + A^-_{ads} \tag{5}$$

In the case of O_2 adsorption, the equation is:

$$e^-_{cb}(TiO_2) + O_{2ads} + H^+ \longrightarrow TiO_2 + OH^{\bullet}_2 \longrightarrow O^{\bullet -}_2 + H^+ \tag{6}$$

By the following reaction, the establishment of H_2O_2 takes place:

$$e_{cb}(TiO_2) + HO_2^{\bullet} + H^+ \longrightarrow H_2O_2 \tag{7}$$

Dissociation of H_2O_2 gives the very reactive $OH^{\bullet}$ radical:

$$H_2O_2 \xrightarrow{h\nu} 2OH^{\bullet} \tag{8}$$

$$H_2O_2 + O_2^{\bullet -} \longrightarrow HO^{\bullet} + O_2 + HO^- \tag{9}$$

$$e_{cb}(TiO_2) + H_2O_2 \longrightarrow HO^{\bullet} + HO^- + TiO_2 \tag{10}$$

2.1.5 Kinetic mechanism used for evaluation of photocatalytic activity

The photocatalytic activity can be characterized by so far known kinetic mechanisms. We monitor one given substance which undergoes structure changes caused by the photocatalyst and appropriate energy amount.

2.1.5.1 Langmuir-Hinschelwood kinetics

This mechanism is one of the mostly used in applying kinetics to photocatalytic reaction although it contains several assumption which are difficult to follow in industrial scale: [2]

- the surface reaction is the rate determing step (the slowest step that influence the rate of reaction the most)
- the reaction takes place between chemisorbed reactants (need of energy for chemisorption)
- the products desorb fast
- assumptions for the Langmuir isotherm

The Langmuir isotherm describes how the amount of adsorbed gas varies with the gas equilibrium pressure at isothermal conditions. It includes following assumptions:

a) uniform surface – the adsorption heat for chemisorption is independent on the surface coverage θ

b) monolayer adsorption –only one molecule can be adsorbed on each active site

c) immobile adsorption

d) dynamic equilibrium between adsorbed and nonadsorbed species

As mentioned above, applying the Langmuir isotherm brings limitations to be faced. Only a few processes can be fully characterized by this mechanism. The biggest problem here is that real surfaces are usually *not uniform* – means that on some sites the molecules will adsorb preferably compared to others. Heat needed for molecule to be chemisorbed on the surface is decreasing with the increasing coverage – the first adsorbed molecule requires the most energy of all. This suggests that the monolayer adsorption is hardly ever probable. It is convenient for the molecule to be adsorbed on another one rather than on the vacant place because of lower energy preference.

The adsorption on surface can be either associative or dissociative depending on whether the whole molecule is adsorbed on one or more active sites. [2]

2.1.5.2 Langmuir-Hinschelwood Mechanism [2]

Considering a simple reaction scheme $A + B \rightarrow AB$, the LH mechanism includes these steps:

$$A + * \xleftrightarrow{k1} A* \tag{11}$$

$$B + * \xleftrightarrow{k2} B* \tag{12}$$

$$A* + B* \xrightarrow{k3} AB* \tag{13}$$

$$AB* \xleftrightarrow{k4} AB + * \tag{14}$$

Firstly, both reagents are adsorbed on the active sites (*). This step is typical for LH kinetics, it assumes adsorption of both reagents before they react together. In the case of heterogenous kinetics, it is usually really fast.

As can be seen from 3rd equation, the surface reaction is assumed to be irreversible step – the *rate* determing *step* (RDS). This is because of the rate determing step approximation – the slowest step is suggested to be irreversible. This is the one influencing the overal rate the most.

In following expressions I use a concetration variable for the rate determination as I dealt with liquid phase adsorbed on solid support. In the case of gas phase, parcial preassures are used.

$$r = r_3 = k_3\theta_A\theta_B = \frac{k_3 K_A c_A K_B c_B}{\left[1 + K_A c_A + K_B c_B + K_{AB} c_{AB}\right]^2} \tag{15}$$

When assuming that the desorbing of product is fast enough (assumption for LH kinetics), we can neglect the product active sites concentration. The reaction rate can be then described as:

$$r = r_3 = k_3\theta_A\theta_B \text{ and } \theta_A + \theta_B + \theta_* = 1 \tag{16}$$

$$r = \frac{k_3 K_A c_A K_B c_B}{\left[1 + K_A c_A + K_B c_B\right]^2} \tag{17}$$

2.1.5.3 The Eley-Rideal kinetics

The main difference between LH and ER mechanism is that the latter one takes into account the possibility of only one adsorbed reagent. This means that the adsorbed species can react with molecules from the liquid phase. The reaction proceeds via physical adsorption. However, Eley-Rideal kinetic mechanism is rarely used compared to Langmuir-Hinschelwood. [2]

2.1.5.4 The Eley-Rideal Mechanism [2]

Considering a simple reaction scheme $A + B \rightarrow AB$, the ER mechanism includes these steps:

$$A + * \xleftrightarrow{k1} A* \tag{18}$$

$$A* + B \xrightarrow{k2} AB* \tag{19}$$

$$AB* \xleftrightarrow{k3} AB + * \tag{20}$$

It is seen that compared to LH, there is one step less – the adsorption of reactant B on the active site of catalyst does not occure. The rate determing step is still the surface reaction – the 2nd reaction in this case.

If we assume again that the product desorbs fast, the overall reaction rate can be expressed as follows:

$$r = \frac{k_3 K_A c_A c_B}{\left[1 + K_A c_A + K_B c_B\right]^2} \tag{21}$$

2.1.6 Suspended vs Immobilized form

Generally, we can work with both type of titania (photocatalyst) – in the form of suspended particles or as a thin film. However, the first mentioned situation is not that often nowadays because it is difficult to recover the photocatalyst from the solution.

The so called immobilized form of photocatalyst – as a thin film layer – is more important for the research in these days.

For the highest photocatalytic activity possible, there are some facts to follow while choosing the right catalyst form. The smaller the particles, the bigger the surface area (= more active sites) and the higher the photocatalytic activity. For this case, one could consider the suspended form as the more "photoactive" than the immobilized one. On the other hand, the problem of recycling is more difficult to solve than the lower activity of the catalyst. The activity for the thin film is considered to be high enough and the manipulation stays for the great advantage in this case. This is the reason why immobilized form of photocatalysis is preffered.[5][6]

2.1.7 Application potential

As the photocatalytic phenomenon is well known for more than 40 years, there are many application connected with it.

2.1.7.1 Self-cleaning surfaces

The self-cleaning surface is supposed to keep itself clean under UV illumination. It characterizes the ability of removing of the impurities from the surface. It is closely connected to well known property of photocatalyst – hydrophility of the material.

Its effect is small afinity of the impurity particle to the surface, while bigger afinity of the water to the surface. Small or no affinity of the particle to the surface is often named as a "hydrophobic effect" – the particle is washed out by the water which spreads over the surface or it can be decomposed by the reactive species created by photocatalysis. This is highly used in industry for easy-to-clean windows or walls.[6]

Products like this were commercially used in Japan for the fisrt time – in highway tunel lamps. These lamps – mostly represented by sodium lamps – emit UV light of about 3 $mW \cdot cm^{-2}$ (at the position of cover glass). This UV light provides a sufficient surface power density for the photocalatytic process to take place. That means the impurities can be decomposed and the cover glass keeps transparent. [6]

A positive water influence has been detected. Even though, the amount of photons absorbed is not sufficient to excite enough electrons (= to remove all impurities), the surface is kept clean because of the additional water effect (superhydrophilic titania properties). This discovery caused the large scale application of titania's self-cleaning properties in exterior construction materials such as plastics, cement, glass or tiles. These materials are said to stay clean for 20 years without any additional maintenance. [6]

Titania coated textiles are another example of using the self-cleaning properties. Meilert et al. demonstrated the decolorization of wine and coffee strains on the cotton under sunlight. [7]

In the case of photocatalysis, the term "hydrophility" is often changed for *"superhydrophility"* which characterizes very good spreading properties – the contact angle of water is close to zero. It is a consequence of big amount of hydroxy groups on the titania surface. These hydroxy groups are created by the dissociation of water followed by the interaction with formed electrons and holes. For hydrophility determination, *contact angle* measurement is used. [9]

2.1.7.2 Antifogging function

By cooling down the steam, the fogging can occure on glassy materials – water droplets are created. However when using the photocatalytic layer, no droplets like this are formed as only a compact layer of water is present.

The water layer can be either thin or thick. The thin layer can evaporate easily. When the water volume is too big, no evaporation occures. However, because of the homogenous layer, the ability to see through the material is still high.

The application of the antifogging function can be found in automobile side-view mirrors production (by TOTO Ltd. in Japan).[7][10]

2.1.7.3 Antibacterial effect

Bacterias like *Escherichia Coli* can be decomposed when using photocatalysis. Using outside conditions, the cell deactivation can be achieved fast. However, taking into account the inside conditions, we must count with approximately three times weaker intensity of the light. The antibacterial properties can be increased by fluorescent lamp and addition of copper or silver. After that, the small amount of UV light is sufficient for cell deactivation. [7][10]

2.1.7.4 Air purification

The widely spread uses of photocatalysis include the decontamination, the deodorization and the disinfection of indoor air. Conventionally available air purification systems are based on filters representing the substrates for adsorbed pollutants. After some time, the filter can loose its abillity because too many particles are adsorbed on it.

Using of photocatalytic filters avoids this problem because pollutants are decomposed so the filter saturation does not occure in a large scale. Moreover, the efficiency of removing of pollution is high in the case of using photocatalysis.

As was mentioned above, the photocatalytic air purification can minimize the odour as well. For this purpose, the deodorizing sheets from titania and active carbon are used. The active carbon is an adsorbent of smell (e.g. from kitchen or refrigerator), while titania removes all the pollutants when the sheet is placed on the sunlight. [7]

2.1.7.5 Water purification

Water treatment represents an important issue and more and more research has been focused on this topic. The advantage of photocatalytic water treatment is mainly that only UV light and appropriate photocatalyst are necessary to be present. The final products of this photocatalytic reaction are mostly CO_2 and H_2O or other nontoxic substances. On the other hand, only waters with low contamination can be treated as the efficiency of the process is not high enough and the flux of UV light is also low. [7]

2.2 Titanium dioxide

2.2.1 Physical properties

Titanium dioxide has a wide spectrum of applications. It is mainly used as a coating pigment and additive in the fabrication of plastics and rubber. Its presence in form of nanoparticles plays an important role in suntan lotion because of light scattering.

It has a high refractive index. Big crystals are transparent, while smaller particles are capable of light scattering and they can be used for creating of highly opaque layers.[11]

Since the establishment of its photocatalytical properties, it has been often used in air and water purification (for its antibacterial properties).

It is mainly used for its high photocatalytic activity, stability against the light, nontoxicity and price availability. Moreover, it has surfactant properties and is stable against corrosion. [12]

In the nature, there are 3 structural modifications of titania – anatas, brookit and rutile.

- *Anatase* occurence is quite rare. It contents traces of Fe a Sn. Its color usually varies from brown to black. The hardness and density properties are similar to rutile. At the temperature of 915 °C the anatase structure changes to rutile. [13]
- *Brookit* is typical for its dark brown to greyish black color caused by the traces of Fe, Nb and Ta. Its structure changes to rutile at 750 °C. [14][15]
- *Rutile* is the most common among the titania modifications. Big crystals are black or reddish brown, small ones are mostly yellow. Its traces are mostly Fe, Cr, Sn and Nb. [14][16]

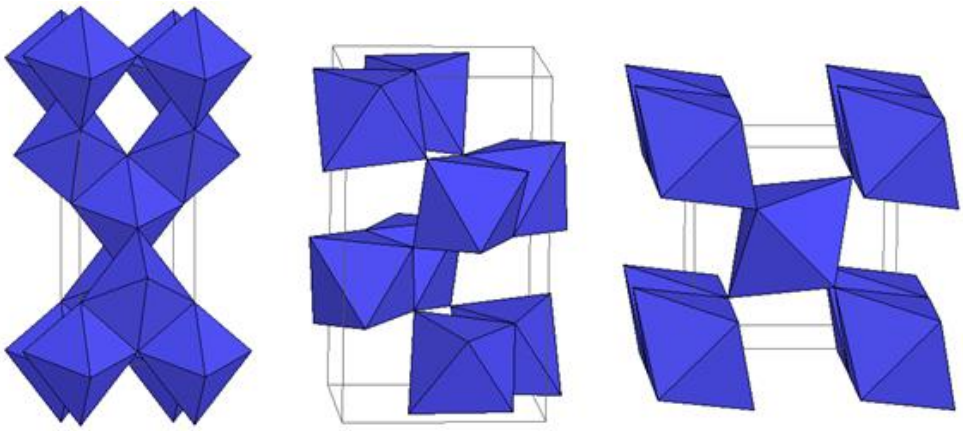

Figure 4 *Three possible structures of TiO_2 – anatase, brookite and rutile.*[17]

The most often used initial grade of titania is called TiO_2 P 25 and is produced by Evonik. It contains 2 titania modifications – anatase and rutile in the ratio 3:1. At normal conditions particles of both types do not interact together. However, when the photocatalysis takes place, there is an interaction between them causing a synergic effect which means this mixture is more photoactive than one would assume from the anatase or rutile individual photoactivity.

Millenium PC10 and Millenium PC50 (both containing only anatase particles but of different sizes) represent other photocatalytic industrial sources.[14][17][18]

2.2.2 Semiconductor properties

The width of band gap is characteristic for each semiconductor. It characterizes the energy barrier (= band gap energy) between the valence band (the highest probability that electron is

there) and the conduction band (free movemement of electrons). The band gap energy shows how much minimum energy is needed for electron to move from valence to conduction band. In the case of insulants, the energy band gap is too big for the electron transition. On the other hand, conductors have their valence and conduction bands overlapping.

After absorption of the sufficient amount of energy, the generation of electron-hole pair takes place followed by the redox processes.

The electric conductivity increases with increasing temperature because of more electrons that are excited to conduction band. [14][19]

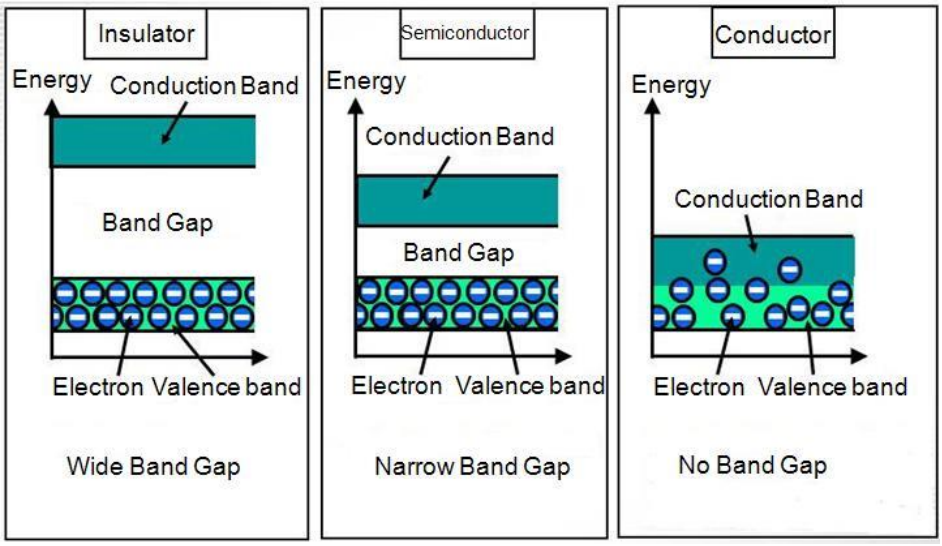

Figure 5 *Valence and conduction bands for insulator, semiconductor and conductor.* [20]

2.2.3 Photocatalytic properties

As said before, the right amount of photon (light) energy is required to activate the semiconductor – catalyst. This means to create the active sites on the catalyst by electron-hole pair establishment. The light from UV or VIS spectra and appropriate semiconductor (with sufficient width of band gap) are needed.

Titanium dioxide is the mostly used photocatalyst, mainly because of its high stability in the solution and the band gap energy corresponding to the UV light (3.2 eV). UV light represents 5 % of the energy of solar spectrum which in a small scale allows the application in outdoor conditions. [10][14]

Nowadays, a lot of research has been focused on the developing of a stable catalyst which could be activated by the VIS light. For example, pigment doping of titania seems to have a promising potential in the photocatalysis development. Pigment electrons can be excited by the energy smaller than the one needed for the excitation of titania electrons. After the excitation takes place, electron flows from the pigment conduction band to the lower conduction band of titania. The following mechanism is the same as mentioned before – reaction with the adsorbed species takes place. [21]

2.2.4 Substrates for photoactive layers coating

Choosing the appropriate substrate for coating of titania layers plays and important role for the overall behaviour of the photocatalyst. The support should meet the following requirements: [22]

- resistant to the oxidising environment
- UV transparent
- generation of low pressure drop
- strong adhesion to the surface
- helping with the contact of photocatalyst and reagent

Many sorts of glass support are used nowadays. There have been other substrates tested (ceramics or aluminium). However, their opacity to radiation represents a big limitation.

The biggest problem when using a soda lime glass is the possible migration of sodium ions which could affect the titania structure. That is why a pretreatment by sulphuric acid is always necessary. [22][23]

The polymeric materials research seems to take a good way. The commercially available poly(ethylene terephthalate) or cellulose acetate are cheap, lightweight, easily shaped and UV transparent.

2.2.5 Preparation methods of TiO_2 layers from liquid phase

One of the most suitable ways of creating thin immobilized catalyst film is the sol-gel method. It is great because of its simplicity, universality and homogeneity.

The technique is based on the change of liquid phase (*sol*) to solid phase (*gel*). Sol is a phase colloid that consists of particles in the range of 1-500/1000 nm. It is thermodynamically unstable – it can turn to gel as the result of coagulation. This means that the stability factor (electric double layer) is disrupted making it possible for the gel to be created in the places of disruption (by connecting them together).This connection leads to a network which is filled by dispersed environment (solvent). Created network gives the system strength, while the solvent contributes to mobility.

Individual steps in sol-gel method: [24]

- *Formation of sol*: by hydrolysis of water solution of metal alkoxide, metal hydroxide is created:

$$M-OR + H_2O \longrightarrow M-OH + R-OH \tag{22}$$

- *Gelation*: formation of gel (network filled by solvent) by polycondensation of hydrolized metal alkoxide – by reaction with nonhydrolized or hydrolized metal alkoxide:

$$M-OR + M-OH \longrightarrow M-O-M + R-OH \tag{23}$$

$$M-OH + M-OH \longrightarrow M-O-M + H_2O \tag{24}$$

- *Gel aging*: more polycondensation reactions take place, the number of disruption points is increased → denser connection of network is created.
- *Gel drying*: removing of water and other liquids from the gel pores at aproximately 200 °C.

- *Calcination* is the typical example of next step, carried out at temperature up to 600 °C, leads to total dehydratation (removing of M-OH molecules at the surface), pyrolysis and conversion to metal oxide.

$$2M(OH)_n \longrightarrow 2MO_{n/2} + nH_2O \quad (25)$$

When applying temperatures greater than 600 °C, the gel can undergo decomposition because the pores present collapse and the rest of the volatile substances leave the gel. [25]

The precursors for this method are usually either titanium buthyloxide or titanium isopropoxide.[24]

2.3 Standards for evaluation of photocatalytic activity

The International Standards Organization (ISO) is the worldwide biggest publisher of international standards. Companies following these standards provide keeping of the given quality and reliability of their products. Every international standard must be reexamined no less than in 3 years after publication. [26]

2.3.1 ISO 10 678; 2010 – The determination of photocatalytic activity of surfaces in an aqueous medium by degradation of Methylene Blue

This ISO method represents a simple evaluation for new photocatalytic materials, photoreactors and light sources. It is based on assesment of photocatalytic bleaching rate of an indicator ink – Methylene Blue (MB).

Use of MB has been decreasing but it is still used in textile, leather and paper industry and therefore it seems more than logical to use it as a test dye. Methylene Blue is a cationic dye, in solid state it is a dark powder, when soluted in water it turns to blue color solution.

The absorption peaks of the dye solution in water give following absorption maxima at: 246, 292 and 664 nm. The absorption maxima at 664 nm could be the effect of chromophore with long conjugated system. On the other hand, the peak at 292 nm might be of the aromatic ring. These statements suggest using the 664 nm peak for decolorization evaluation while using the peak at 292 nm for the analysis of the dye degradation. [26][27]

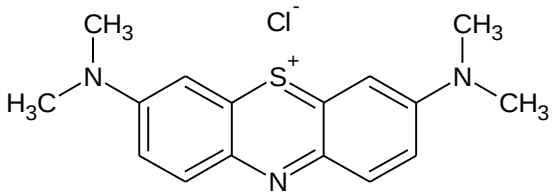

Figure 6 *Methylene Blue.*

Methylene Blue degradation can be described as a complete mineralization. However, the mineralization process takes more time than the photobleaching of MB.

$$C_{16}H_{18}N_3SCl + 25.5\ O_2 \rightarrow HCl + H_2SO_4 + 3\ HNO_3 + 16\ CO_2 + 6\ H_2O \qquad (26)$$

The apparatus for standard measurement contains a sample (typically 10 cm plate) with photocatalytic layer and the cylinder fixed on the sample (3-4.7 cm diameter). The sample must be exposed to UVA light before starting the standard assesment. At *"conditioning step"*, 35 ml of MB solution ($2 \cdot 10^{-5}$ M) is poured into the created vessel and left for 12 hours in the dark. After that, the concetration of MB in the solution must be higher than 10^{-5} M. If not, the conditioning step must be done again until it meets the requirements.

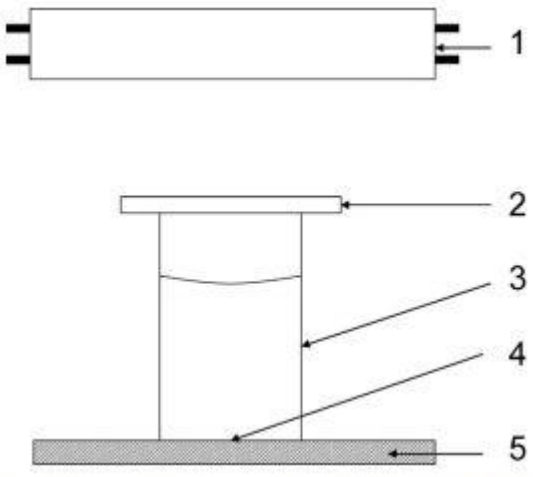

Figure 7 *Apparatus for Methylene Blue standard ISO method – 1) source of UV light, 2) glass cover, 3) testing cylinder, 4) irradiated area, 5) sample. [26]*

Then another 35 ml of MB solution is placed into the vessel and the UV transparent glass cover is put over it. After that the irradiation of the system by UVA light (1.0 $mW \cdot cm^2$) begins and the solution is stirred every 20 min. The change of absorbance as a function of time is measured by spectrophotometer directly or by sampling (absorbance detection at 665 nm). The irradiation process lasts 3 hours or less – in the case of faster decolorizing of the MB solution. The reaction temperature is recommended to be 23 ± 2 °C.

The blank experiment in the dark conditions is performed as well. Then the photonic efficiency of the active sample is calculated according to following equation:

$$\xi_{MB} = \frac{100 \cdot r\left(\mathrm{MB}^{+}\right)}{I_{\mathrm{UV}}} \tag{27}$$

Where *r(MB+)* represents the rate of MB bleaching ($molecules \cdot cm^{-2} \cdot s^{-1}$), I_{UV} is iradiance (number of $photons \cdot cm^{-2} \cdot s^{-1}$).

If the photonic efficiency is bigger than 0.1%, the experiment should be done once again with the irradiance source 0.25 $mW \cdot cm^{-2}$.

The benefit of using this method is surely its simple and easy performance. On the other hand, the used dye must have a high purity with $\varepsilon_{MB} = 7.4 \cdot 10^4$ $M^{-1} \cdot cm^{-1}$ at 664/665 nm. The standard is given for low photoactivity samples $\xi < 0.1\%$. Higher photonic efficiency is not suitable for the evaluation according to this standard, and is probably caused by mass transfer effects which are not assumed in this method. It is suggested that MB would be more suitable for water purification standards rather than for PCA evaluation of self-cleaning films. [26][28]

Several changes are recommended in this method: the UV light source should be more specified: "original narrow band emitter in the range 320-400 nm" should be replaced by more specific "UVA light with an emission peak at 365 nm with a 20 nm bandwidth" (black light blue fluorescent tube source with europium-doped strontium fluoroborate or borate phosphor is suggested). In original ISO method, the pH range of the reaction solution was not defined. According to further experiments, pH 5.5-6.0 seems relevant. The stirring of the solution should be provided as well. Also changing the irradiance source for weaker

one, when the photonic efficiency requirement is not met ($\xi < 0.1\%$), does not seem reasonable. It was proved that the kinetics of MB photobleaching depends non-linearly on incident irradiance. As long as the irradiance decreases, the photonic efficiency increases. [28]

2.3.2 ISO 22 197: Test methods for air-purification performance of semiconductor photocatalytic materials

Three methods for photocatalytic air purification have been published. They differ mainly in the pollutant, whose removal is studied: [26]

- nitric oxide (ISO 22197-1: 2007)
- acetaldehyde (ISO 22197-2: 2011)
- toluene (ISO 22197-3: 2011)

All the three test methods have the same photoreactor system. The illumination source is the UVA light which is applied on a sample (50 × 100 × 5 mm) in a quarz or borosilicate glass. The pollutant is in the mixture with air. The inlet and outlet gas streams are regularly analyzed to evaluate any change. The material of reactor must be inert to UV light and pollutant. Stainless steel is the most suitable material to be used.

At the beginning the test gas flows into the photoreactor without any illumination (ca. 30 min before turning on the light). After starting the experiment (detected by turning on the light), the pollutant concentration in time is detected.

Every air-purification standard differs in the concetration of test pollutant, overall gas stream flow rate, sample run test time and system for analysis. [26]

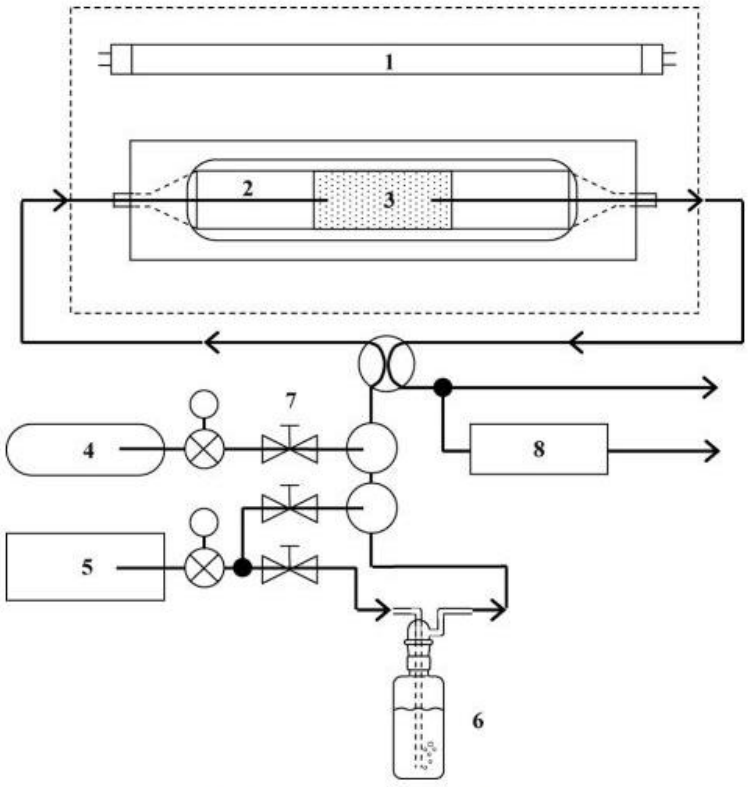

Figure 8 *Irradiation setting for the air purification ISO standards. (1) UV light, (2) glass cover, (3) tested sample, (4) standard gas – test pollutants, (5) air source, (6) humidifier, (7) mass-flow controllers, (8) pollutant gas analyzer. [26]*

2.3.3 ISO 10676; 2010: Test method for water purification performance of semiconductor photocatalytic materials by measurement of forming ability of active oxygen

This method is closely connected to wastewater treatment under UV light illumination. The test pollutant is represented by dimethyl sulfoxide (DMSO) – organic solvent used in industry. On the other hand, it is not well studied wastewater pollutant so its use in the case of water purification test method does not seem appropriate. Other frequent pollutants such as Methylene Blue, Acid Orange 7, phenol, 4-chorophenol and dichloroacetic acid would be more suitable instead. [26]

The known mechanism of DMSO's degradation could be the reason why DMSO is a test pollutant in this ISO method.The fast reaction with hydroxyl radicals gives methane sulfinic acid which undergoes further oxidation.

The overall process is given:

$$(CH_3)_2SO + 2O_2 \rightarrow CH_3SO_2H + CO_2 + H_2O \quad (28)$$

$$CH_3SO_2H + O_2 \rightarrow 2CH_3SO_3H \quad (29)$$

$$CH_3SO_3H + 2O_2 \rightarrow H_2SO_4 + CO_2 + H_2O \quad (30)$$

At the beginning, the sample is pretreated by UV light. Then the sample (10 cm^2) is placed under the UV light source (irradiance 2 $mW \cdot cm^{-2}$) and the circulated 5 mm deep polluted water stream (10 ppm of DMSO) is allowed to flow through.

The amount of DMSO is being analyzed during 5 hours of illumination via the ion or gas chromatography. The suggested room temperature is 20-25 °C. [26]

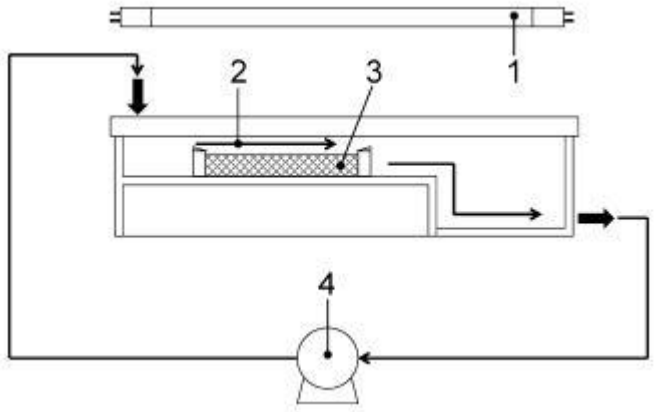

Figure 9 *Irradiation setting for the DMSO water purification ISO standard. (1) UV light source, (2) water stream with 10 ppm DMSO, (3) tested sample, (4) peristaltic pump.[26]*

2.3.4 ISO 27448:2009: Test methods for self-cleaning performance of semiconductor photocatalytic materials – measurement of water contact angle

This method is known as the one based on "photoinduced superhydrophilic effect" (PSH). It uses an oleic acid and determines its degradation by changing of water droplet contact angle during illumination (the wettability is increased). The contact angle is measured until it reaches the value of 5° – then the test is suggested to be finished. [26]

The reaction describing the decomposition process is:

$$C_{18}H_{34}O_2 + 25.5\,O_2 \rightarrow 18\,CO_2 + 17\,H_2O \quad (31)$$

Firstly, each sample (10 cm^2) is pretreated by UV illumination. Secondly, the oleic acid is placed on the sample – either manually or by dipping. When the manual way is choosen, the sample must be weighted and the 200 µl of organic compound is placed in the centre of the sample so the created surface is homogenous (usually done by non-woven cloth). The weight of oleic acid on the sample should be 2 ± 2 mg.

In the case of dipping, the sample is placed in the solution of oleic acid and then pulled out at the rate 60 $cm \cdot min^{-1}$. Finally, the sample is dried at 70 °C for 15 min. No specification about the mass of oleic acid on the sample is given.

Next step is the contact angle measurement – each sample is tested at 5 different places before and during UV irradiation (for manual coated samples: 2 mW/cm^2, for dipped ones 1 mW/cm^2). It is recommended to carry out the experiment 5 times with 5 samples prepared in the same way.

According to the ISO standard, the initial and final values of contact angle should be recorded as well as the irradiation time. [26]

2.3.4.1 Contact angle

Contact angle is defined as and angle between the surface plane and the tangent of the drop. The contact angle measurement provides a good way in prediction how the material is going to behave when deposited on the support. As seen in the Figure 10, it is not only the property of adsorbed material, support material and surrounding environment are important as well. All these 3 parameters, each characterized by the value of surface tension, decide whether the adsorbent is spreading over the surface or not.

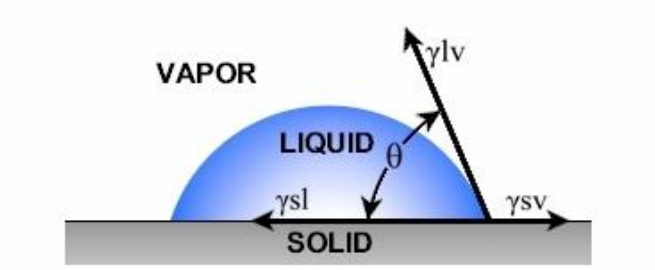

Figure 10 *Three different surface tensions effecting the drop shape. [29]*

If we consider a drop on the solid surface, *Young's equation* describes the effect of the forces acting on the drop – by the relation between surface tensions and the contact angle.

$$\gamma_{SV} = \gamma_{SL} + \gamma_{LV}\cos\theta \quad (32)$$

The value of contact angle indicates whether the liquid drop is spreading on the support or not. If the contact angle is greater than 90°, the surface is non-wetting. In opposite case – the contact angle is smaller than 90°, the liquid is spreading on the surface meaning the surface is wetting. The smaller the angle, the better the wetting ability. If the contact angle is close to zero (complete wetting) the surface is called *superhydrophilic*.

The Young's equation considers the surface to be an ideal plane without any roughness. Actually this kind of surface is hard to find. We can often observe 2 different contact angles values for the same system. This phenomenon is characterized by the term *"hysteresis"*. Then we distinguish between the apparent contact angle and the true one. The relation between them depends on the value of *surface roughness*. [29][30]

$$\cos\theta_{app} = R_{rough}\cos\theta_{true} \tag{33}$$

The surface roughness is the ratio between actual surface area and the apparent surface area and is equal (ideal case) or greater than 1. In the case of wetting surfaces, the apparent contact angle is smaller than the true one. [29][30]

2.3.5 ISO 27447:2009: Test method for antibacterial activity of semiconducting photocatalytic materials

In this case the model bacteria are usually *Escherichia colis*. The standard is valid for photocatalytic ceramic materials or other materials produced when coating or mixing with photocatalyst. In the case of testing permeable or rough materials, use of different method is suggested.

There are 2 main methods: a *film adhesion method* which is used for evaluating the photocatalytic properties of flat surface materials with photocatalytic coating and a *glass adhesion method* which is suggested for assesment of photocatalytic antibacterial properties of cloth materials.

In the case of film adhesion method, *Staphylococcus aureus* and *Escherichia Coli* are conveniant for evaluation. For glass adhesion method, *Staphylococus aureus* and *Klebsiella pneumonidae* are suitable.

Detailed preparation from the parent strains are given for each of the tested bacteria. [26]

2.3.6 ISO 10677:2011: Ultraviolet light source for testing semiconducting photocatalytic materials

This ISO method deals with the selection of the right UV light source during evaluation of photocatalytic activity.

The standard recommends xenon arc lamp for photocatalytic samples being exposed to the sun. The emmision in 300-400 nm is similar to emission of sun.

Black light fluorescent lamps use one phospor and a blue filter to keep most of the light emitted being in the UVA light region. According to the phospor used, two types of Black light fluorescent lamps are known: europium-doped fluoroborate (UV emission peak at 368-371 nm, a bandwidth 20 nm) and lead-doped barium silicate (UV emission peak at 350-353 nm and a bandwidth 20 nm).

The photocatalytic activity depends on the spectral distribution and the radiant intensity of the UV light. That is why the radiometer is important to be used for the UV irradiance assesment. The UV irradiance should be detected at least 15 min after turning on the lamp, at the beginning and at the end of the experiment period. [26]

2.4 Recognized methods for evaluation of photocatalytic activity

Several other models are applied to evaluate the effectiveness of photocatalytic properties of semiconductor, even they are not ISO standards. Some of them are used even more often for the photoactivity assesment as they are easier and faster than the standard methods.

2.4.1 Stearic acid test

The stearic acid (SA) layer is deposited on a photocatalytic film. Then the photocatalytic decomposition dependency on time is evaluated. This simple method is often used for self-cleaning glass testing for several reasons: [31]

- SA is a suitable compound for photocatalytic evaluation of solid films deposited outside and inside as well.
- When the photocatalyst is not present, SA is very stable under UV illumination (no photolysis occures).
- The kinetic of SA degradation is usually zero-order and the thickness of SA film does not effect the photocatalytic activity.

The overall reaction of SA decomposition takes into account CO_2 and H_2O as final products. [33]

$$CH_3(CH_2)_{16}CO_2H + 26\,O_2 \rightarrow 18\,CO_2 + 18\,H_2O \qquad (34)$$

The possible ways of PCA evaluation are:

1. Gas chromatography expressing the amount of generated CO_2.
2. Ellipsometry for assesment of decreasing thickness of SA layer.
3. Infra-red absorption to evaluate how the SA film is removed. SA absorbs in the wavelength region 2700-3000 cm^{-1}.
4. Water contact angle is an indirect method of PCA evaluation. It faces some limiting requirements – it cannot be used for evaluation of hydrophobic, rough or porous surfaces.[31]

2.4.2 Terephtalic acid test

Transparent terephtalic acid (TPA) layer is placed over the photocatalytic surface. After UV irradiation, fluorescent hydroxyterephtalic acid (HTPA) is formed. This formation can be detected via spectrofluorimeter. [34]

This method is considered to be accurate, sensitive and reproducible enough for the photocatalytic evaluation. Moreover, TPA is stable against photodegradation and transparent in VIS and UVA region.

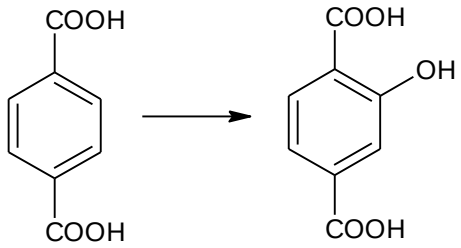

Figure 11 *Degradation of terephtalic acid (left) to hydroxyterephtalic acid (right).*

First of all, a lot of research has been done dealing with photocatalyst-TPA as a solid-liquid system. In this case, the formation of HTPA is a result of reaction between TPA and hydroxyl radical. However, this method is not appropriate for self-cleaning evaluation. The solid-solid system with more concentrated TPA and high adsorption on the photocatalytic surface seems more suitable for the self-cleaning assesment. The proposed mechanism of TPA degradation is via photogenerated holes. [34]

TPA evaluation test has been gaining a great popularity because of its fastness and simplicity. It can be also used for flat and rough surfaces. [31]

2.4.3 Using of indicator ink

Indicator inks provide a simple and inexpensive method of photocatalytic evaluation. Using of dyes as indicator inks is convenient – not only can we measure the change in time (the decrease of absorbance), but we can observe the color change as well – so the detection can be done only by a human eye. Therefore, for commercial uses the dyes with the biggest color change are preffered as they can be detected easier.

In the case of dyes used as indicator inks, in PCA testing there is a big advantage – a lot of research has been done so far. The reason is quite clear – up to 20% of the textile total world production of the dyes is released in the wastewaters, this means the degradation of dyes in the industrial wastewaters calls for the attention. Most of the textile dyes are stable against degradation while wastewater treatment. Physical techniques (adsorbtion on activated carbon) are only postponing the degradation problem (it is not necessary to deal with the dye in the water but further in the adsorber). That is why the photocatalysis plays an important role in this field of study – it enables the total decomposition of dyes and we do not have to deal with desorption of the products. [35]

The number of redox dyes that can be used for photocatalytic activity evaluation is limited. Only a few dyes create forms of different colors and are stable under normal conditions.

2.4.3.1 2,6-dichloroindophenol (DCIP)

One of the most used dye for PCA evaluation is 2,6-dichloroindophenol. However, it has one big disadvantage – the storage stability of the dye in solution is a big challenge to face. Even the solar light can damage the dye structure as it undergoes a photolysis itself.

Its mixture is usually prepared with glycerol for more radical generation which increases the reaction rate. [33]

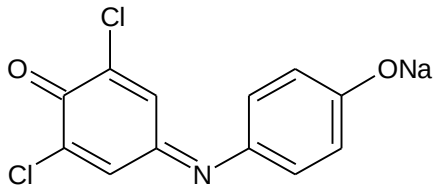

Figure 12 *2,6-dichloroindophenol.*

2.4.3.2 Acid Orange 7

It is an anionic orange dye often used in textile and paper industry. It is soluble in water but not in organic solvents. Its big disadvantage is that it is almost non-biodegradable which causes its high abundance in wastewaters.

It has a strong absorption peak (λ_{max} = 485 nm) in VIS region, however, in the UVA the absorption is low. There are two important intermediates of the photodegradation: sulfanilic acid and 1-amino-2-naphthol. These are often detected when the degradation of Acid Orange 7 is evaluated. [27][35]

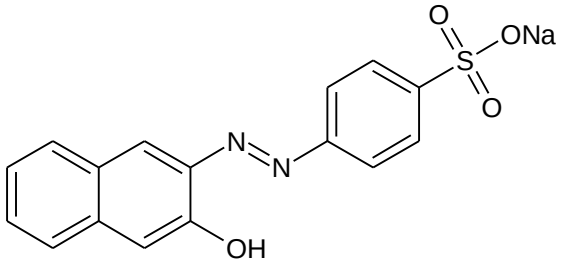

Figure 13 *Acid Orange 7.*

2.4.3.3 Resazurin

Another dye which is used as an indicator ink is Resazurin. Its reduction to Resorufin can be indicated visually because of color change – from blue to pink.

For photocatalytic assesment, Resazurin is often used in a mixture with glycerol, which leads to faster reaction rate. [26]

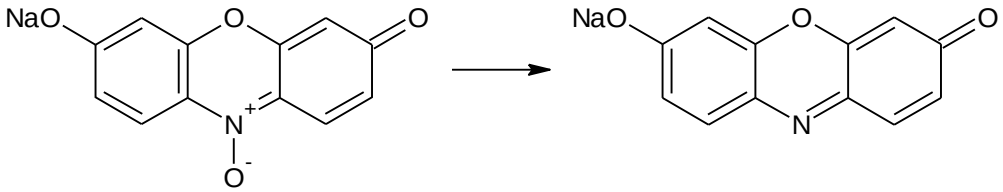

Figure 14 *Structures of Resazurin (blue, left) and it reduced form – Resorufin (pink, right).*

2.4.3.4 Solvent Violet 11

This purple indicator ink is quite rare in evaluation of photocatalytic properties. However, its big advantage is its solubility in many organic solvents (aceton, ethanol) which can make the ink deposition easier because of higher viscosity compared to aqueous solution.

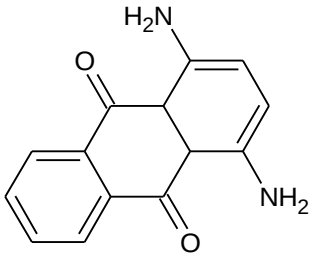

Figure 15 *Solvent Violet 11.*

3 THE AIM OF THE WORK

Lately, the photocatalytic activity assesment has been very often based on titania-indicator ink thin films. The evaluation by monitoring of stearic or terephtalic acid proved good results, however, the visible color change is preffered because it provides easier detection method even for unexperienced user. This is the case of colorful thin films. On the other hand, there are still challenges to face, the suitable indicator ink for PCA detection should have a rapid degradation rate under UV illumination which should be followed by easily detectable color change. Moreover, the ink's deposition should provide layer with good structure, so the PCA evaluation represents accurate results.

In the experimental part of my diploma thesis, I tried to transfer the knowledge gained from the study of literature to experiments I performed.

The experimental part was done according to the following aims:

- To optimize the apparatus for measuring of the degradation rate of indicator ink decouloring – changing the LED diode for white one so differently colored dyes could be tested.
- Another of my tasks was to optimize the composition of the ink suitable for depozition by piezoelectric printing. I tested 7 dyes and evaluated their suitability for photocatalytic activity evaluation.
- After selection of the appropriate indicator inks, I focused on optimizing of the printing conditions for inks's deposition.
- Finally, I dealt with the apparatus optimization by applying the photodiode-multimeter system for detection.

4 ANALYTICAL METHODS

4.1 UV-VIS Spectroscopy

The basis of this method is the absorption of UV and VIS light by diluted solutions of molecules which causes the excitation of valence electrons.

Molecular spectra (MO) are created by bonding between atomic orbitals (AO) – 2 atomic orbitals form 2 molecular orbitals of different energy. The one with energy lower than original AO is called *bonding*, the anotherone with higher energy is *non-bonding*. Electron pair in the ground state is in the bonding MO. After the absorption of energy (given by the energy difference between two given MO), the electron transfers to non-bonding MO. [36]

4.1.1 Fundamentals

When the radiant flux Φ_0 passes through the cuvette with the solution, partial reflection, dispersion and absorption occure. It is assumed that the main part of the flux is absorbed. [36]

Transmittance (T) expresses the relative radiant flux that passed through the cuvette – it is a ratio between the radiant flux passed through the sample and the initial one.

$$\mathrm{T} = \frac{\Phi}{\Phi_0} \tag{35}$$

Absorbance is the negative value of transmittance logarithm. Measuring of the transmittance is a widely used spectroscopic technique. However, in most cases, the absorbance values are presented. It is used for qualitative evaluation – for identification of substances as well as for quantitative evaluation – when evaluating the concentration of a molecule in given solution. For the accuracy of the experiment it is advised not to work with values higher than A = 1.

$$A = -\log T = \log \frac{\Phi_0}{\Phi} \tag{36}$$

Absorbance is an additive quantity – when the radiant flux is absorbed by more than one component, the overall absorbance is given by the sum of absorbance of each component.

The Beer-Lambert-Bouguer (BLB) law describes the linear dependency of absorbance on a concentration (ε is the molar absorption coefficient, l is the cuvette length). The BLB law is valid for concentrations up to 10^{-2} mol/dm^3.

$$A = \varepsilon \cdot \mathrm{l} \cdot \mathrm{c} \tag{37}$$

4.1.2 USB-650 Red Tide Spectrometer

Most of my measurements were done by a USB-650 Red Tide Spectrometer with a fiber connection to a computer device. This provides a simple way of absorbance evaluation without any necessary manual handling.

When the light enters the spectrometer, it reaches the connector part. There is a slit with rectangular aperture behind the connector and its size determines how much light passes through the optical bench. The next part of the spectrometer which the light reaches, is a filter limiting the wavelength regions of the light before entering the optical bench. After

that, the light passes collimating mirror and is reflected onto the grating where the light is diffracted and then further directed to the focusing mirror. The focusing mirror directs the light spectra to a detector plane, where the light passes through the optional attached detector component to increase the efficiency of light collecting (e.g. by reducing the amount of stray light). The collector itself has the function of a convertor of optical signal from the light into the digital one. The digital signal is then transformed to SpectraSuite application. [37]

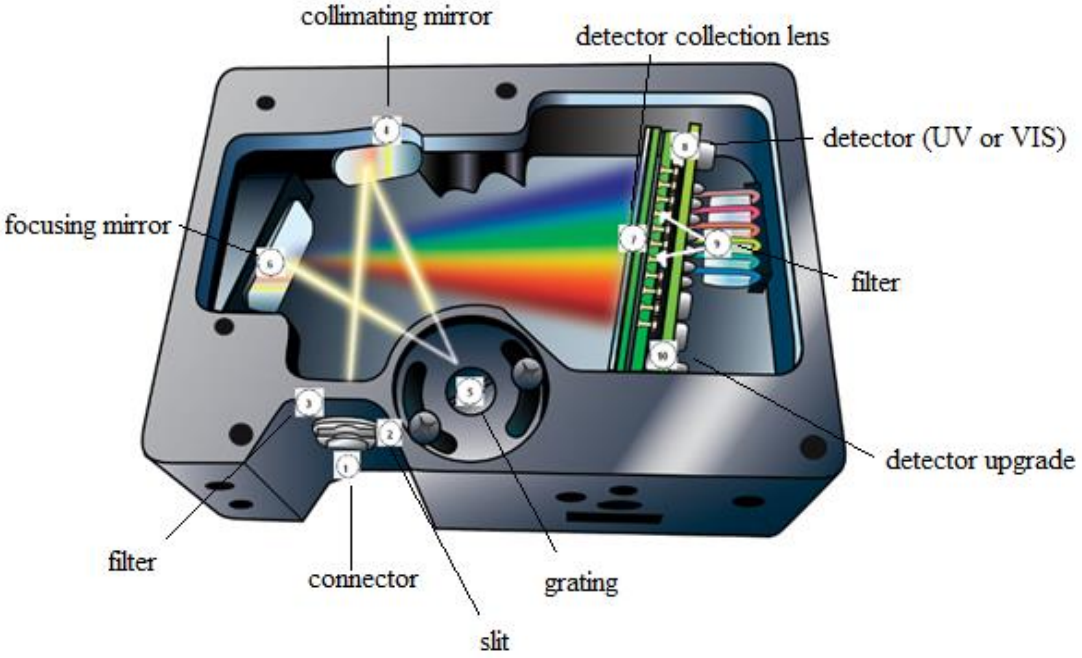

Figure 16 *USB-650 Red Tide Spectrometer. [37]*

4.2 Stylus profilometry

Profilometer is a device for measuring of the roughness of surface. There are two main types: stylus and optical. While the optical profilometer uses light source for the surface detection – a non-contact technique, the stylus profilometer's detection uses a probe (usually made from hard material) – it is a contact technique.

When using the stylus profilometry, the height of a sample is detected by a probe movement on the sample. The measurement of the height is done by monitoring the force of the sample against the probe while moving along. The technique moves in coordinate system X, Y and Z. Any change in Z direction can be used for evaluation of surface structure.

As this is the contact method, high sensitivity and resolution is provided. On the other hand, sensitivity to soft surfaces and probability of probe contamination by the surface must be considered. Moreover, the technique can even damage some surfaces. [39]

Figure 17 *DektakXT Stylus Profiler.[40]*

4.3 Material printing

There are many coating techniques to be used for substrate coating, e.g. dip-coating, spin-coating and spray-coating. Lately, inkjet material deposition (material printing) has been growing in importance. The deposition of a low viscosity liquid drop on a substrate is done by a thermal or piezoelectric print head. The great advantage of this method is that the precisely printed area can be set, different patterns can be printed and most of the ink is consumed for the deposition on the substrate (there are little losses while cleaning of the print head and purging).

A selection of the appropriate viscous solvent is very important. There are many solvents suitable for coating techniques, but not for material printing, e.g. cyklohexane is a great solvent when using a dip-coating method, however, in the case of material printing, it faces problems with high volatility (resulting in a fast evaporation from the print head nozzles), low surface tension and low viscosity.

There are 2 types of the deposition of the material in dispersed form – continuous and drop-on-demand printing. [41]

4.3.1 Drop-on-demand printing

During drop-on-demand printing, the drops are not released continuously. They are created by pressure in the inkjet head. According to the drop releasing, this technology is further divided into thermal and piezoelectric printing.

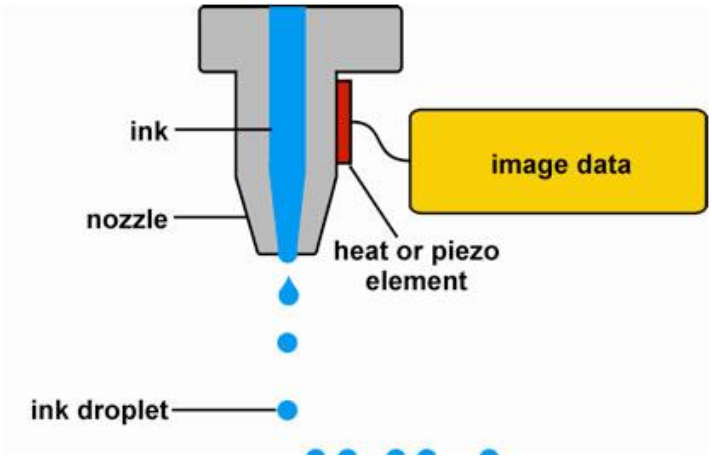

Figure 18 *Drop-on-demand printing. [42]*

In the case of thermal printing, the heat is important for the droplets releasing. By increasing the temperature of the solution, the bubble is created in the nozzle. Because of the pressure effect, the bubble explodes on the substrate. After that, another bubble is created and the mechanism repeats. When using this method, it is necessary to use a thermally stable solution and cooling system. This means that for the creation of a single bubble, the solution must be both, heated and cooled down.

Piezoelectric printing uses piezo-crystal in the inkjet head. When there is a sufficient current applied, the pressure for the droplet releasing is created. This method stands out because there is no need for thermally stable solution. [41]

4.3.2 Continuous printing

As the name suggests, the expelling of the droplets in this case is continuous. There is a droplet generator in the inkjet head which divides the solution into single droplets. The piezo crystal makes the droplets enter the space between electrodes at high frequencies (50–175 kHz), which are responsible for the formation of charged droplets. The charge of the droplet is important as it determines how much the droplet is going to be deflected when passing through the deflector. The deflected droplets are recycled.

There are two types of deflection: *binary* and *multilevel*. In the first case, the case of binary deflection, the undeflected drops are printed, while the multilevel deflection prints the deflected droplets. [41]

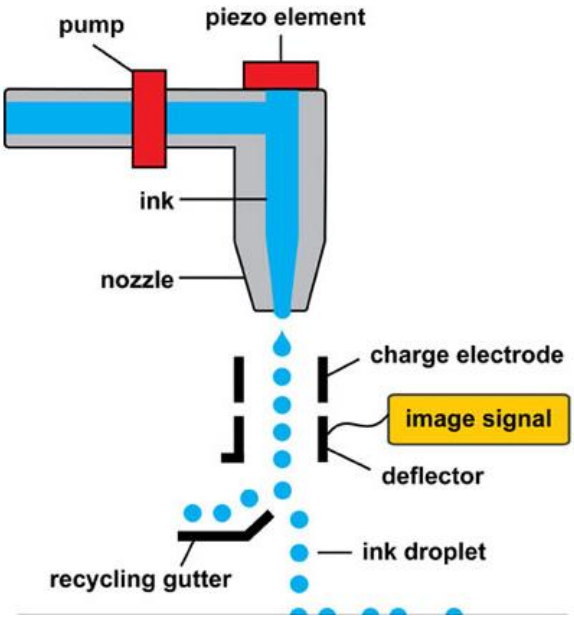

Figure 19 *Continuous printing [42]*

4.3.2.1 FujiFilm Dimatix 2831 Printer

This printer is a drop-on-demand kind of device. The electric signals cause the deformation of piezo crystal and the releasing of the droplet from the nozzle. Figure 22 shows the drop expelling in time periods. The inkjet head consists of 16 nozzles, which can be heated up to 70 °C, leading to decrease of viscosity, mainly in the case of polymer solution. The substrate is placed on a heated plate (up to 60 °C), which can contribute to the evaporation of solvent (increasing the overal rate of printing).

We can print films with the maximum size 20 × 30 cm with 25 mm in thickness. The typical size of the droplet is 1-10 pl. [43]

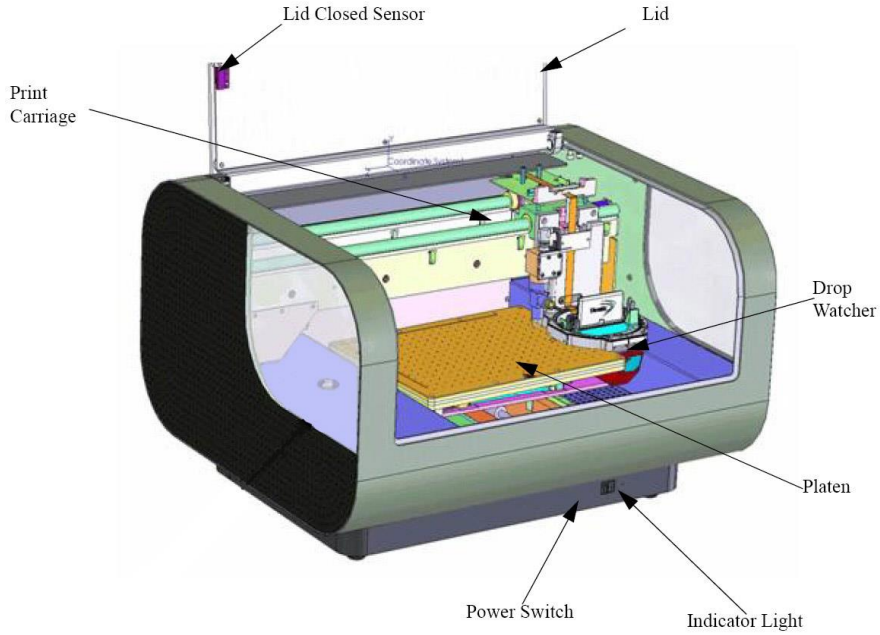

Figure 20 *Dimatix Fujifilm 2831 Printer.[43]*

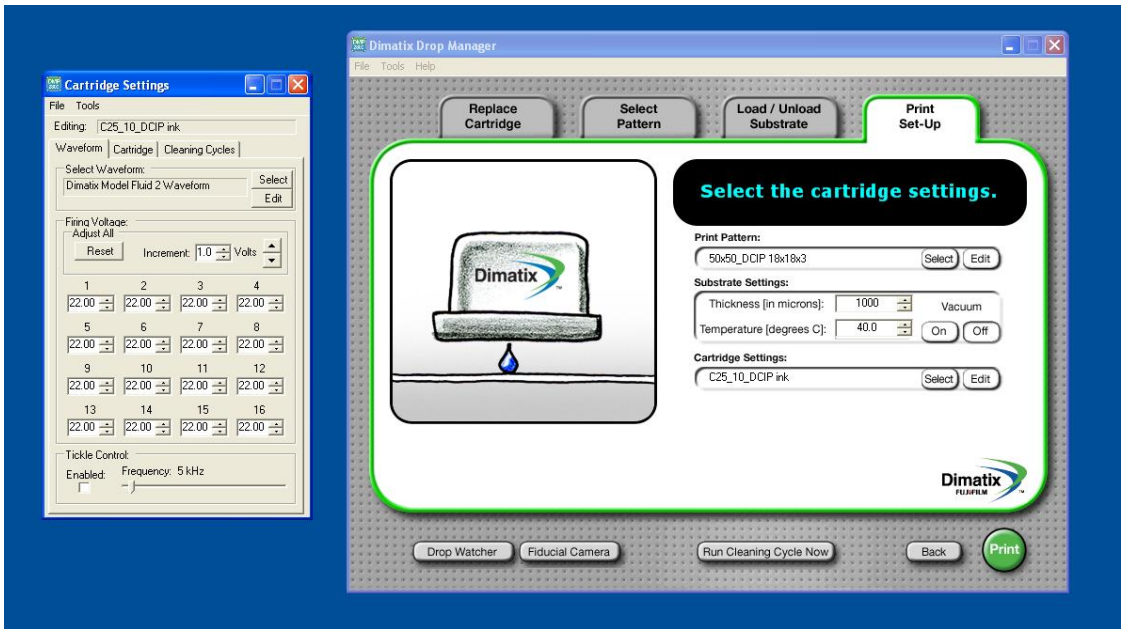

Figure 21 *Conditions for printing set-up on Dimatix Fujifilm 2831 Printer.*

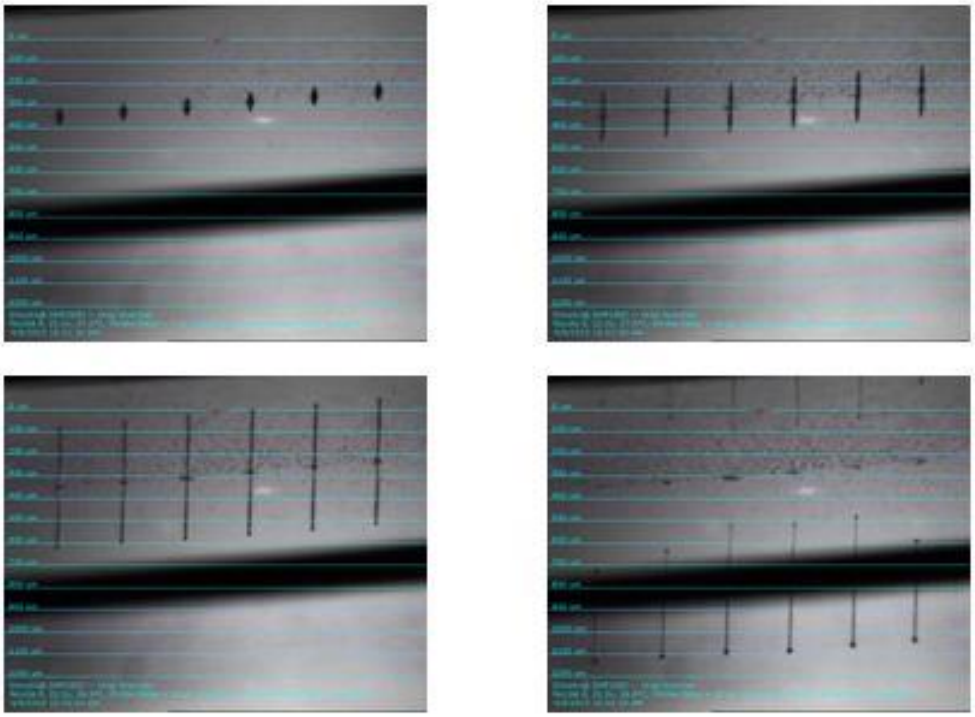

Figure 22 *Dimatix drop expelling in 7, 10, 19 and 58 µs.*

5 EXPERIMENTAL PART

5.1 Used Materials and Devices

5.1.1 Chemicals and Materials

- E5 sol (already prepared, composition: Xylene, Triton X, demineralized water, TTIP)
- Glass substrate, 5 × 5 cm and 2.5 × 7.5 cm
- Polyvinylpyrrolidone, Fluka Analytical
- Isopropylalcohol, Penta
- 2-propoxyethanol, Fluka Analytical
- Glycerol, Lachema
- 2,6-dichlorindophenol, Sigma Aldrich
- Methylene Blue, Centre for Organic Chemistry Ltd.
- Direct Blue 10, Centre for Organic Chemistry Ltd.
- Reactive Blue, Centre for Organic Chemistry Ltd.
- Solvent Violet 1, Sigma Aldrich 1
- Resazurin, Sigma Aldrich
- Acid Red 1, Centre for Organic Chemistry Ltd.
- 5% $NaHCO_3$, pH = 8.35

5.1.2 Devices

- UV LED Reactor
- USB-650 Red Tide Spectrometer
- Analytic Scale Scaltec SPB 32
- Dimatix Materials Printer DMP 2800
- Bruker Detak XT Profilometer
- Double beam UV-VIS Spectrophotometer Spektronic Unicam Helios α
- Digital Multimeter UT70B
- Maya 2000 Pro, High Sensitivity Spectrometer

5.1.3 Software

- Microsoft Word 2007
- Microsoft Excel 2007
- SpectraSuite, Ocean Optics
- Vision V3.50
- Vision 64
- Origin 8
- Adobe Photoshop
- UT 71AB Multimeter Software
- Ocean View, 1.5.0

5.2 Sample preparation

5.2.1 Sol preparation and printing – E5

The titania sol was prepared by adding 15.3 ml of xylene to 2.5 ml of Triton X (nonionic surfactant). The mixture was blended on a magnetic stirrer with addition of 0.06 ml of demineralised water. After 10 minutes of stirring, the solution was transparent and 1.0 ml of TTIP could be added, changing the color of the solution to yellow. [22]

The microscopic glass plates, on which the sol was deposited were treated in boiling 9 M sulphuric acid for 1 hour to remove the surface sodium ions which could migrate into the titania layer and then influence the crystallization and all titania's properties. After that, the glass was placed in the mixture of Triton X and propan-2-ol and then dried.

The substrate size on which the titania sol was deposited was 5 × 5 cm (E5-A) and 2.5 × 7.5 cm (E5-B). The deposition proceeded via Dimatix Materials Printer. The substrate sample was heated to 40 °C and all 16 nozzles were used while printing. The drop spacing was 20 μm and the printing angle was set to 45°. In the case of 5 × 5 cm glass plates, only one layer of titania was printed, while in the case of 2.5 × 7.5 glass plates, 1-4 TiO_2 layers were prepared. After printing the titania layer, the substrate was calcined for 4 hours at 450 °C.

5.2.2 Titania substrate pretreatment

Before every dye deposition, the substrate was pretreated with 5% $NaHCO_3$ (pH= 8.5) to keep the dye-titania composition alkaline before printing. Some of the tested dyes are acid-base indicators and they can change the color under acidic conditions even before UV-irradiance.

After the alkaline pretreatment, the samples were washed with distilled water and dried.

5.2.3 Indicator ink preparation and printing

The chemical composition of the solution of indicator ink was quite simple and samples differed only a little from each other – depending on which solvent they were soluble in. 2,6-dichloroindophenol and Solvent Violet 11 were soluble in organic solvents (isopropanol), while the rest of the dyes were only water-soluble.

Finally, I choose to work with 7 dyes in total, 2 of them were soluble in isopropanol and 5 in water. This was the only difference in their composition.

Table 1 *Composition of prepared indicator inks.*

	DCIP	**AR1**	**DB10**	**MB**	**RB**	**Res**	**SV11**
10% PVP in IPA	3 ml	3 ml	3 ml	3 ml	3 ml	3 ml	3 ml
PrEt	3 ml	3 ml	3 ml	3 ml	3 ml	3 ml	3 ml
IPA	3 ml	–	–	–	–	–	3 ml
H_2O	–	3 ml	3 ml	3 ml	3 ml	3 ml	–
GLY	0.1 ml	0.1 ml	0.1 ml	0.1 ml	0.1 ml	0.1 ml	0.1 ml
Dye mass	30 mg	30 mg	30 mg	30 mg	30 mg	30 mg	30 mg

The prepared dye solution was then filtered (45μm syringe), used for "drop experiments" or placed into the printer head for further deposition on the pretreated substrate for "printed experiments".

5.2.4 Photocatalytic testing

The LED reactor was used for the photocatalytic activity evaluation. The system was composed of 2 LED diodes – the first one was white and the second one emitted light at 340 nm. Emission spectrum of UV LED was measured and normalized (Figure 23).

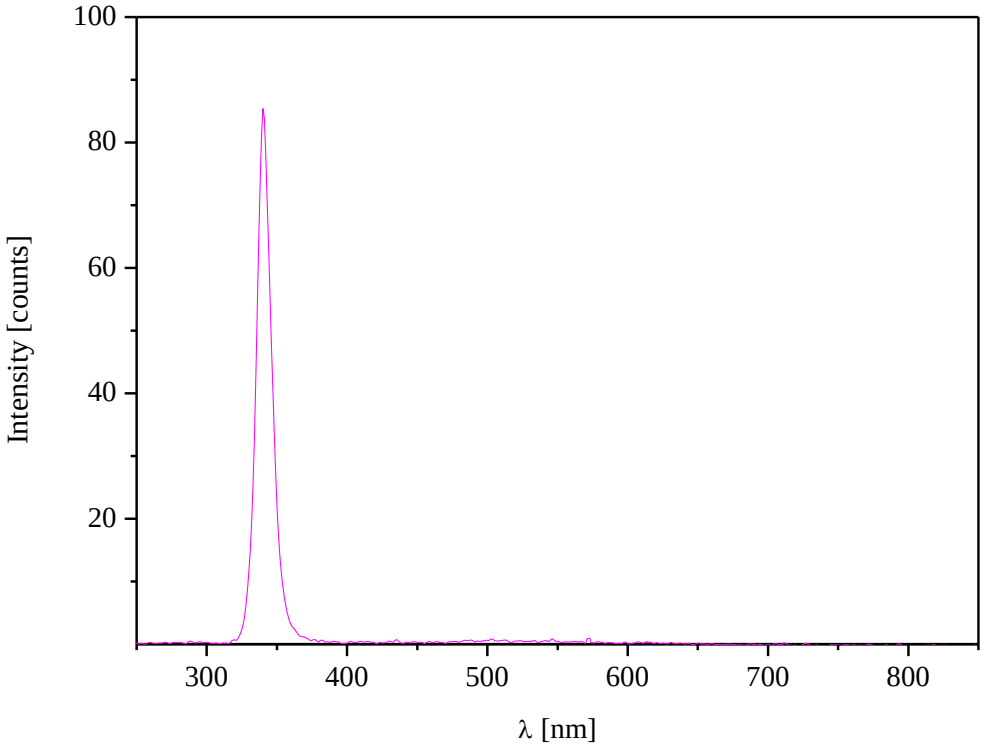

Figure 23 *UV LED emission spectra with the maximum at 340 nm.*

The original reactor set up was changed a bit because of the apparatus optimization. While the original LED diode's emission was at 650 nm, I wanted to focus on the research of dyes with various color, not only in blue region and that is why I decided to replace the "blue" diode with the white one. The UV LED was kept under the current of 25 mA during the measuring.

The sample was placed in the middle of the reactor plate, so both diodes could fully illuminate it. The light went through the sample and the colimator optics which was connected to spectrophotometer. The data from the spectrophotometer were transformed to the computer via USB cabel. Before the measuring, the reference spectrum was taken (glass + Titania) as a baseline (100% transmittance) and then the "dark spectrum" was measured. After that, the spectra from the sample (glass + titania + indicator ink) were measured and the absorbance maximum was calculated.

The data were processed via Ocean SpectraSuite Programme. The absorbance detection was set to 20 nm wavelength region. The particular wavelength region was choosen according to the position of the peak of absorbance. The obtained values were then averaged for a set time of 15 min.

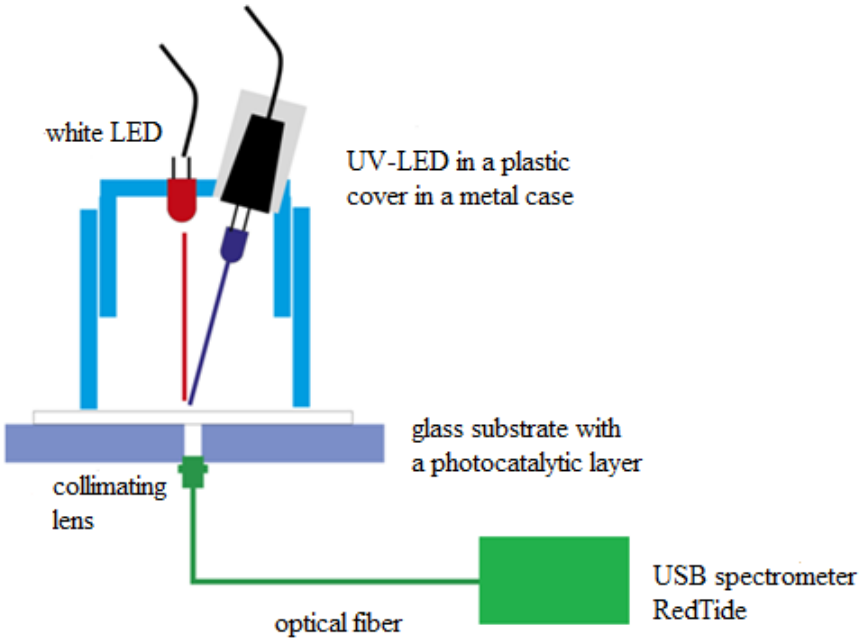

Figure 24 *The reactor system for photocatalytic activity measurement – with white LED and UV LED (340 nm).*

In the last part of my thesis I focused on another method that can be used for photocatalytic evaluation. I used the UV LED reactor I was working with before and substituted the detection part (spectrophotometer, optical fiber and reflector sight) with photodiode connected to a multimeter. Red filter was used for reduction of the wavelength light region. In comparison to the previous type of measuring, where the average absorbance was calculated according to the absorbance values from the selected 20 nm wavelength region, the results of this measuring were obtained by the response to the light characterizing the "red region" (caused by the red filter).

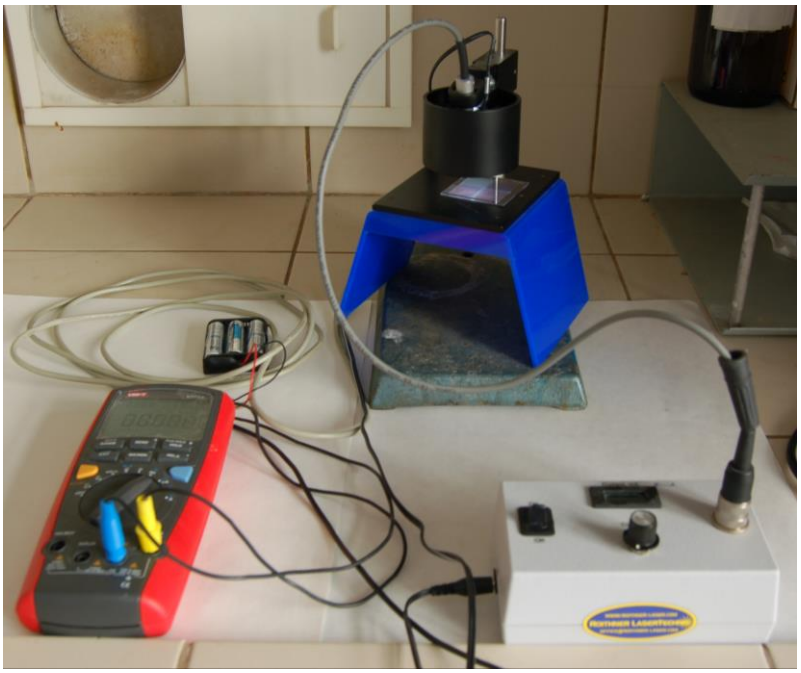

Figure 25 *Optimized apparatus for photocatalytic activity measurement – a photodiode based light-to-frequency convertor connected to a multimeter.*

5.2.5 Photocatalytic activity evaluation

When it came to the evaluation of photocatalytic activity data from "printed experiments", I decided to use only the most suitable indicator inks for PCA: Methylene Blue and Resazurin. The drop experiments were used for the discussion of the selection of further tested dyes. In my opinion, the non-selected dyes were not suitable for photocatalytic activity evaluation.

Because the dyes used for the experiments had different degradation characteristics, I decided to evaluate just the initial rate – the rate until the absorbance drops to 90% of the initial value. For this analysis I used following equation, considering the BLB law validity.

$$r_i = \frac{dc_i}{dt} \tag{38}$$

6 RESULTS AND DISCUSSION

6.1 Drop experiments

The initial phase of my research consisted of so called "drop experiments" which helped to evaluate the speed of degradation of tested dyes. The purpose of this simple experiment was to choose suitable samples to be printed on Dimatix Materials Printer and tested further.

With the help of the dropper, the drop was applied on the glass substrate with pre-printed TiO_2 photocatalytic layer E5-A. The size of the drop was not limited by any special requirements. The drop deposition was followed by approximately 20 minutes long waiting for the drop to dry. The experiment began by acting of UVA-light on the sample for 15 min. The decrease of the absorbance was detected in the highest wavelength region (20 nm). The experiment was performed 5 times with each of the dye solutions.

There were 7 dyes choosen for the testing, 3 of them (DCIP, RES, MB) are well known indicator inks often discussed in the scientific literature, while the remaining 4 ones are mostly textile dyes often used in industry.

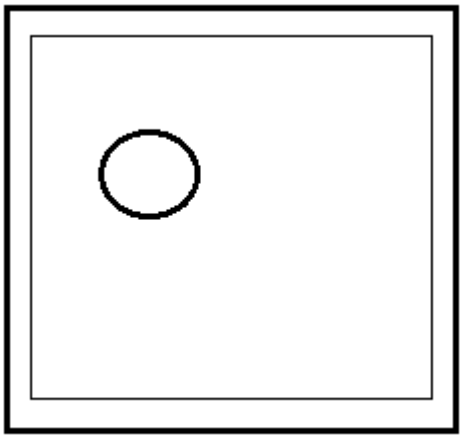

Figure 26 *Scheme of the drop deposited on the glass substrate and titania photocatalytic layer (grey square).*

6.1.1 Evaluation of the drop experiments

In the case of all 5 experiments with 2,6-dichoroindophenol, the increase of absorbance is seen at the beginning of the experiment. This was probably caused by the fact that the tested samples were not dry enough, so the absorbance kept growing for the first minute. The further degradation of DCIP ink was very fast, especially the first 5 minutes. Although DCIP is known for its fast degradation, it is facing its big disadvantage – instability during normal conditions, as it changes colour very fast even in daylight.

The results for Direct Blue 10, Reactive Blue and Methylene Blue were similar – since they differed significantly, so it was difficult to decide whether the ink yields to degradation or not. The reason for this difference could be the different size of the deposited drops. The drops with smaller size (detected by the smaller absorbance value) degraded faster than the bigger ones. This is caused by the fact that smaller drop has smaller barrier for the light to be adsorbed on active sites of titania. Moreover, in the case of the smaller drop, there is lower ratio of the dye that is supposed to be decomposed to regenerated electrons and holes. However, as mentioned before, I considered this method to be a simple way of

evaluation, whether the dye is degradable or not and consequently, the size of the drop was not essentially important.

Degradation behaviour of Resazurin was quite unexpected, considering that this dye is very often used in self-cleaning evaluation. Almost no degradation occurred.

In the case of Acid Red 1 and Solvent Violet 11 there was almost no degradation observed either.

- 2,6-dichloroindophenol

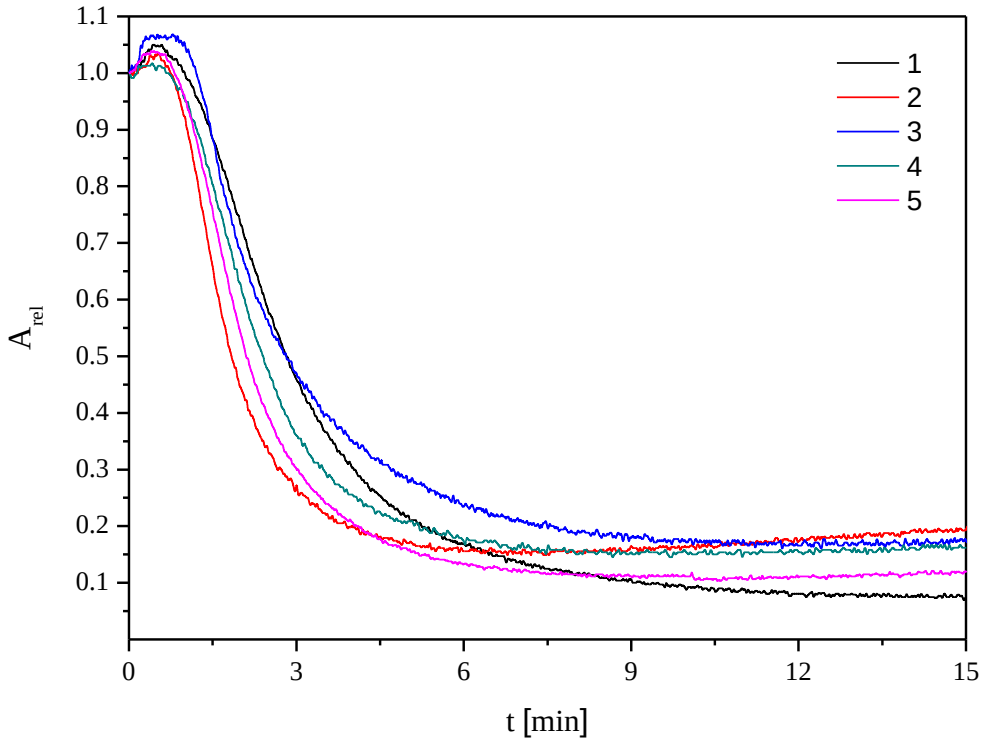

Figure 27 *Absorbance on time dependence for the wavelength of 630-650 nm.*

- Direct Blue 10

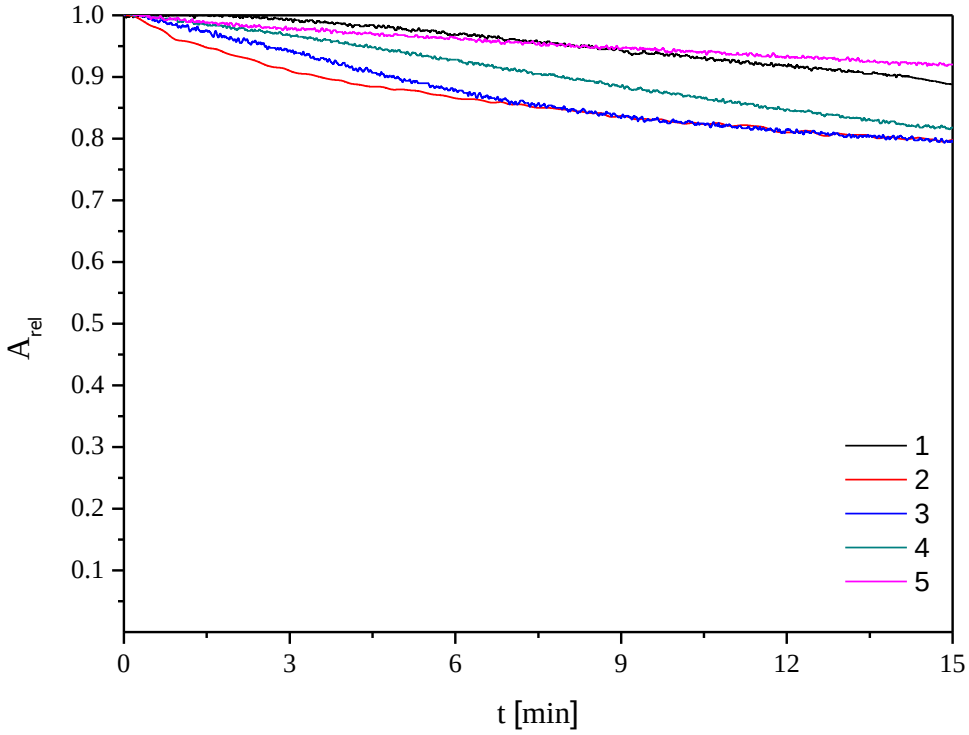

Figure 28 *Absorbance on time dependence for the wavelength of 580-600 nm.*

- Methylene Blue

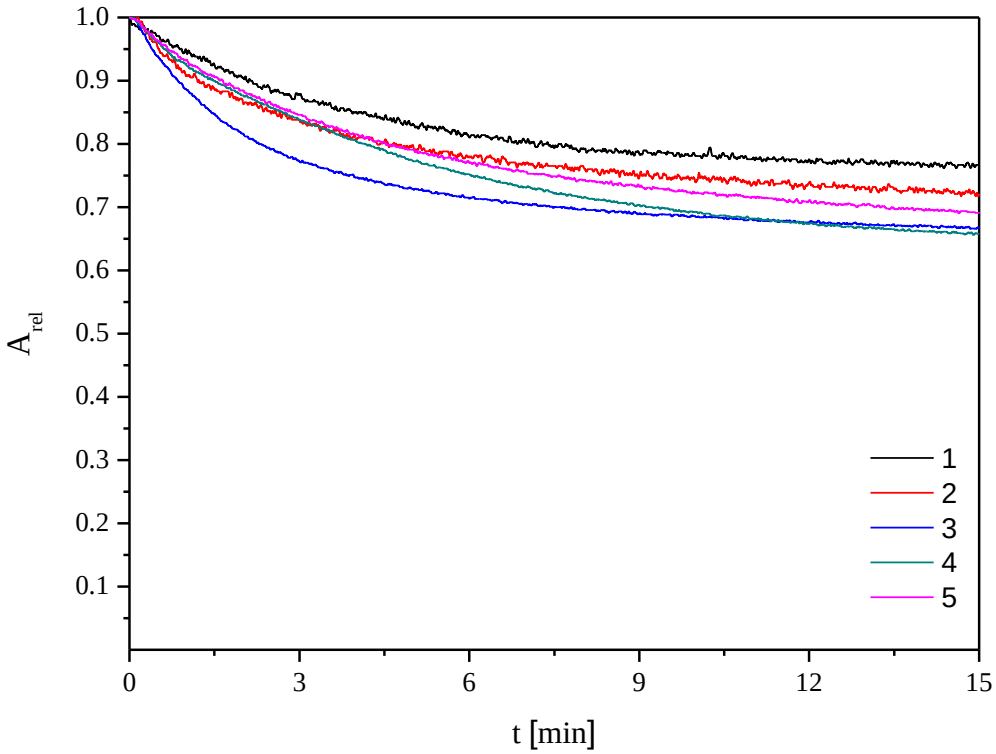

Figure 29 *Absorbance on time dependence for the wavelength of 570-590 nm.*

- Reactive Blue

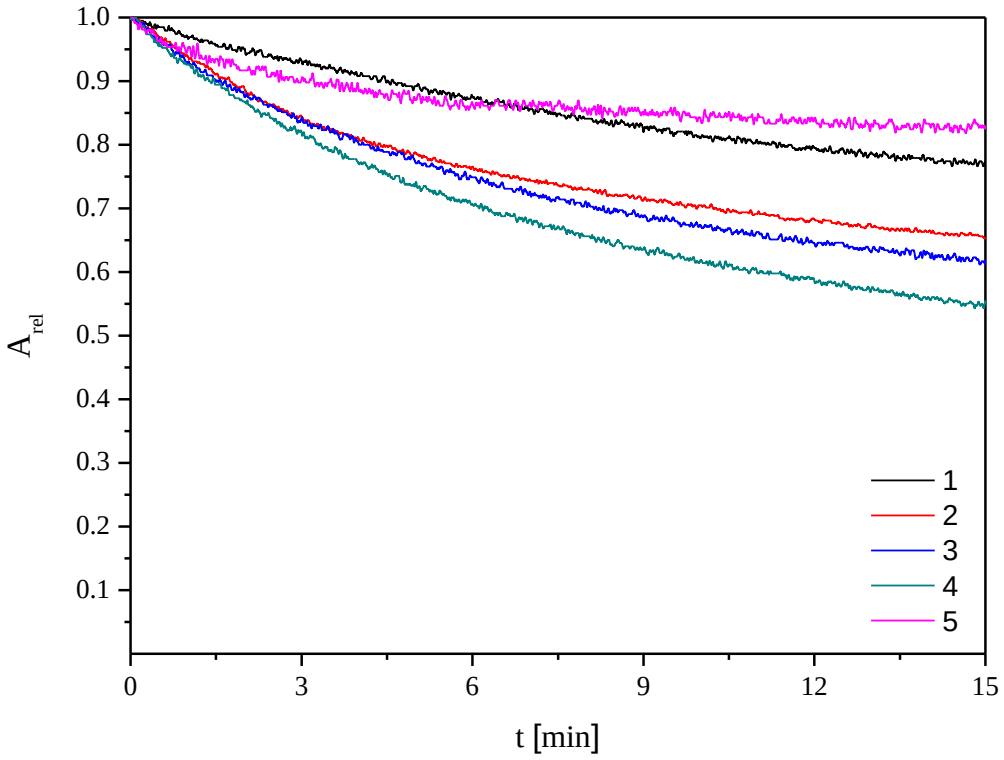

Figure 30 *Absorbance on time dependence for the wavelength of 600-620 nm.*

- Acid Red 1

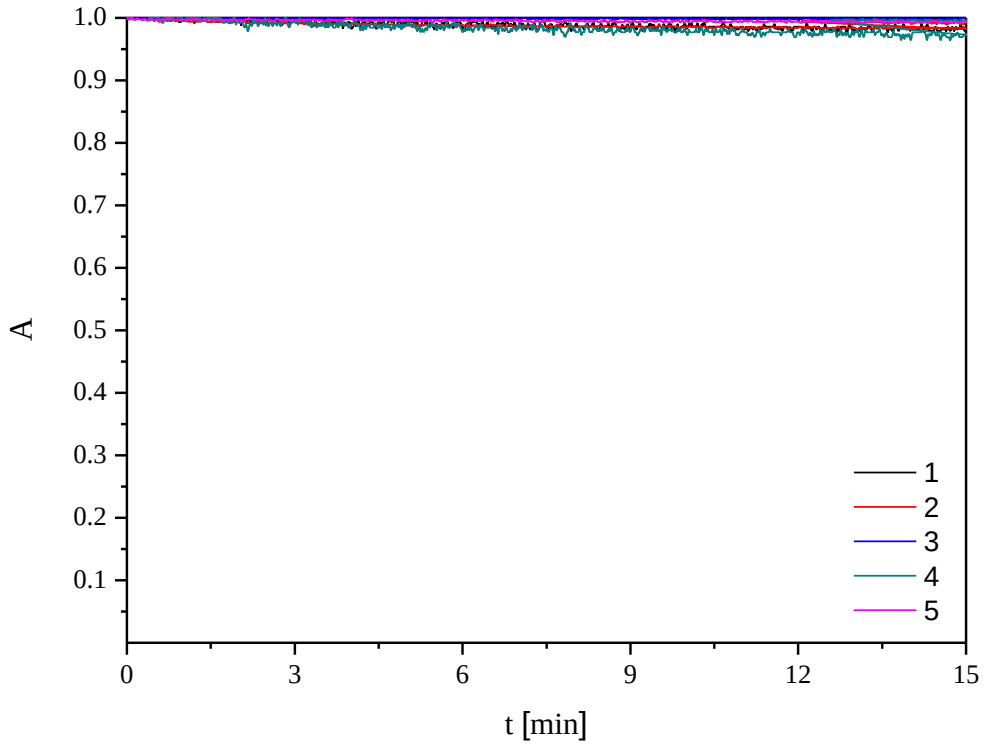

Figure 31 *Absorbance on time dependence for the wavelength of 540-560 nm.*

- Resazurin

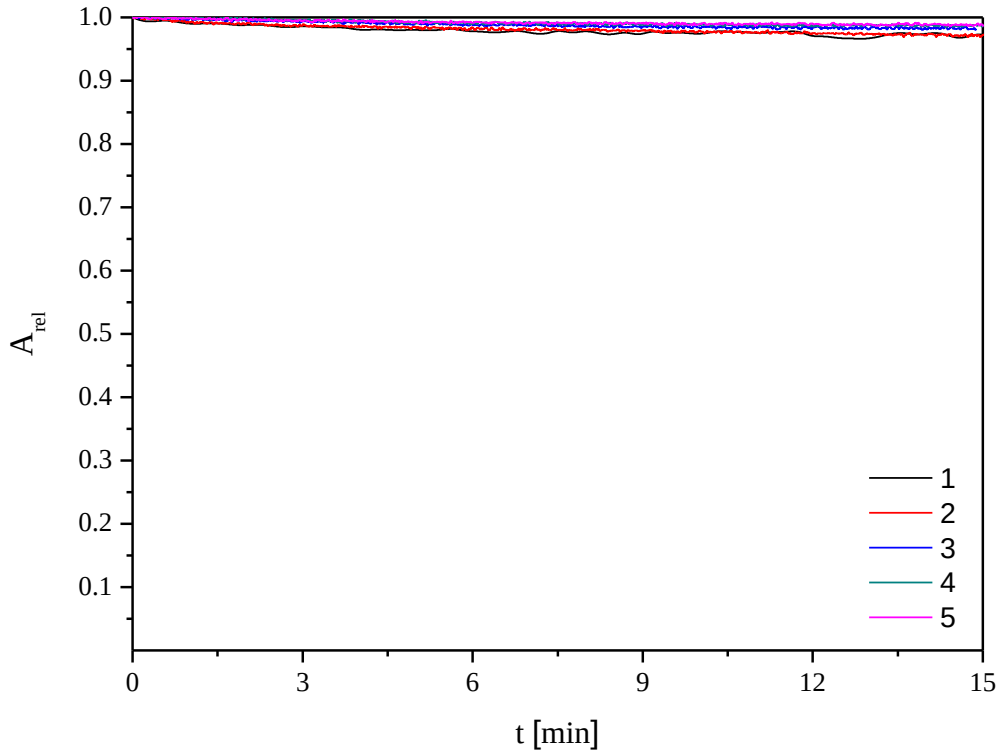

Figure 32 *Absorbance on time dependence for the wavelength of 565-585 nm.*

- Solvent Violett 11

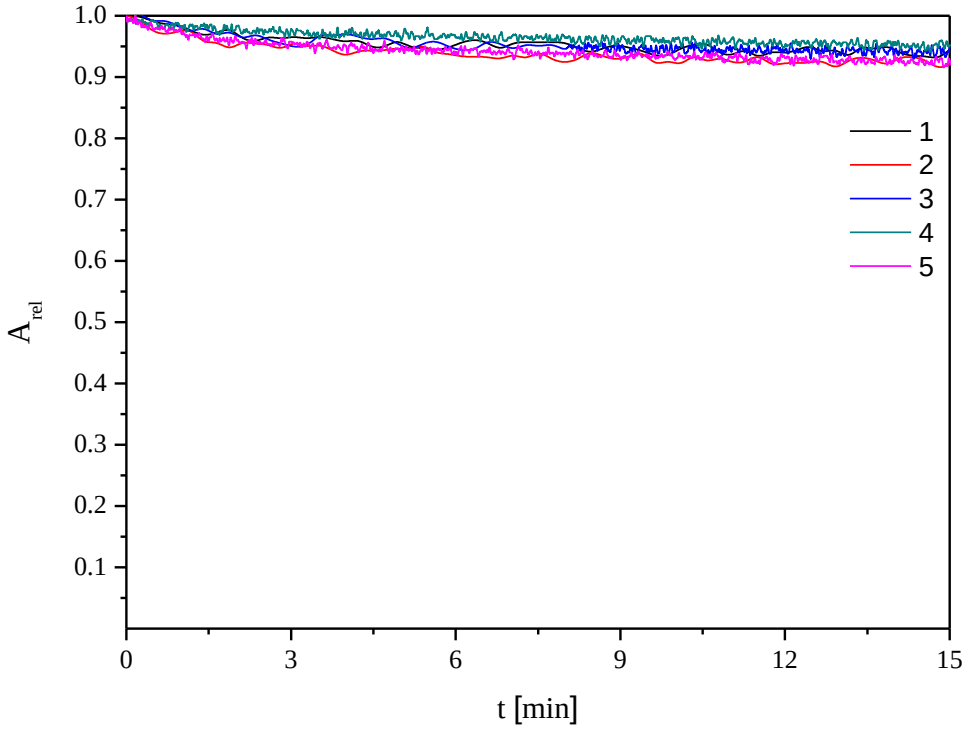

Figure 33 *Absorbance on time dependence for the wavelength of 560-580 nm.*

6.2 The stability tests

The stability tests of dye solutions were performed as well. The dye was dissolved either in isopropanol or in water, and placed in the vial. The sample was left in the laboratory. During several weeks, the stability tests were carried out by measuring of the absorbance spectrum.

According to the stability tests, except for DCIP, all the samples appeared to be stable under the laboratory conditions.

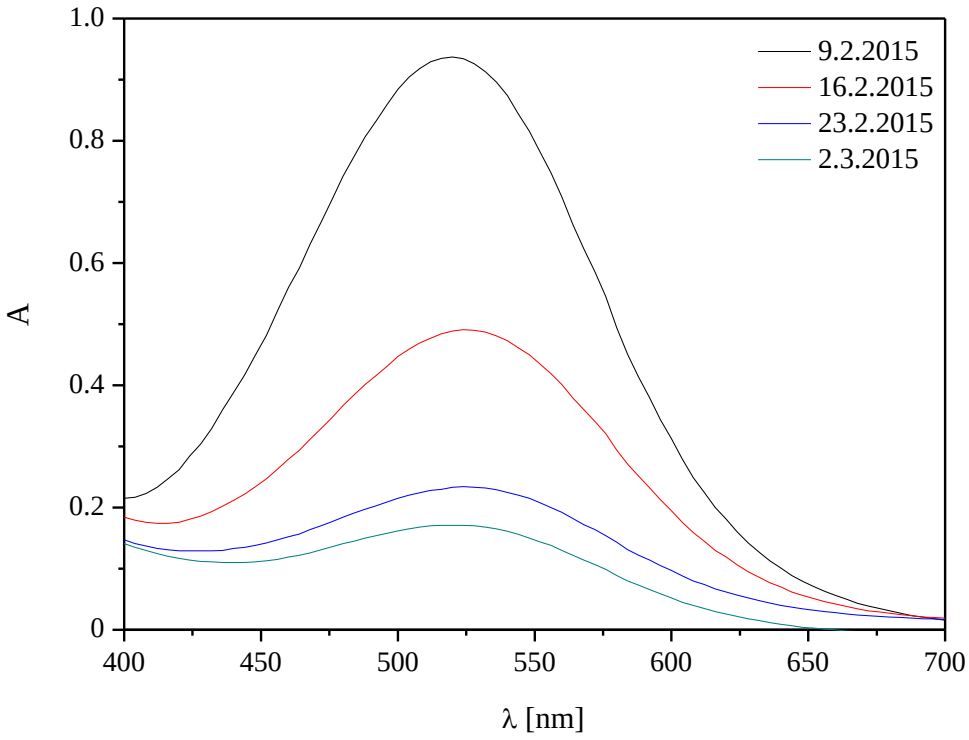

Figure 34 *Stability test for DCIP.*

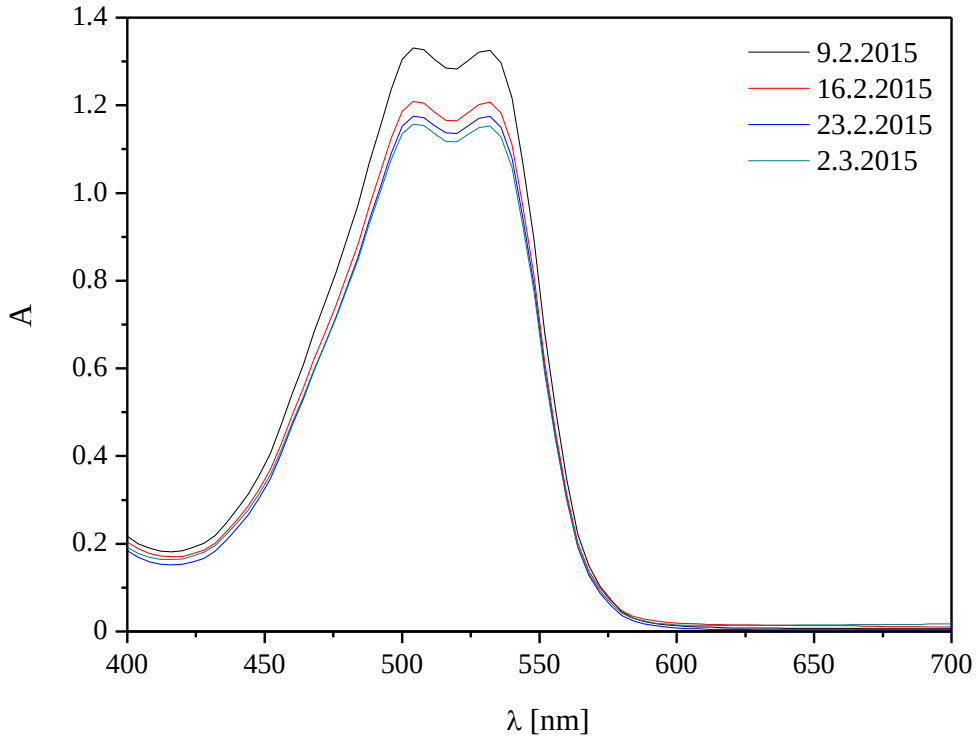

Figure 35 *Stability test for AR1.*

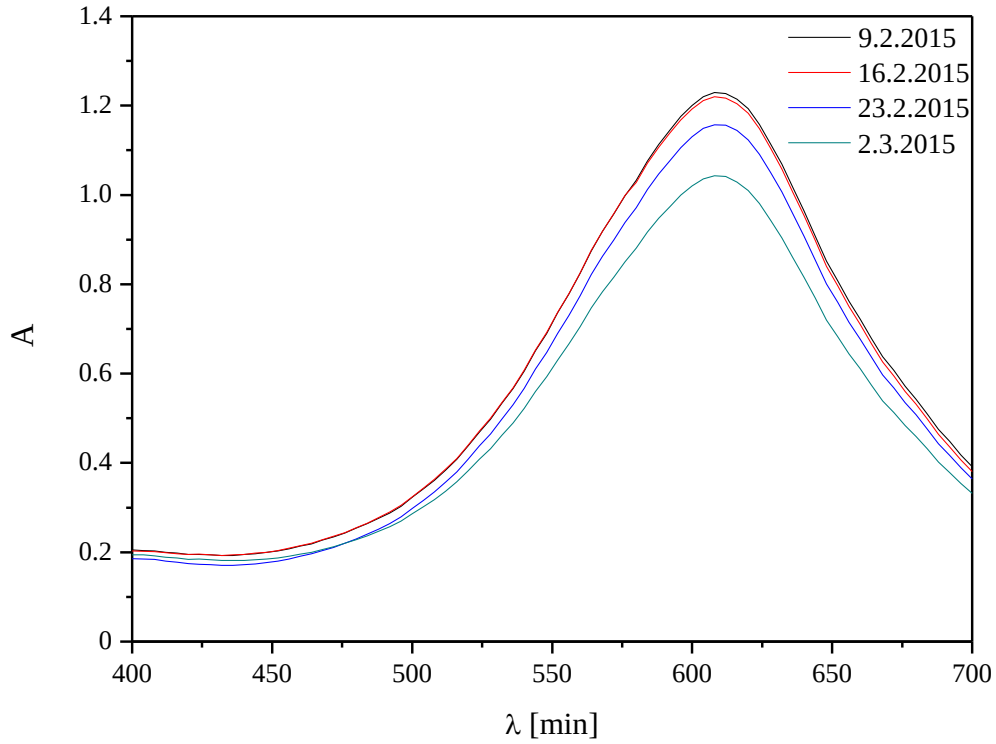

Figure 36 *Stability test for DB10.*

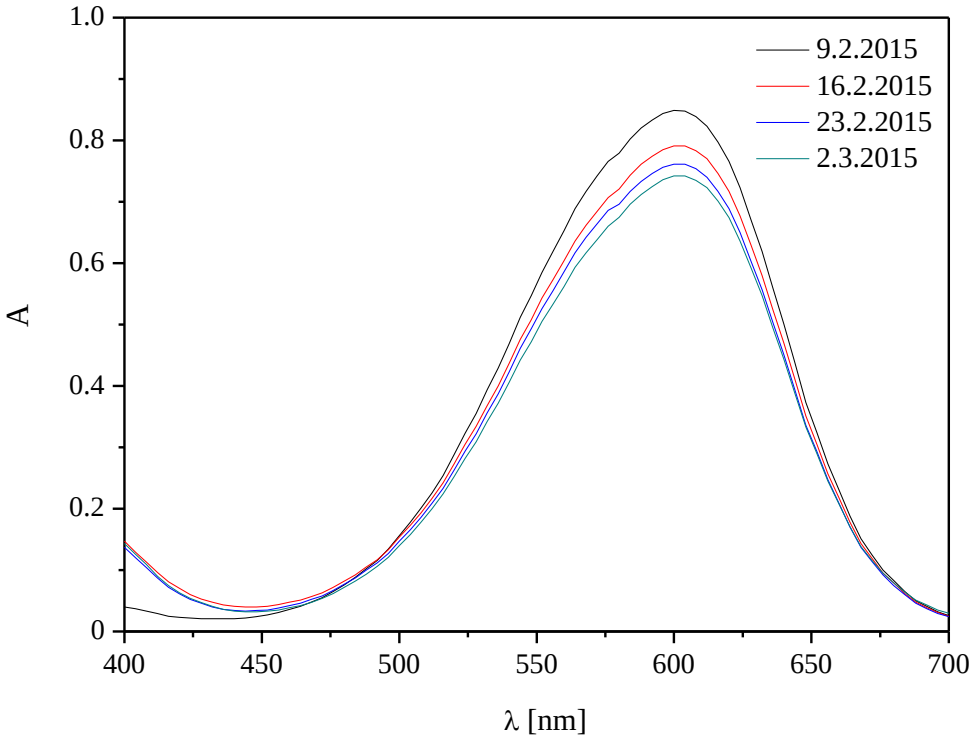

Figure 37 *Stability test for MM.*

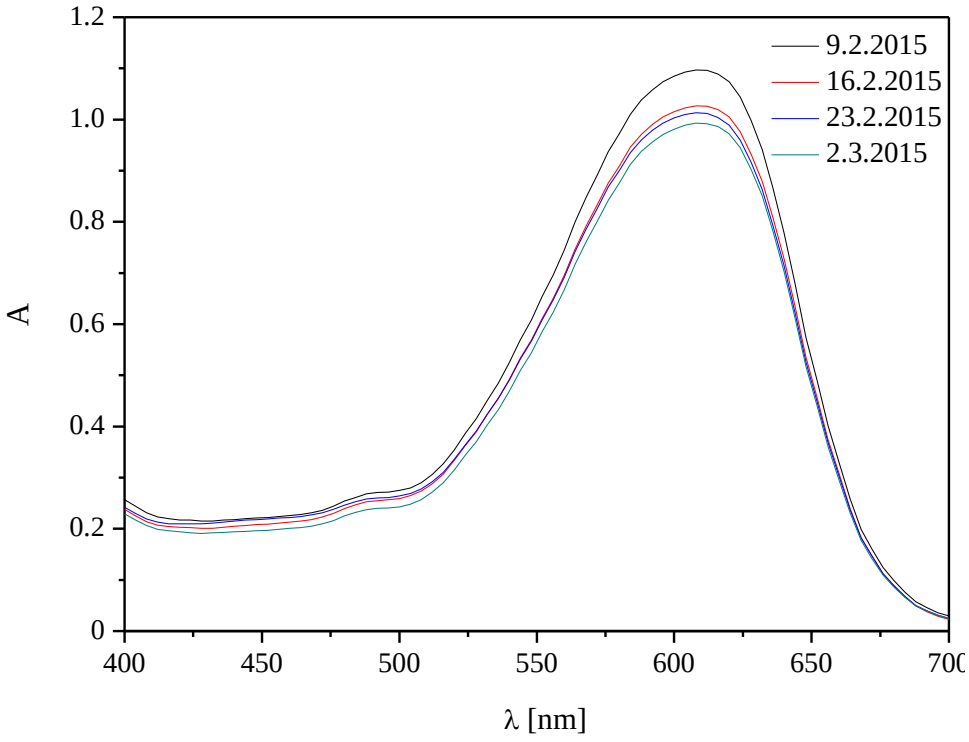

Figure 38 *Stability test for RB.*

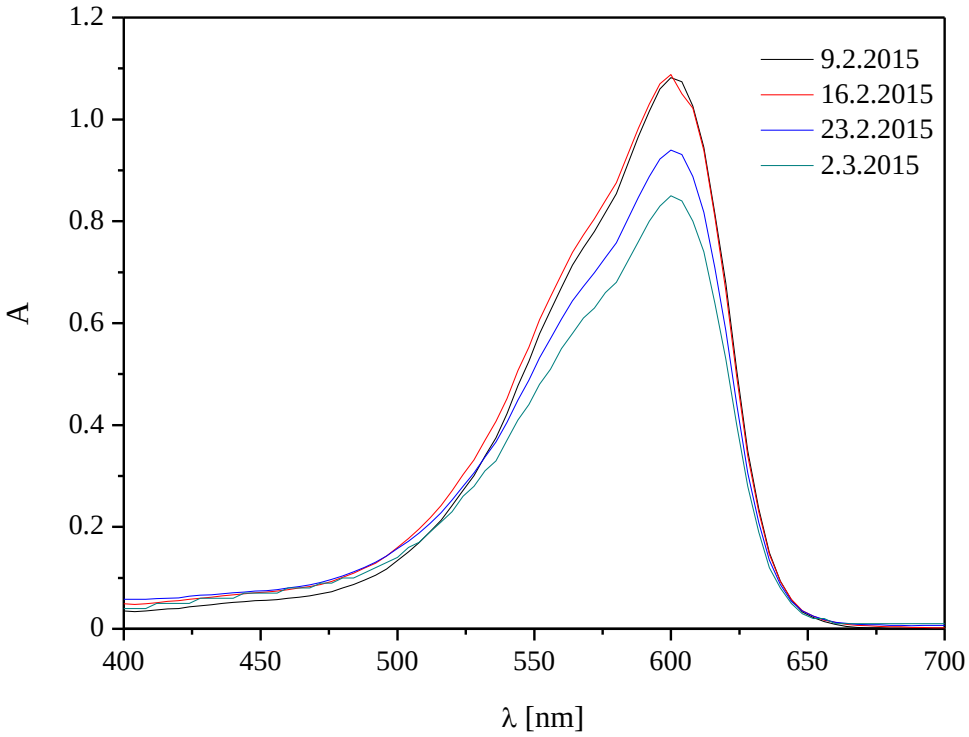

Figure 39 *Stability test for RES.*

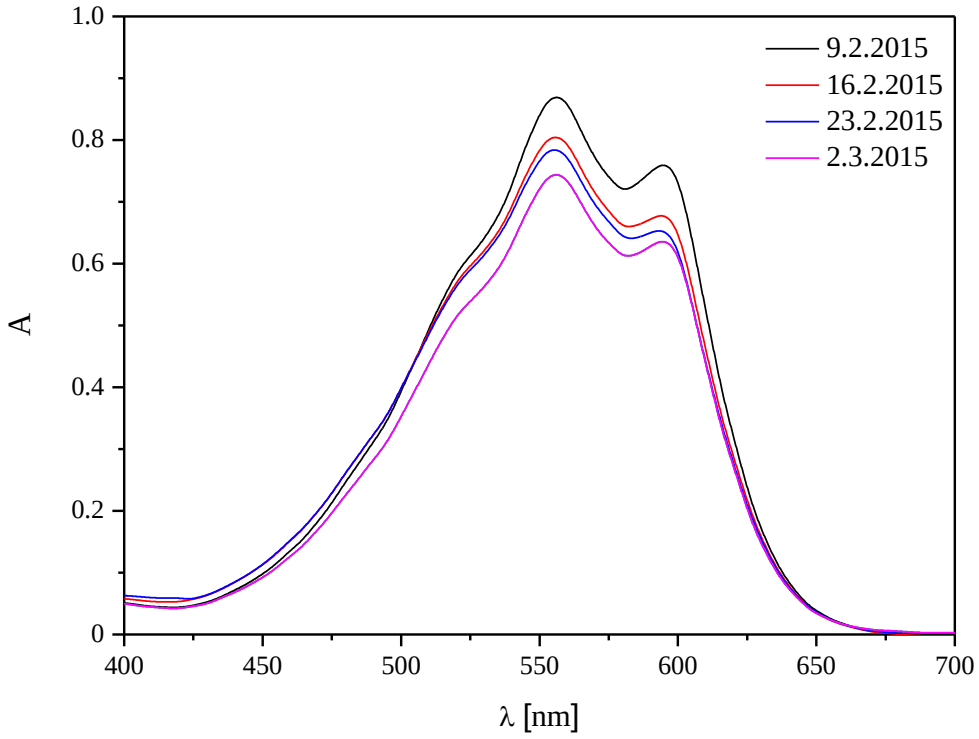

Figure 40 *Stability test for SV11.*

6.3 Printed layers experiments – E5-A

According to the results from previous experiments, dyes with the degradation rate that was high enough and with good stability test, were choosen to be printed on the Dimatix Materials Printer. The only exception was Resazurin, as almost no degradation was observed in the drop experiments of this substance. However, I decided to carry out printed experiments with Resazurin as well, to see if it would behave the same way in the experiment with printed layers.

A photolysis experiment was performed and the photodegaradation ability of the dye itself was tested without any catalyst's layer. This was done with the sample of 1 layer of indicator ink.

The glass substrate was 5 × 5 cm and the layers were deposited in the same way as in Figure 41: 1-3 layers of dye were printed on the substrate and the lower right corner was left as a reference (only titania layer was present).

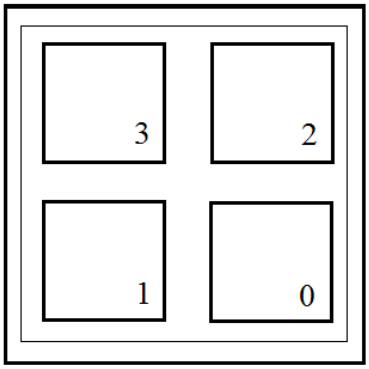

Figure 41 *The tested substrate, squares 0-4 represents the number of layers of printed dye on the titania photocatalytic layer (grey square)*

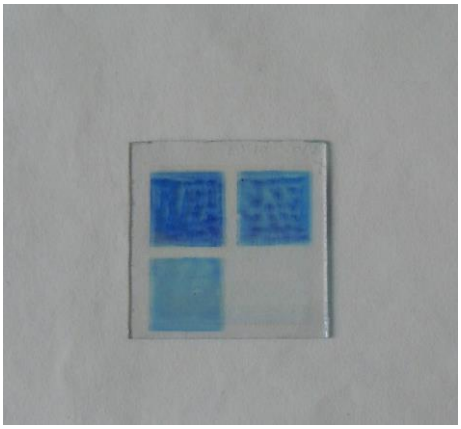

Figure 42 *E5-A sample with 1-3 layers of Methylene Blue printed.*

Following dyes were choosen for further printing testing: Direct Blue 10, Methylene Blue and Resazurin.

6.3.1 Direct Blue 10

Direct Blue 10 is highly water-soluble dye. The dye solution was prepared with 30 mg of DB10. However, the printed layer was too weak to be measured and it could not even be

tested in 3 layers. When I increased the number of layers, the surface became wrinkled which I did not consider to be suitable for accurate evaluation of photocatalytic activity.

The results implied the increase of the Direct Blue 10 content, which meant doubling of the value (60 mg of dye was used to prepare the solution). The printed sample structure was better than the previous one. The reason for this was definitely the higher dye content in the printed layer as well as the higher desk temperature (50 °C) and the printing angle (21°).

Table 2 *The printing conditions for original and concentrated Direct Blue 10 solution.*

	DB10	2 x DB10
Printing angle	6.8°	21°
Desk temperature	40 °C	50 °C
Drop spacing	30 µm	30 µm

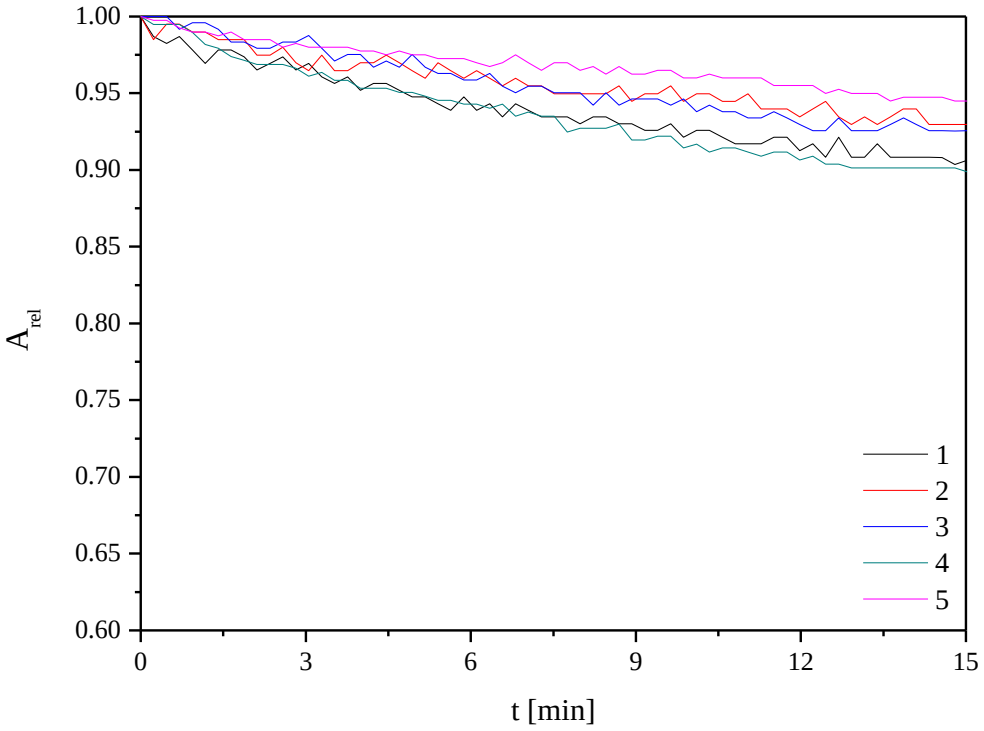

Figure 43 *Direct Blue 10 degradation – photolysis test: relative absorbance as a function of time in 600-620 nm.*

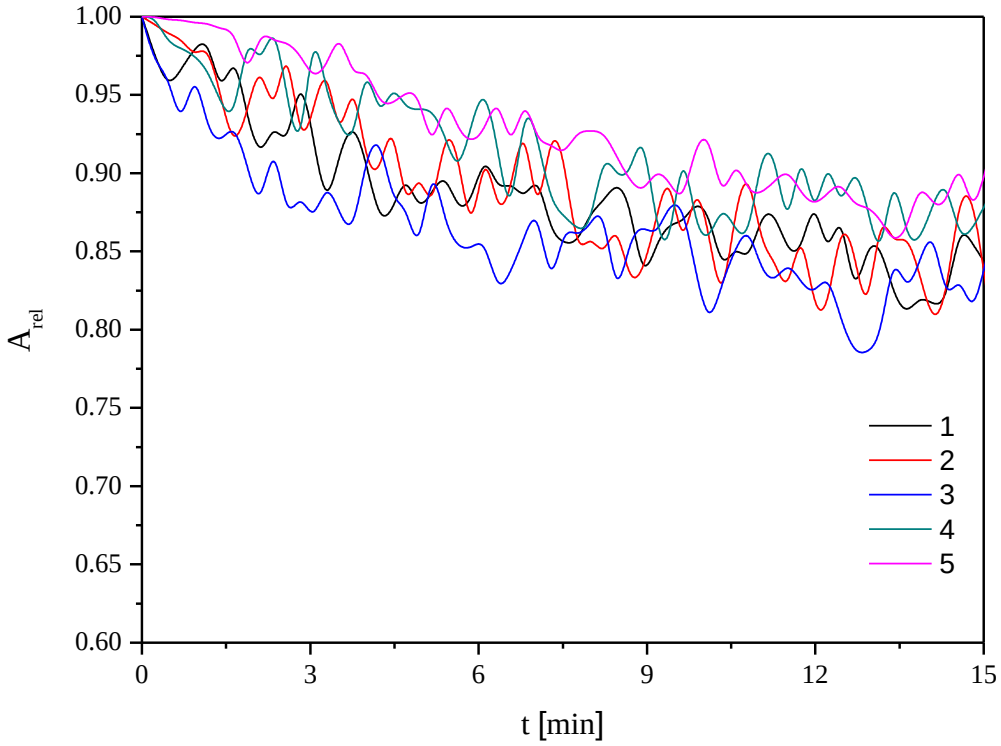

Figure 44 *Direct Blue 10 degradation – 1 layer: relative absorbance as a function of time in 600-620 nm.*

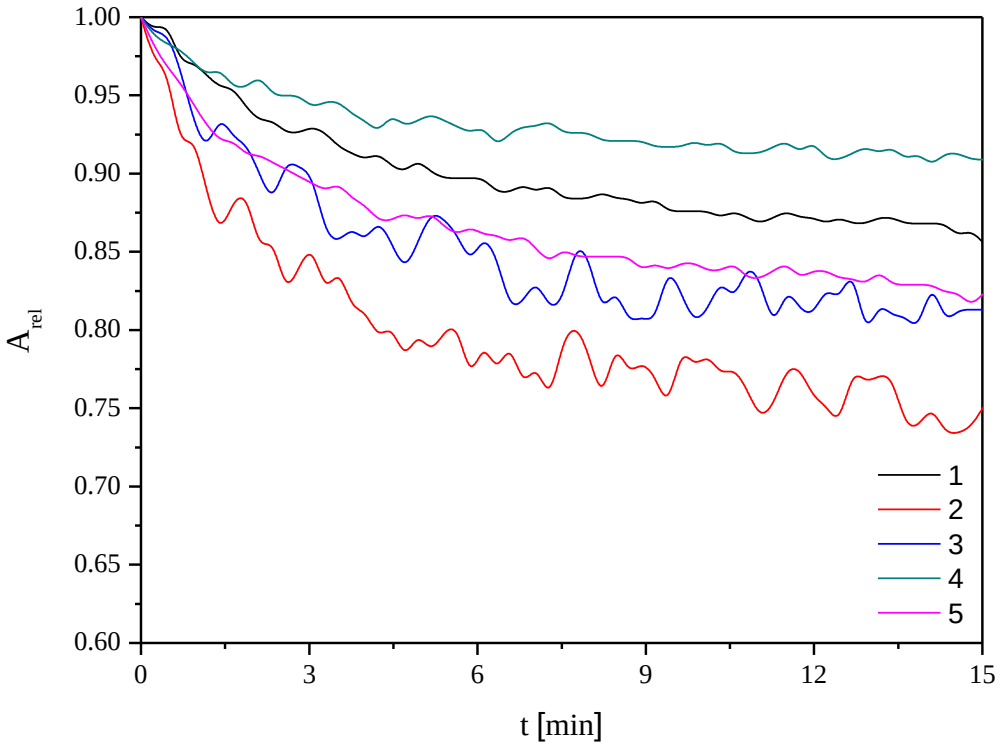

Figure 45 *Direct Blue 10 degradation – 2 layers: relative absorbance as a function of time in 600-620 nm.*

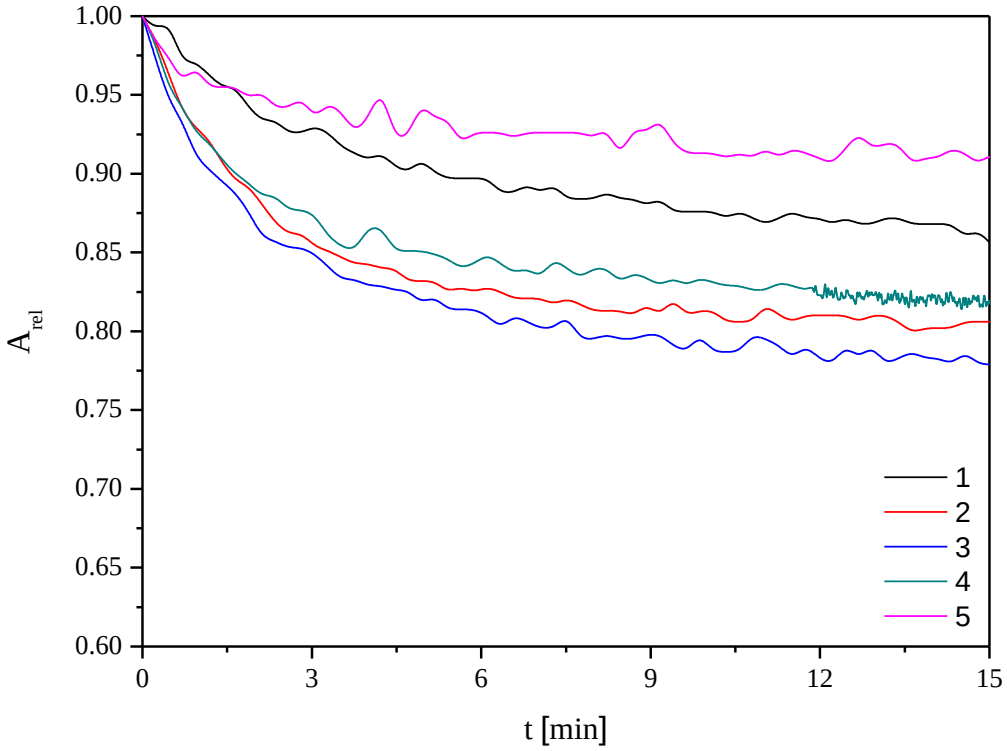

Figure 46 *Direct Blue 10 degradation – 3 layers: relative absorbance as a function of time in 600-620 nm.*

Direct Blue 10 results differed quite a lot so I decided not to evaluate any kinetic results.

6.3.2 Methylene Blue

Similarly to the case of Direct Blue 10 indicator ink, Methylene Blue is also highly soluble in water. I faced the same problems while printing the sample – the printed layers were too weak to be measured and even the increased number of layers did not help because of inappropriate structure.

As a result I decided to double the dye content in the solution. The printing conditions stayed the same as for Direct Blue 10.

Table 3 *The printing conditions for original and concentrated Methylene Blue solution.*

	MB	2 x MB
Printing angle	6.8°	21°
Desk temperature	40 °C	50 °C
Drop spacing	30 µm	30 µm

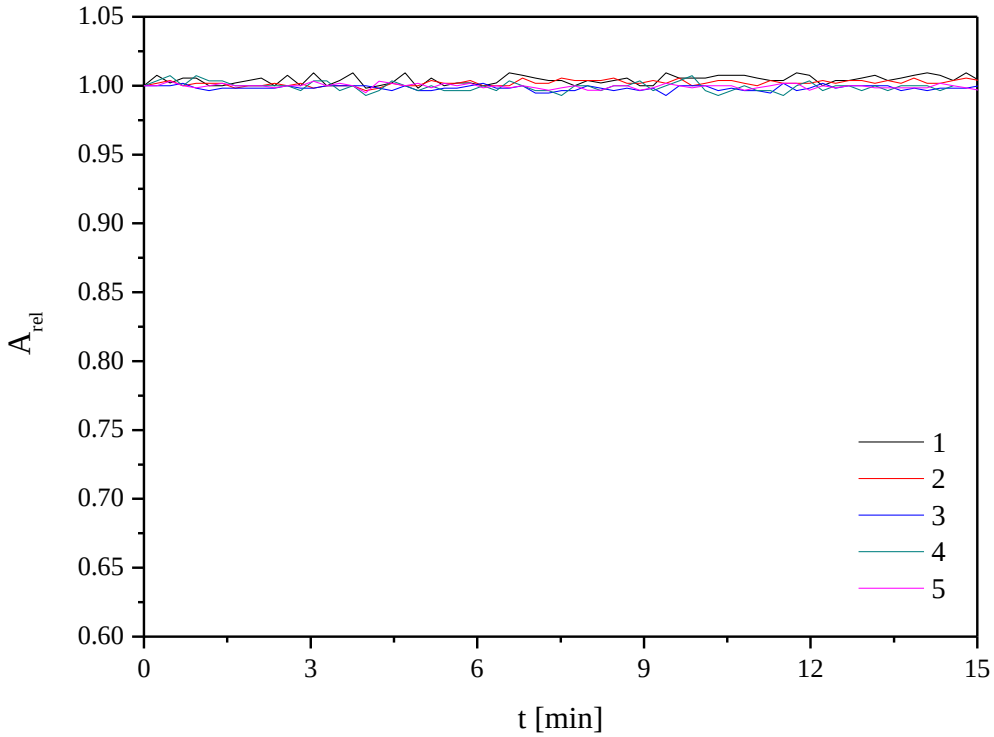

Figure 47 *Methylene Blue degradation – photolysis test: relative absorbance as a function of time in 580-600 nm.*

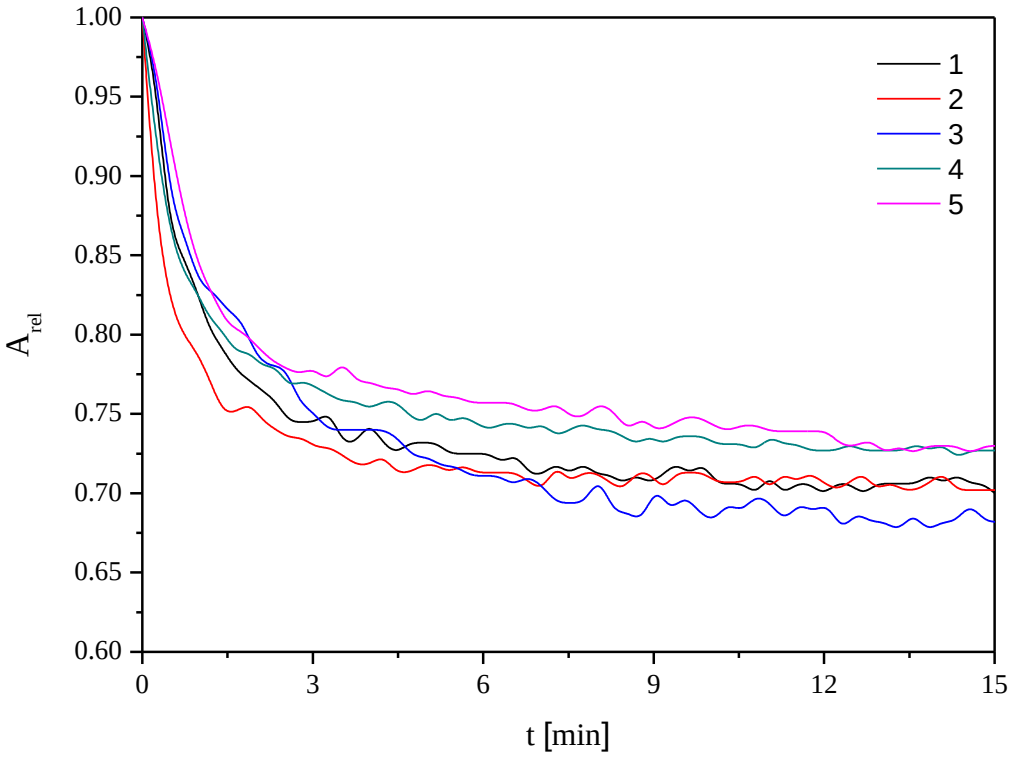

Figure 48 *Methylene Blue degradation – 1 layer, relative absorbance as a function of time, measured in 580-600 nm.*

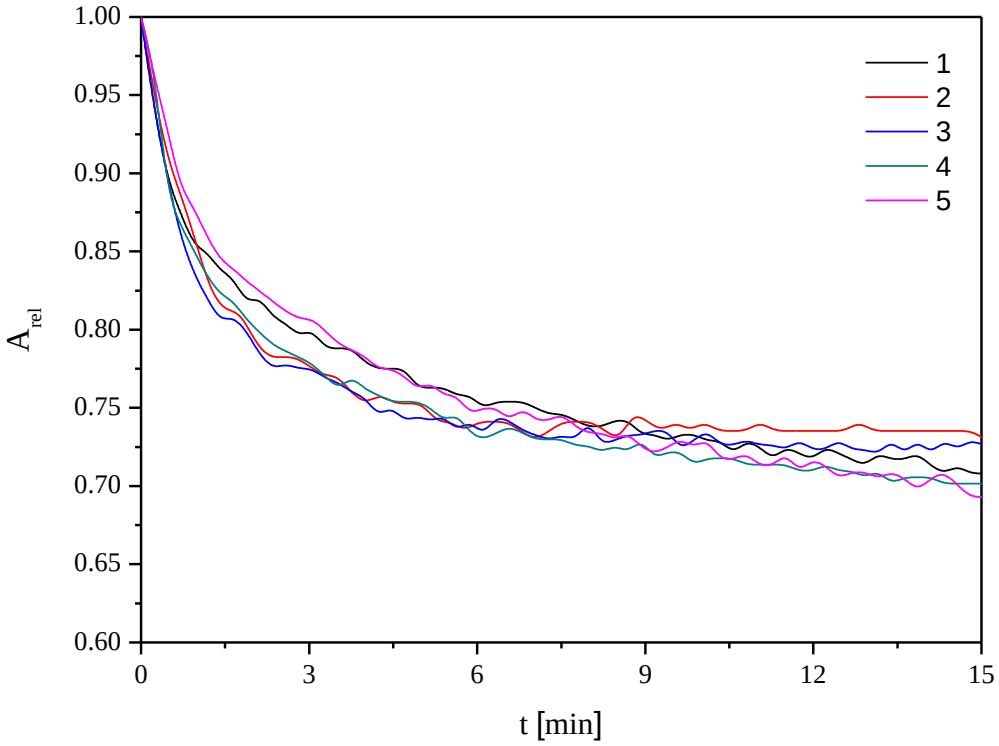

Figure 49 *Methylene Blue degradation – 2 layers, expressed by decrease relative absorbance as a function of time, measured in 580-600 nm.*

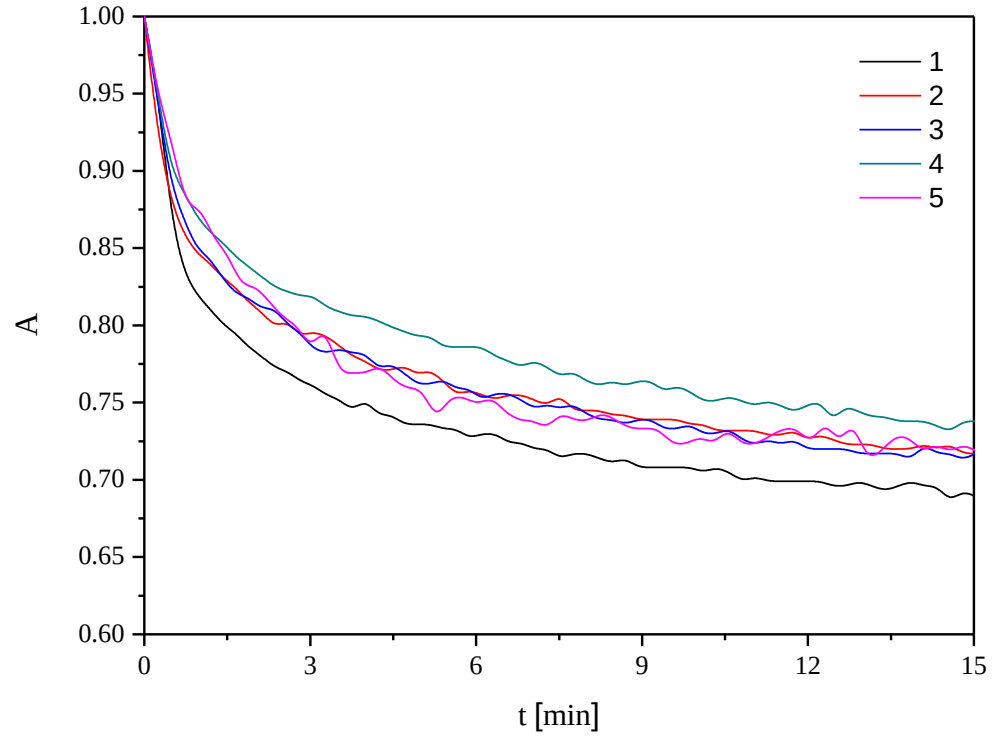

Figure 50 *Methylene Blue degradation – 3 layers, relative absorbance as a function of time, measured in 580-600 nm.*

I calculated the rate up to the point where the degradation reached 90% of the relative indicator ink absorbance value. The data were put into a column graph.

Table 4 *Average initial degradation rate for 1-3 MB layers .*

	1 layer	2 layers	3 layers
Rate [min^{-1}]	1.808 ± 0.047	1.897 ± 0.061	1.875 ± 0.038

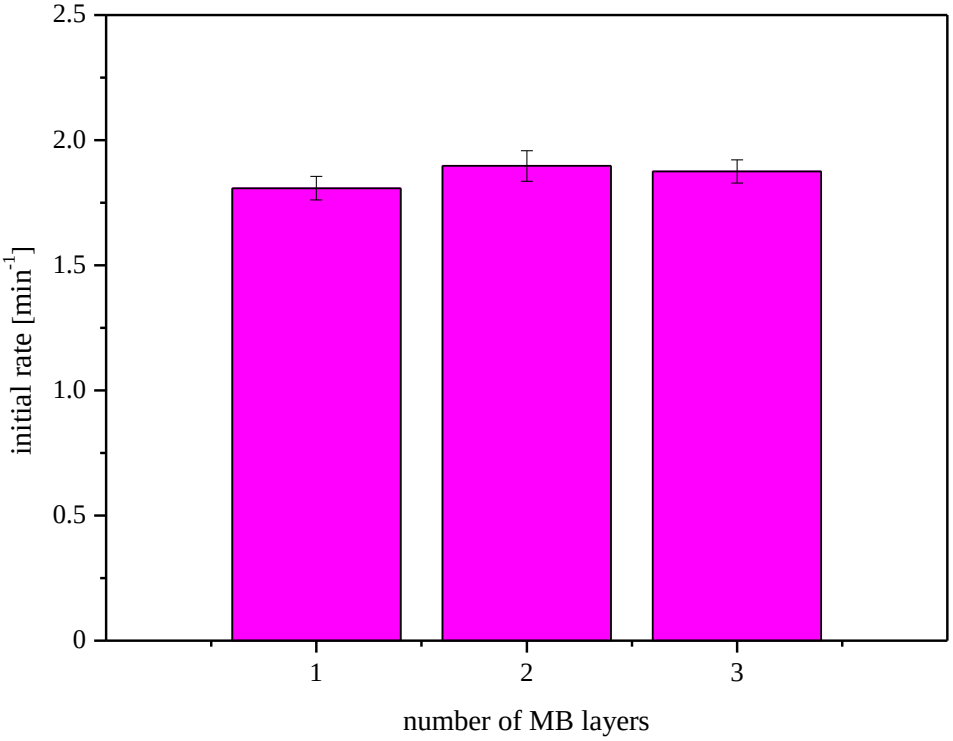

Figure 51 *Average initial rate dependance on numbers of MB layers.*

6.3.3 Resazurin

Resazurin was chosen for the printing experiment, although the drop experiments did not prove its degradation to be fast enough. On the other hand, it is a widely discussed indicator ink in the literature I have studied. Thus, I decided to apply the printing experiment on this dye as well, to see if the printed layer would influence the degradation rate.

The dye content of the layer seemed sufficient for the evaluation so the original preparation process was chosen.

Table 5 *The printing conditions for Resazurin solution.*

	Resazurin
Printing angle	6.8°
Desk temperature	40 °C
Drop spacing	30 μm

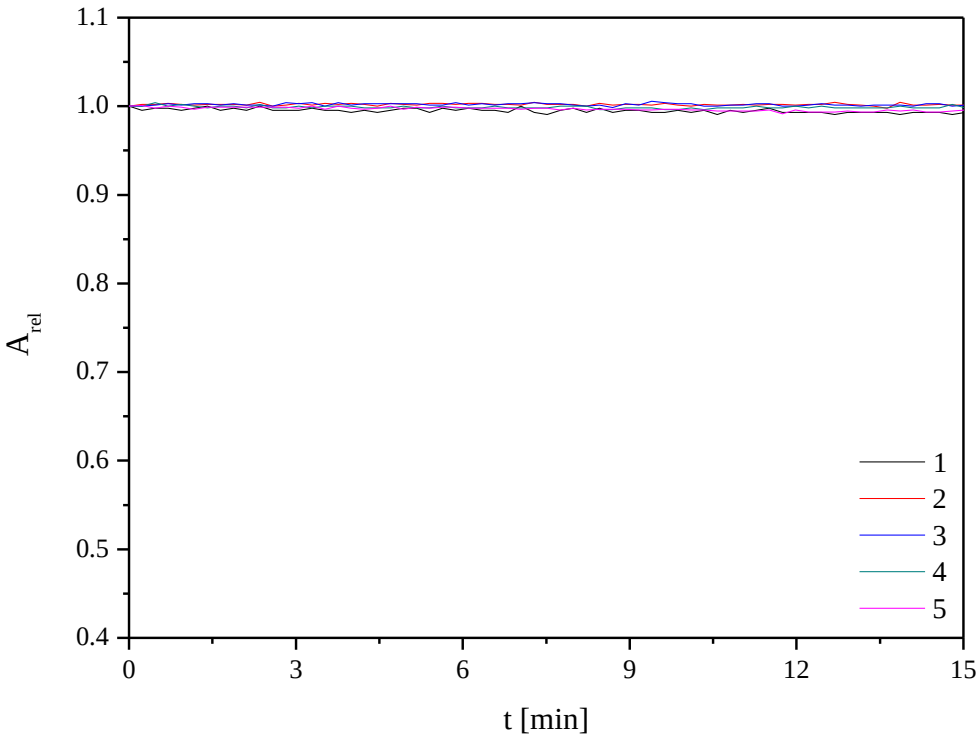

Figure 52 *Resazurin degradation – photolysis test: relative absorbance as a function of time in 565-585 nm.*

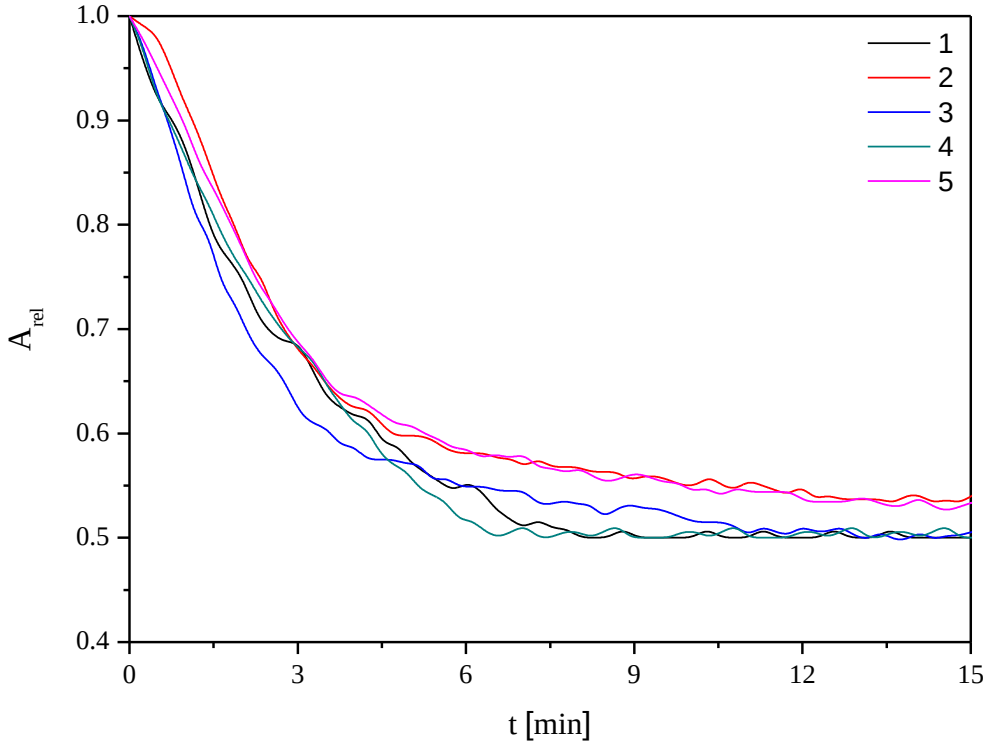

Figure 53 *Resazurin degradation – 1 layer: relative absorbance as a function of time in 565-585 nm.*

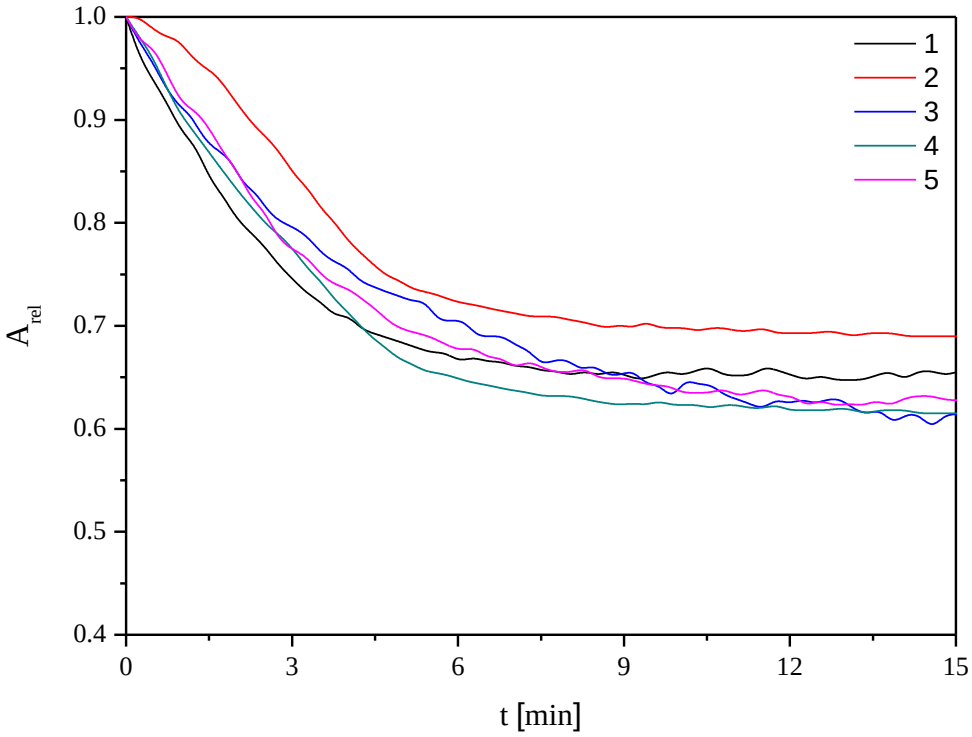

Figure 54 *Resazurin degradation – 2 layers: relative absorbance as a function of time in 565-585 nm.*

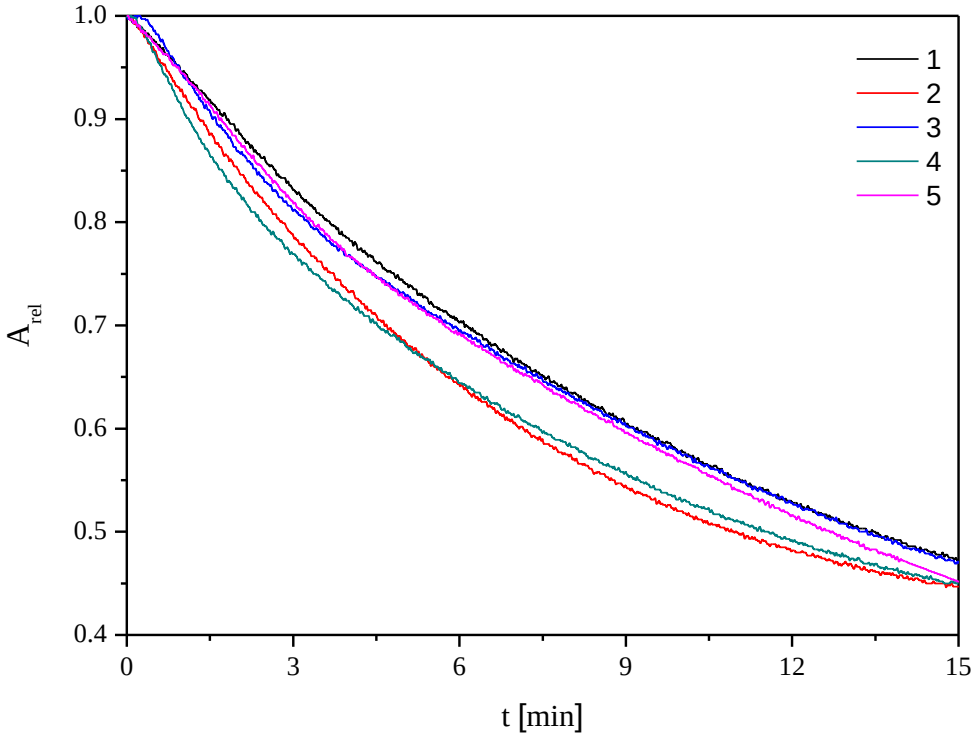

Figure 55 *Resazurin degradation – 3 layers: relative absorbance as a function of time in 565-585 nm.*

I evaluated the average initial rate from 5 obtained values for each layer experiment. The column graph was plotted as well.

Table 6 *Average initial rates for 1-3 RES layers on 1 titania layer.*

	1 layer	2 layers	3 layers
Rate [min^{-1}]	1.080 ± 0.238	0.822 ± 0.293	0.619 ± 0.130

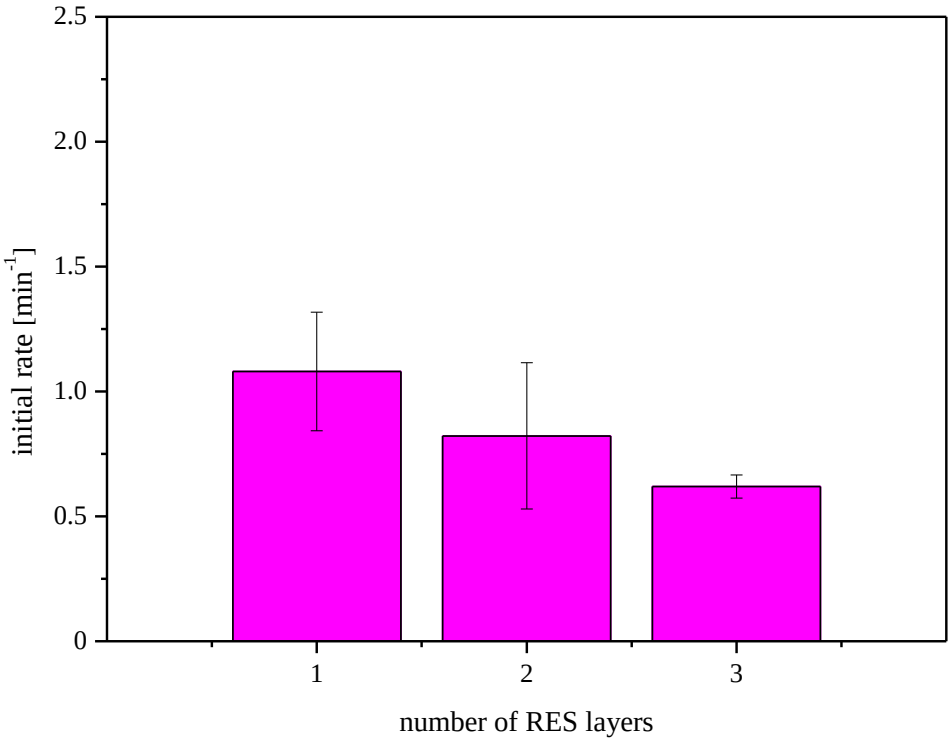

Figure 56 *Average initial rates for 1-3 RES layers.*

6.3.4 Discussion of printed layers experiments E5-A

When observing the dependance of absorbance on time, it can be seen that Resazurin was the indicator ink that degrades the most. This is true especially in the case of 3 layers, where the degradation reaches almost 50%. The results of Methylene Blue seemed also adequate, as even though the degradation was not that high, it reached ca. 75% for 2 and 3 layers as well. The results for Direct Blue 10 were difficult to assess. However, it can be seen that the results of Direct Blue 10 were the worst of all 3 tested dyes.

I evaluated only the results from the experiments with Methylene Blue and Resazurin. The results from Direct Blue 10 experiments differed a lot from each other. Consequently, the calculation of the average initial degradation rate (up to 90% of initial absorbance value), similarly to the remaining two substances, would give a final value that would not make any sense.

Since the kinetics models for the photocatalytic dye degradation in polymer layer are quite complex, I decided to evaluate the initial rate – until the absorbance reached 90% of the initial absorbance value. In this case, Methylene Blue showed better results – especially in the case of 3 layers, where the initial rate degradation was more than tripled compared to Resazurin.

The results shows that at the beginning of the experiment, the Methylene Blue degradation is quite fast, however, after approximately 1.5 min in all 3 cases of different layer numbers, it decreases. All in all, in this first 1.5 min, it reaches approximately 85% of the initial absorbance value, suggesting that it reaches half of the total dye decomposition in this stage.

On the other hand, Resazurin is characterized by slower degradation rate at the beginning, but the rate does not decrease so rapidly after it reaches 90% of initial absorbance value as it was in the case of Methylene Blue.

Both printed inks' solutions seemed stable enough under UVA light when TiO_2 was not present.

6.4 Printed layers experiments E5-A – optimization and stability testing

Two indicator inks – Resazurin and Methylene Blue were selected for further experiments. The printing conditions were optimized to achieve better surface structure. The drop spacing was set for 20 μm, the printing angle was changed to 21°, so that there were more drops per surface area printed than under previous conditions. The surface temperature was set for 40 °C. Only one layer of indicator ink was printed, because it achieved the best structure qualities during previous experiments.

Another aim of this part was to find out, whether the dye undergoes the same degradation rate when it is freshly printed, as well as in the case of testing carried out some days later. The samples were tested for 4 days – 1st, 2nd and 4th days' results were recorded.

6.4.1 Methylene Blue

6.4.1.1 Characterization of printed layers

The E5-A glass substrate consisted of 0-3 layers of an indicator ink on titania photocatalytic layer. Firstly, the thickness of the titania layer was measured and then the thickness of different amounts of colorful layers was detected. In each thickness measuring, the experiment was measured 3 times and than the average value and standard deviation was determined.

Table 7 *Stylus Profilometry measurement of thickness for Methylene Blue.*

	0 layer of Dye	1 layer of Dye	2 layers of Dye	3 layers of Dye
Thickness [μm]	0.316	0.356	0.626	0.693
SD	0.007	0.027	0.054	0.065

The more dye layers were added on the titania surface, the bigger the thickness was. However, it can be seen that the layer thickness is not additive. The difference between the thickness of 0 and 1 layer was small. In the case of 2 layers of dye, the thickness value was almost doubled compared to 1 layer. In the case of deposition of 2 and 3 layers, the results can be explained by different interaction between the wet layer and the dry one from previous printing compared to the interaction between titania and 1st layer of dye.

6.4.1.2 Methylene Blue Stability test

Similarly to the printed experiments evaluation, 5 experiments were performed. According to the stability test, the results from 1st day of testing were the best. The fresher the printed indicator ink layer, the faster the degradation.

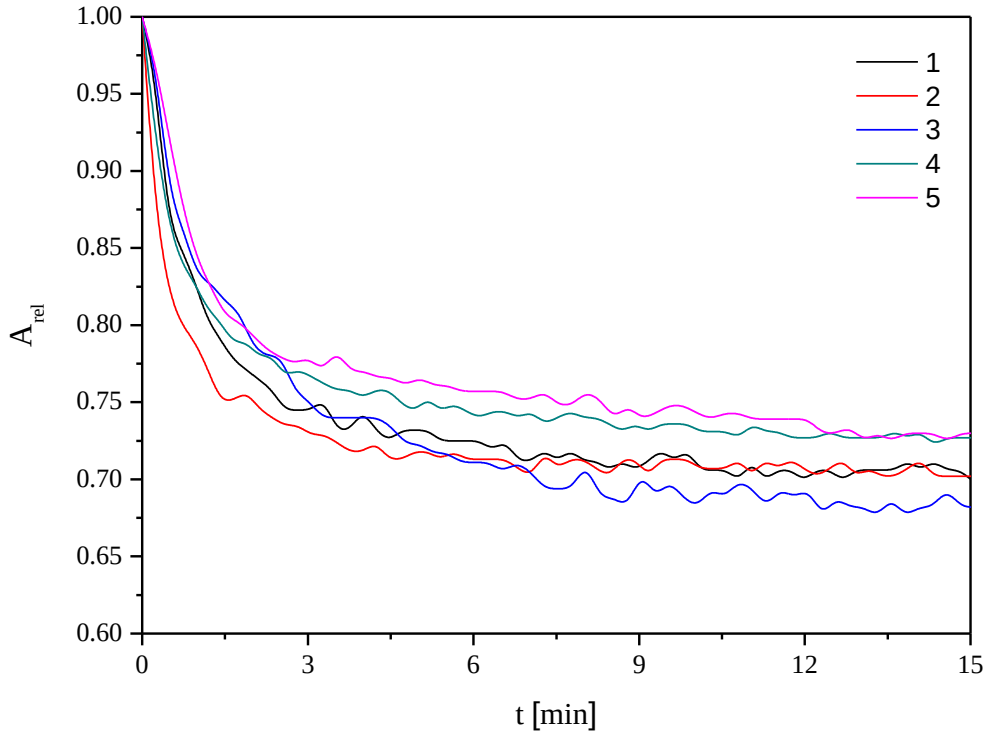

Figure 57 *MB – Stability test, 1st day.*

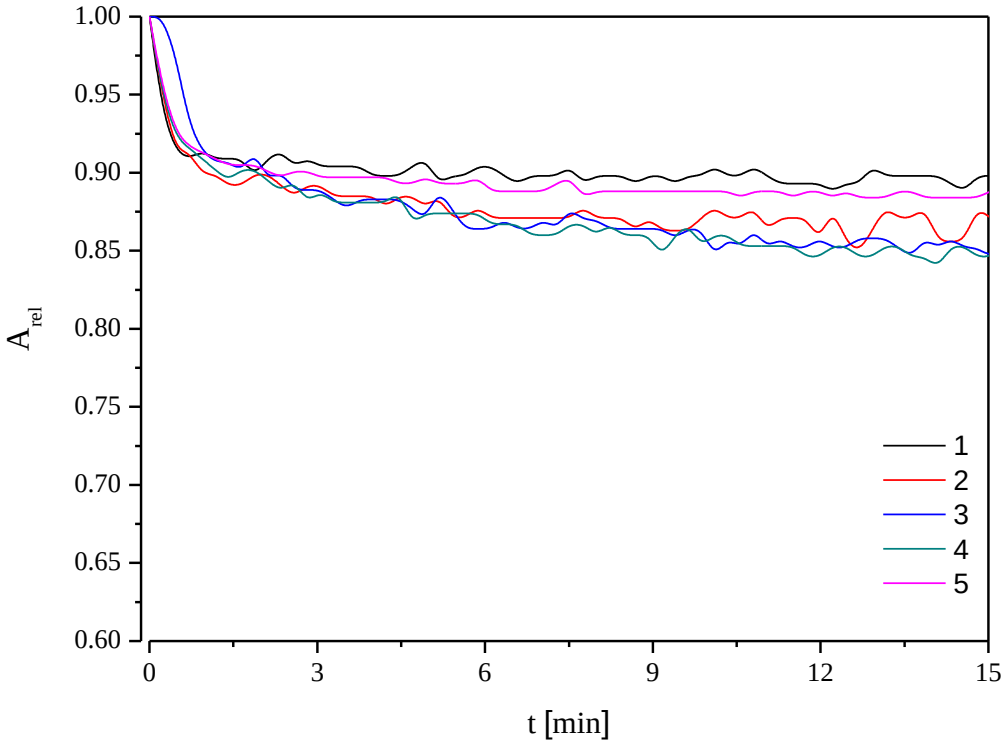

Figure 58 *MB – Stability test, 2nd day.*

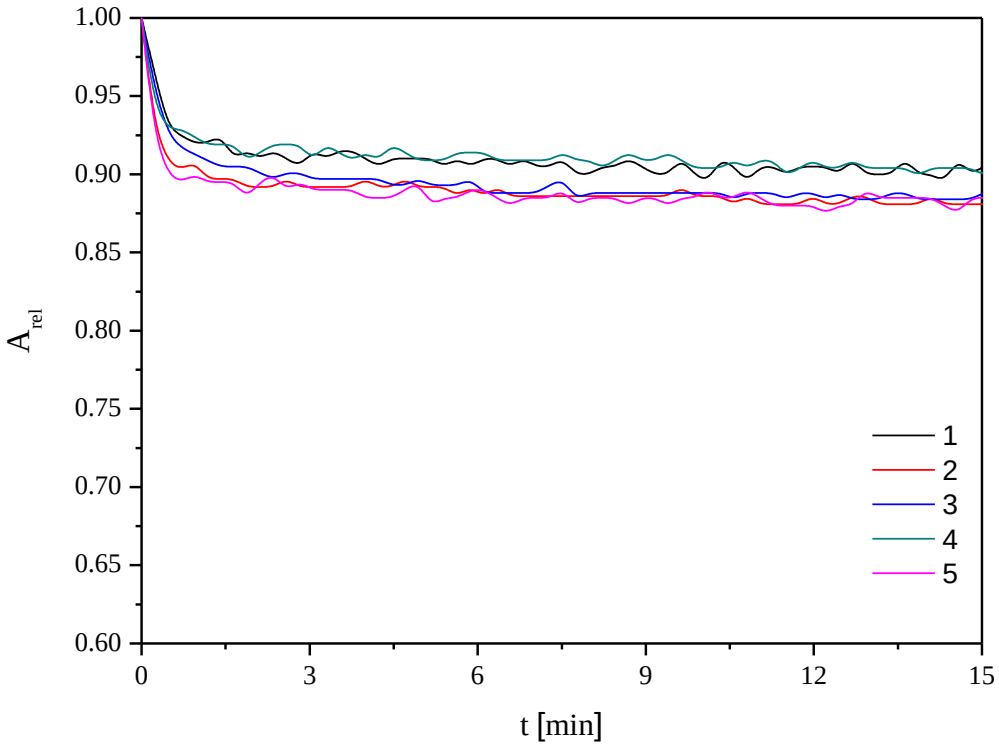

Figure 59 *MB – Stability test, 4th day.*

6.4.2 Resazurin

6.4.2.1 Characterization of printed layers

The procedure for the Stylus Profilometry in the case of Resazurin was the same as in the case of Methylene Blue. The titania glass sample was the same, so the values for thickness of titania are equal to values seen in Methylene Blue case.

The thickness values for different amount of layers of Resazurin had similar tendency as in the previous case. Again, the values of 2 and 3 printed layers of the dye differed significantly from the value of 1 printed layer.

Table 8 *Stylus Profilometry measurement of thickness for Resazurin.*

	0 layer of Dye	1 layer of Dye	2 layers of Dye	3 layers of Dye
Thickness [µm]	0.316	0.338	0.610	0.618
SD	0.007	0.022	0.063	0.052

6.4.2.2 Resazurin stability test

This stability test showed that the freshly printed indicator ink can achieve up to 50% degradation under UVA light illumination. When the sample got older, the degradation ability decreased.

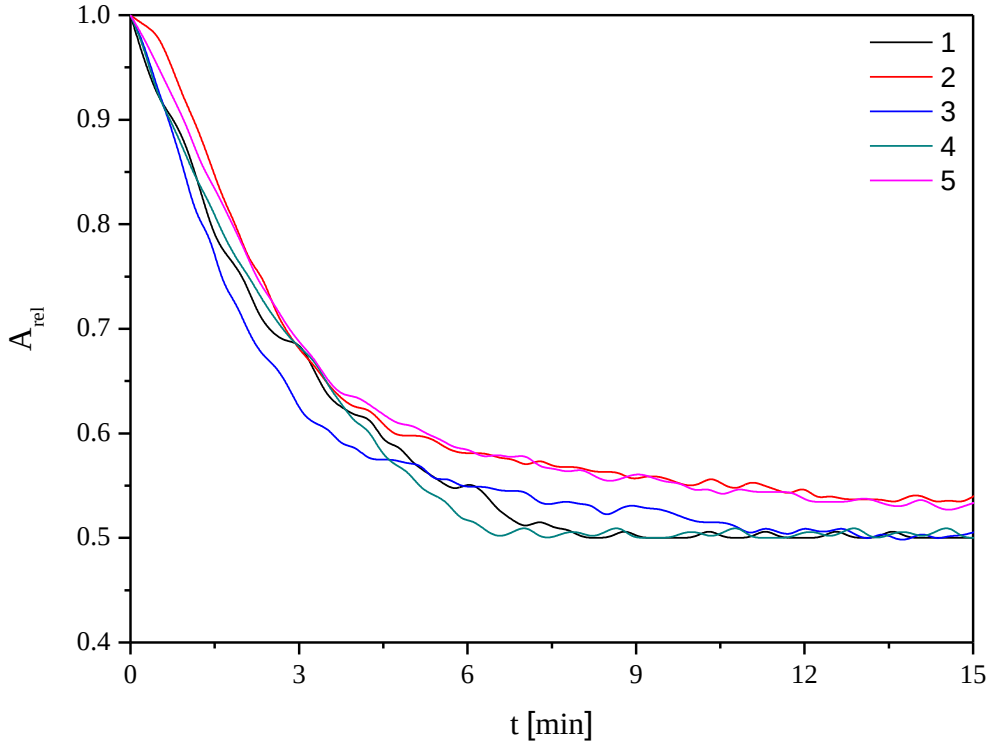

Figure 60 *RES – Stability test, 1st day.*

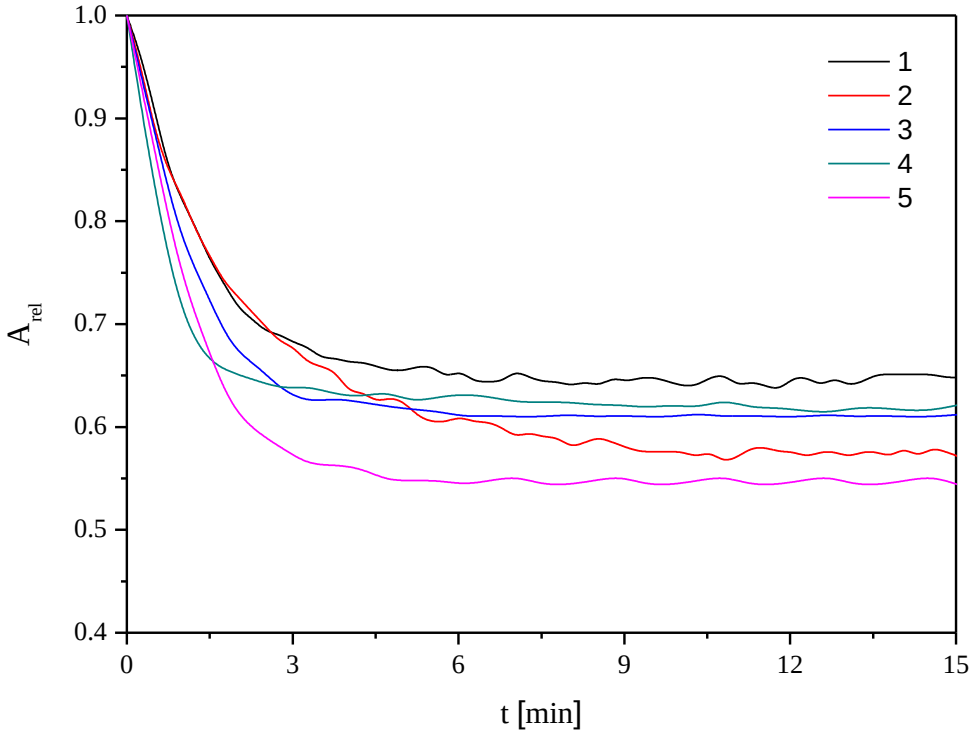

Figure 61 *RES – Stability test, 2nd day.*

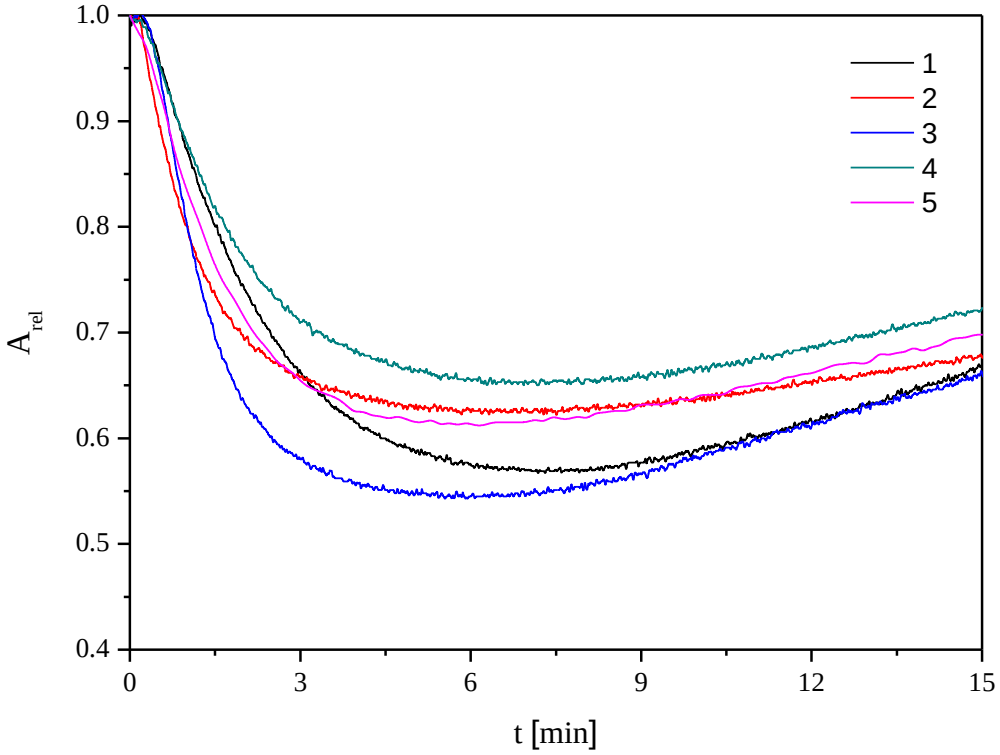

Figure 62 *RES – Stability test, 4th day.*

6.5 Printed experiments – E5-B

Unfortunately, the E5-A photocatalytic substrate's structure was damaged, when the kinetics of optimized printed layers was supposed to be tested, and consequently, it was not possible to prepare more E5-A samples from the sol.

Due to the damaged samples, I had to select another sample to carry out the optimized experiment. E5-B had the same composition and was available. It contained glass plates with 1-4 titania layers.

The glass substrate was 2.5 × 7.5 cm and the layers were deposited in the same way as shown in the Figure 63: 1 layer of indicator ink was printed on the glass substrate in the left corner and the right corner was left as a reference (no indicator ink). The glass substrate consisted of 1-4 titania layers.

In the previous experiments I observed different photocatalytic activity for the two dyes tested. My assumption was that Methylene Blue with its lower overall degradation rate is more suitable for testing of more active photocatalytic surfaces, while Resazurin could be preferred in the case of less active photocatalytic surfaces. In conclusion, I tested the dyes on different number of titania layers to find out whether the degradation rate can be influenced when using different number of photocatalytic films.

Taking into account my previous results, I decided to maintain the 1 layer structure of indicator ink. In this case, the number of titania layers was the variable, while the number of indicator ink's layer was constant (=1).

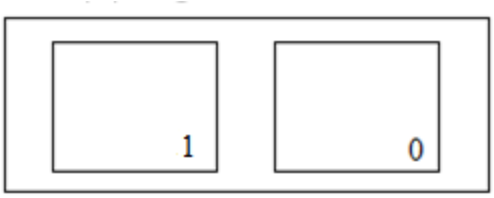

Figure 63 *E5-B substrate with 1 or 0 layer (reference) of deposited indicator ink.*

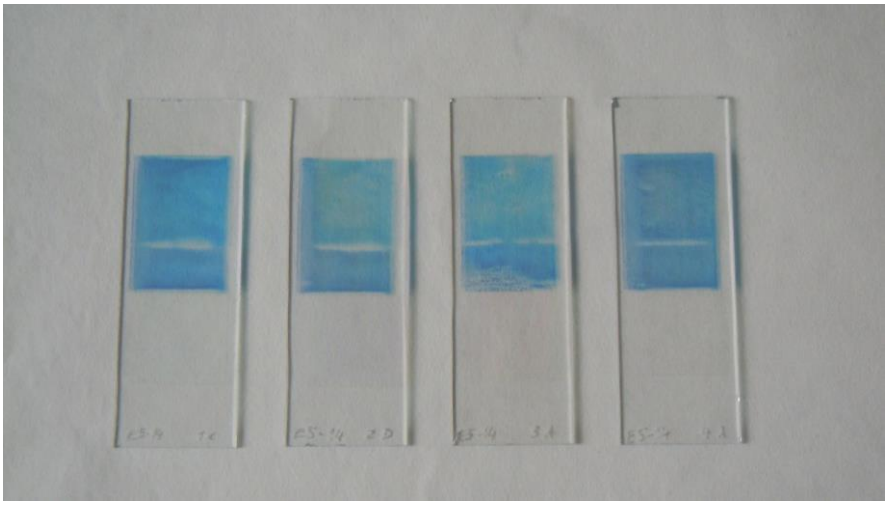

Figure 64 *E5-B samples with 1-4 TiO_2 layers and 1 layer of Methylene Blue.*

6.5.1 Methylene Blue

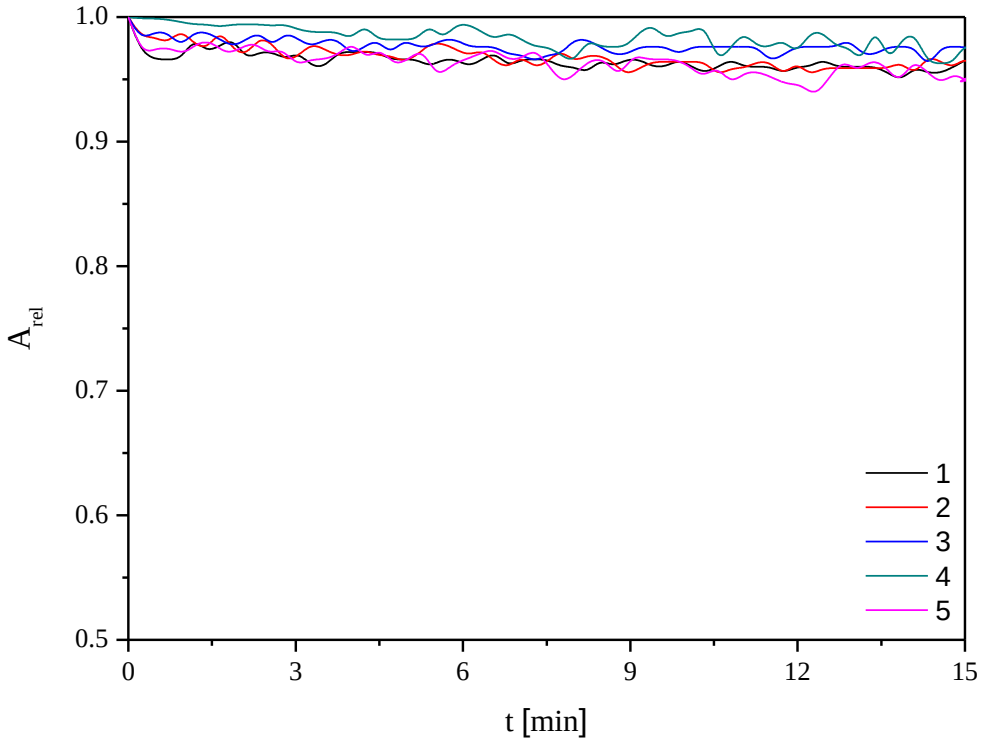

Figure 65 *1 layer of Methylene Blue, 1 layer of titania: relative absorbance as a function of time in 580-600 nm.*

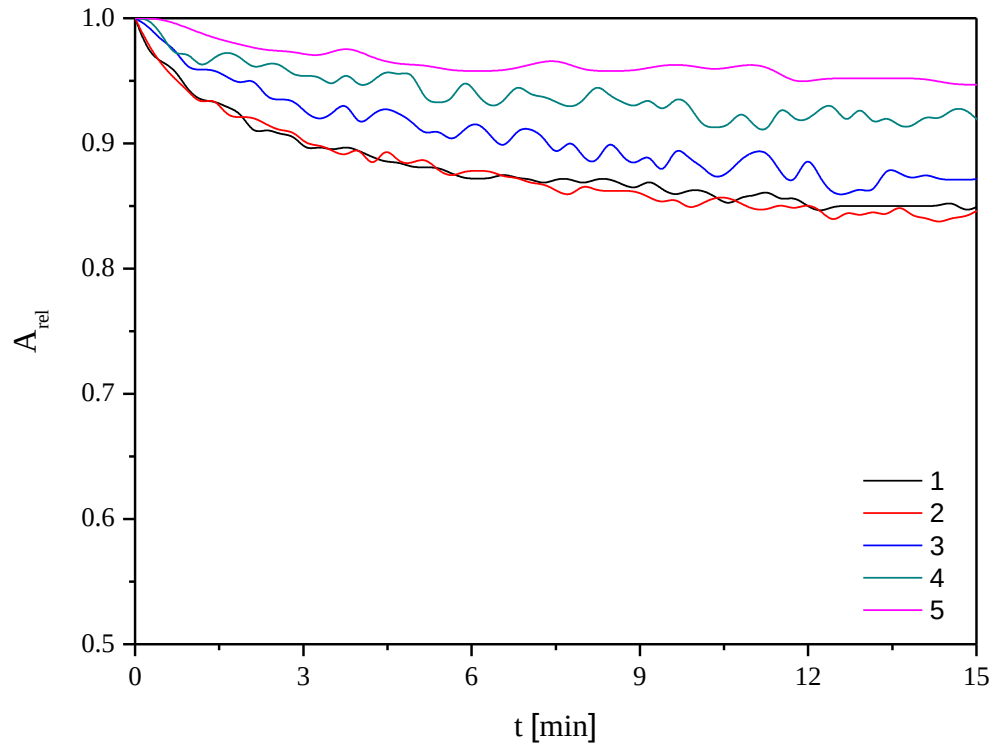

Figure 66 *1 layer of Methylene Blue, 2 layers of titania: relative absorbance as a function of time in 580-600 nm.*

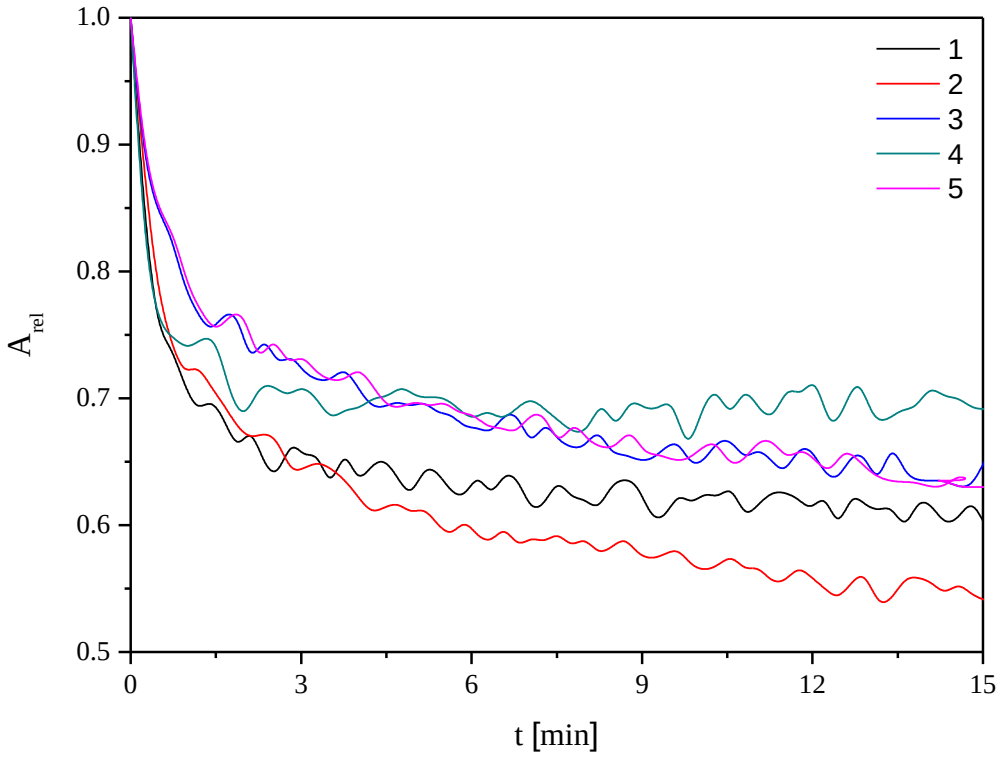

Figure 67 *1 layer of Methylene Blue, 3 layers of titania: relative absorbance as a function of time in 580-600 nm.*

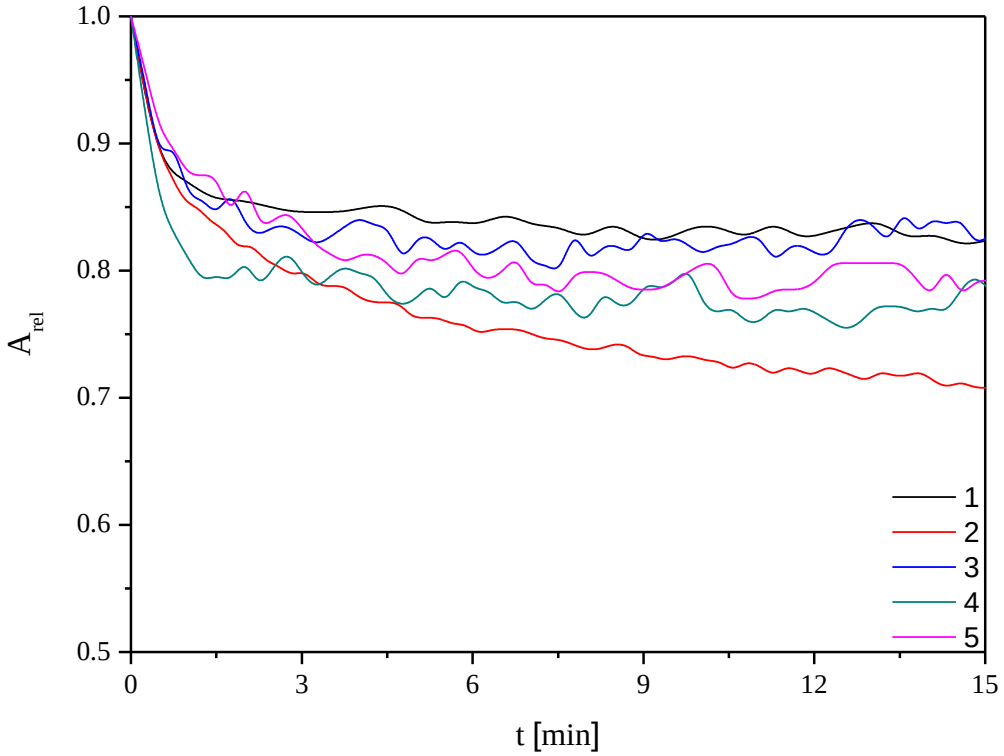

Figure 68 *1 layer of Methylene Blue, 4 layers of titania: relative absorbance as a function of time in 580-600 nm.*

The results for MB with the usage of 1 or 2 layers of photocatalyst, did not show any significant initial rate values. In each case, the 5 experiments differed significantly from each other. Under these circumstances, I decided to evaluate only MB initial degradation rate for 3 and 4 titania layers.

It can be seen that the highest absorbance drop was detected in the case of 3 layers of TiO_2. Lower value of initial rate, when 4 layers of TiO_2 are used, is probably caused by the damaged structure.

Table 9 *Average initial rate of 1 layer of MB for 3 and 4 titania layers.*

	3 layers	4 layers
Rate [min^{-1}]	3.580 ± 0.211	1.576 ± 0.355

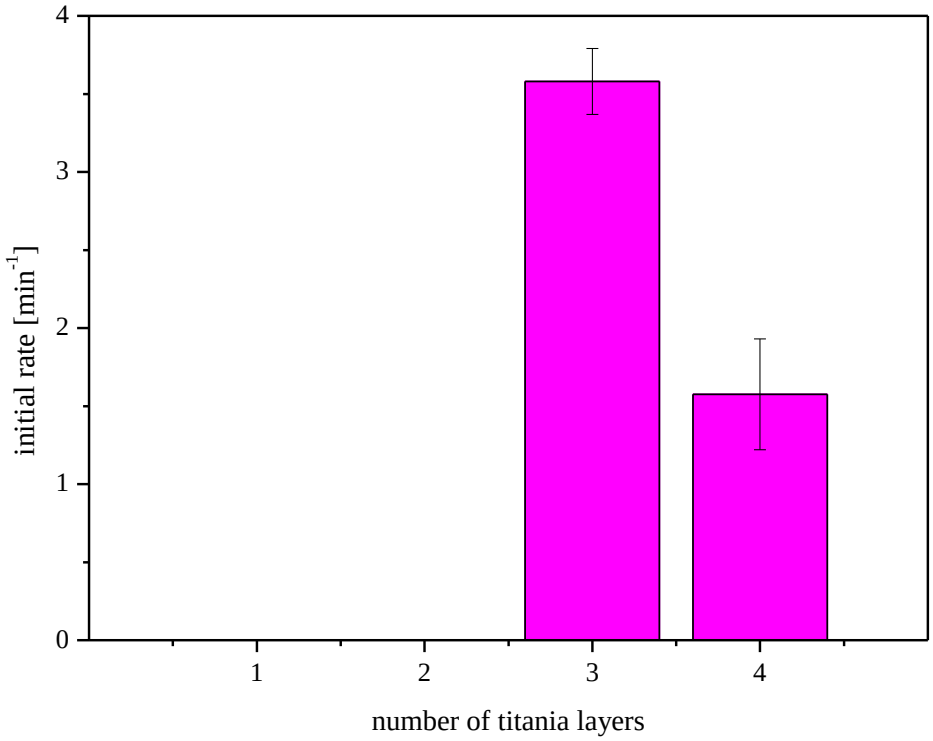

Figure 69 *Average initial rates for MB on different number of titania layers.*

6.5.1.1 The layer thickness evaluated by Stylus Profilometry

Average thickness was again determined from 3 measurements. With increasing titania's number of layers, the thickness increased as well, except for 4 layers of TiO_2. The relatively low titania thickness in the case of 4 layers is probably the result of damaged structure.

Average thickness of 1 layer of titania and 1 layer of indicator ink was relatively high compared to other measurements. This fact suggests that the thickness of the deposited layer depends on the substrate – the results are different when the indicator ink is deposited on 1 layer of photocatalyst from deposition on more layers of photocatalyst.

Table 10 *Results from Stylus Profilometry thickness measurement measurement (L represents "layer", T "titania" and I "indicator ink").*

	1 LT	1 LT + 1LD	2 LT	2 LT + 1LD	3LT	3 LT + 1LD	4LT	4 LT + 1LD
Thickness [μm]	0.100	0.617	0.372	0.641	0.457	0.561	0.331	0.564
SD	0.015	0.023	0.026	0.051	0.042	0.052	0.042	0.044

6.5.2 Resazurin

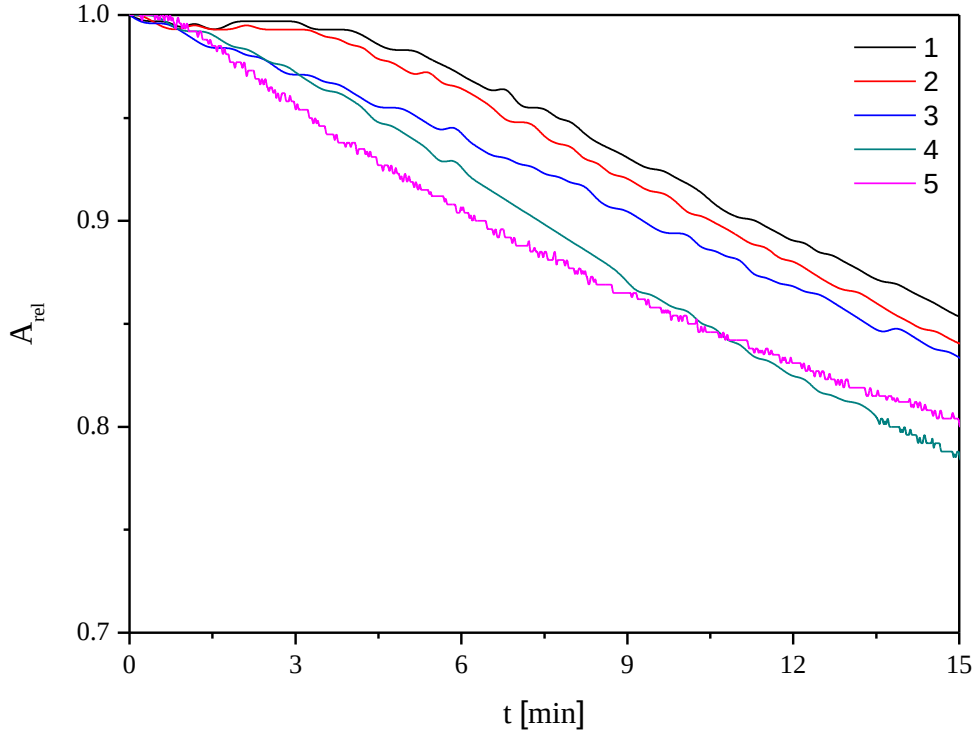

Figure 70 *1 layer of Resazurin, 1 layer of Titania: relative absorbance as a function of time in 565-585 nm.*

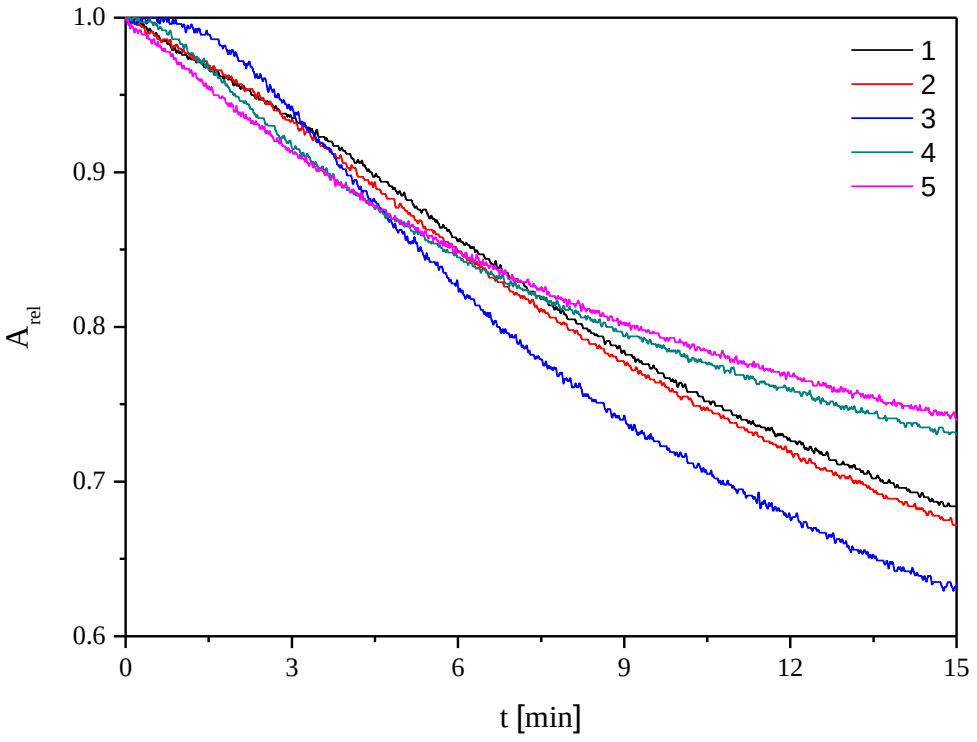

Figure 71 *1 layer of Resazurin, 2 layers of Titania: relative absorbance as a function of time in 565-585 nm.*

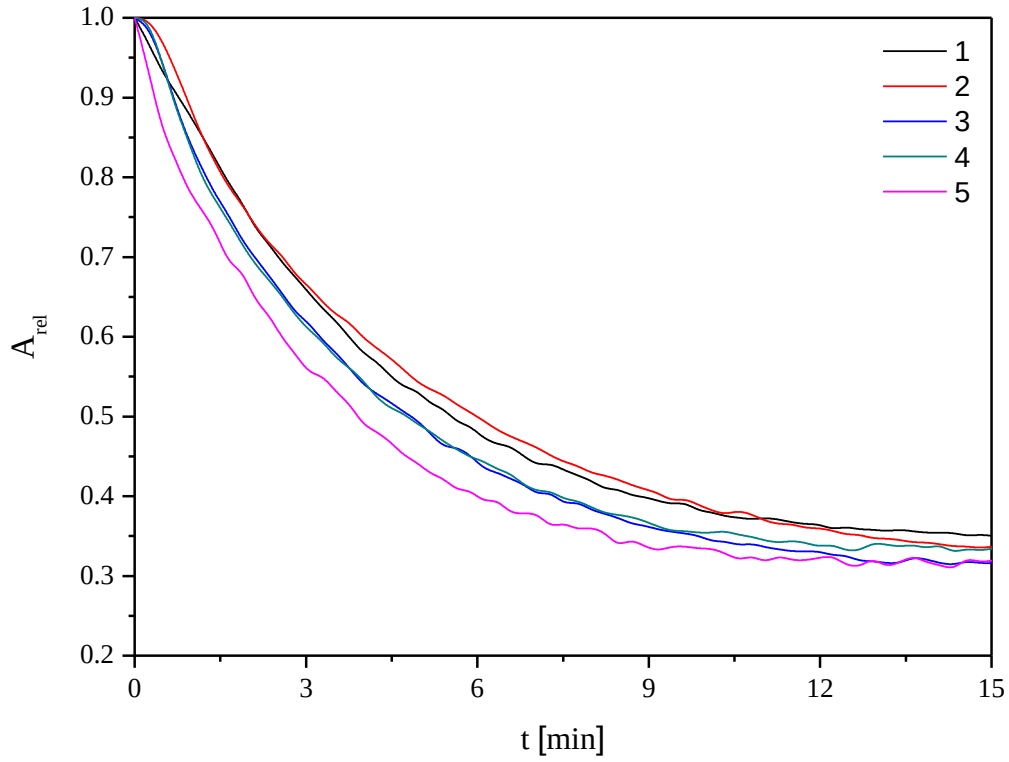

Figure 72 *1 layer of Resazurin, 3 layers of Titania: relative absorbance as a function of time in 565-585 nm.*

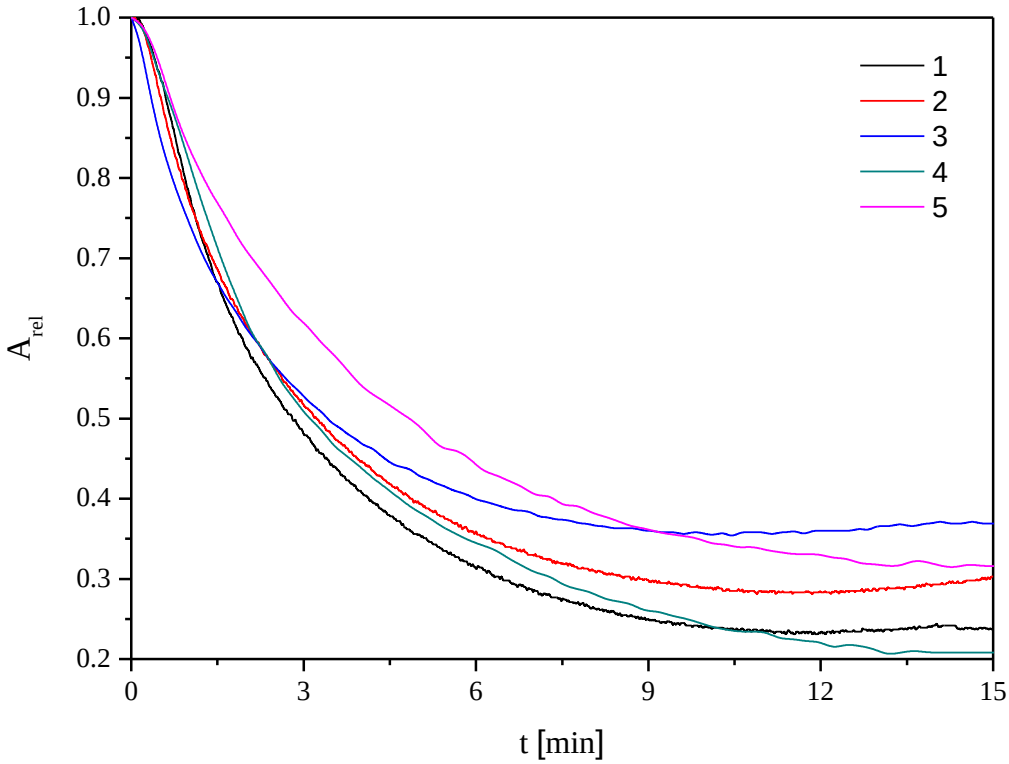

Figure 73 *1 layer of Resazurin, 4 layers of Titania: relative absorbance as a function of time in 565-585 nm.*

The results for all the initial rates of 4 different numbers of titania layers can be seen in the table below. Once again, the average initial reaction rate was calculated according to 5 values of initial rates. The column graph is given bellow as well.

Table 11 *Average initial rates for RES in the case of 1-4 titania layers.*

	1 layer	2 layers	3 layers	4 layers
Rate [min^{-1}]	0.107 ± 0.028	0.231 ± 0.025	1.321 ± 0.320	1.578 ± 0.353

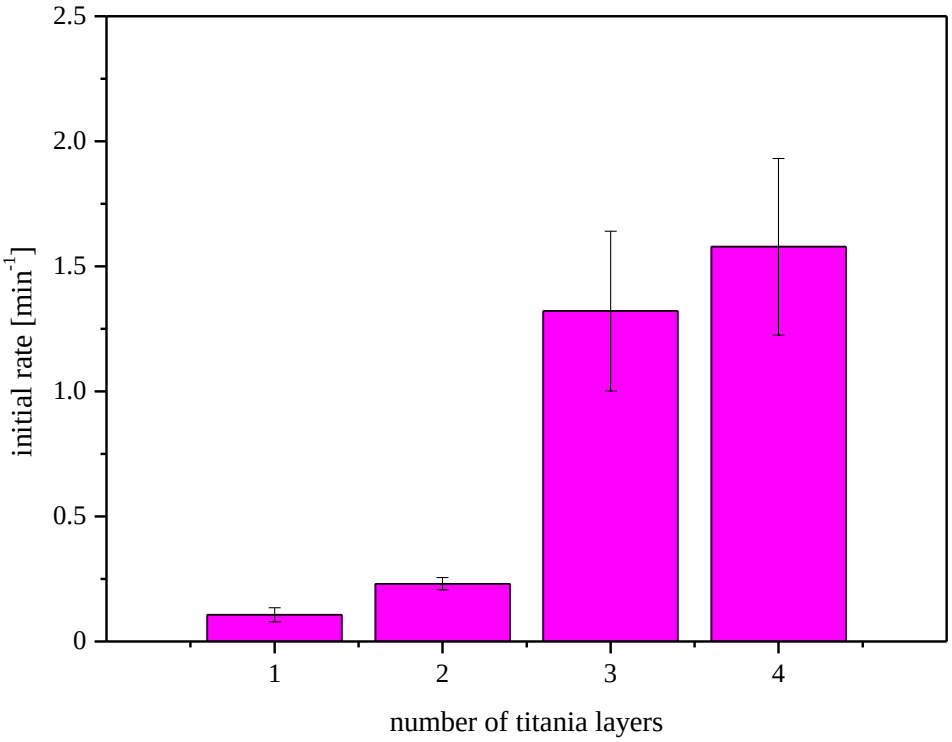

Figure 74 *Average initial rates for RES on different number of titania layers.*

6.5.2.1 The layer thickness evaluated by Stylus Profilometry

I measured 1 sample three times and calculated the average value. In the table below, the average thickness and its standard deviation can be seen.

Table 12 *Results from Stylus Profilometry thickness measurement (L represents "layer", T "titania" and I "indicator ink").*

	1 LT	1 LT + 1LI	2 LT	2 LT + 1LI	3LT	3 LT + 1LI	4LT	4 LT + 1LI
Thickness [μm]	0.100	0.551	0.372	0.557	0.457	0.564	0.331	0.654
SD	0.015	0.091	0.026	0.100	0.042	0.043	0.042	0.030

The results given by Stylus Profilometry suggested the same tendency as in the previous case of Methylene Blue. Similarly, the value for 1 layer of titania and 1 layer of indicator ink was relatively high.

6.5.1 Discussion of printed layers experiments E5-B

In all of the experiments, 1 layer of indicator ink (Resazurin or Methylene Blue) was tested. The variable was number of TiO_2 layers.

The MB results for 1 and 2 photocatalytic layer were not suitable for initial rate evaluation. Therefore, I cannot compare the dye degradation of Resazurin and Methylene Blue.

Resazurin results revealed the dependency of number of titania layers on the initial degradation rate – the more TiO_2 layers, the faster the initial rate.

Likewise, for E5-A printed layers results, the average initial rate was bigger in the case of Methylene Blue (for 3 layers), even though the observed absorbance drop in time suggested the opposite results. The 4 titania layers showed almost the same results for the average initial rate, for both MB and RES.

6.5.2 Apparatus Optimization

The last part of my experimental thesis was to find out whether the indicator ink degradation can be evaluated by different methods other than spectrophotometry. I used the same apparatus as in the previous testing with a little adjustment. Instead of spectrophotometric detection, I used a photodiode-based light-to-frequency convertor connected to a multimeter. I was able to measure the response from the light passing through the sample in kHz unit. A red filter was placed on the photodiode to eliminate certain wavelength range.

The measurement was done on glass sample with 3 layers of titania E5-14 and 1 layer of Resazurin. This sample was chosen in agreement with the previous results – it reached sufficient initial degradation rate and in 15 min the absorbance decreased to approximately 35% of the initial value. Again, 5 measurements were carried out.

I detected the response to light passing through the sample. In the graph below, the *y* axis represents the ratio between the response to the light passing through the sample with 3 layers of titania and 1 layer of dye (I) and the response to the light passing without any barrier (I_0).

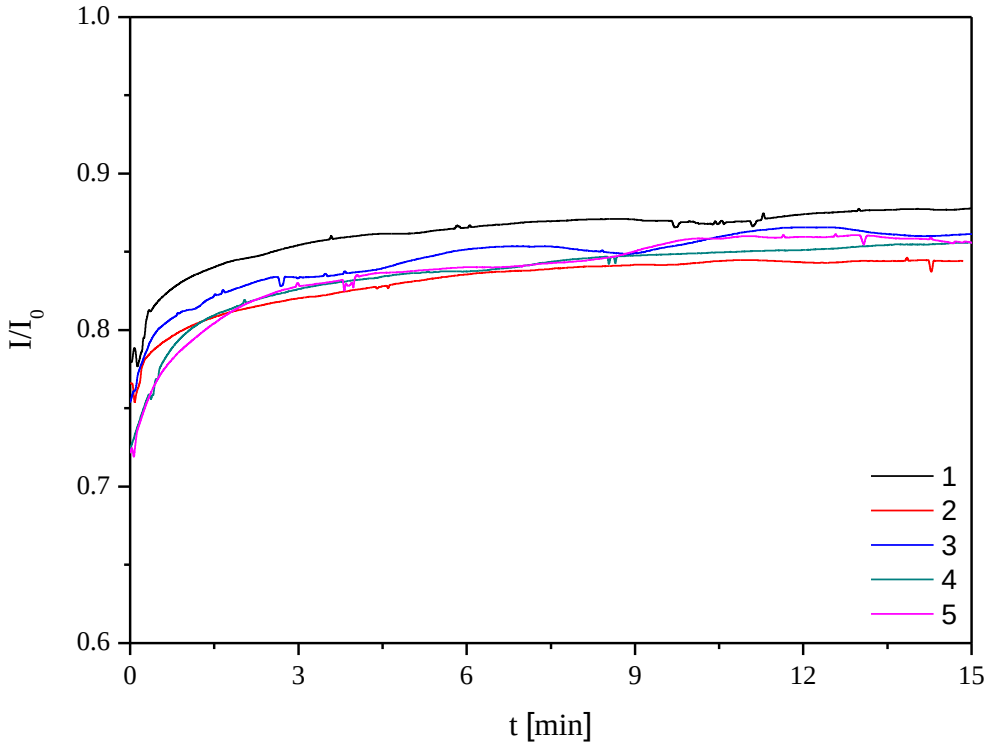

Figure 75 *Multimeter measuring – dependancy of the light response on time*

In the previous case – when using the spectrophotometer system for detection – the dependance of absorbance on time was evaluated, whereas the absorbance was given by a SpectraSuite programme as the average value from 20 nm region (this was because absorbance is defined for a given wavelength value).When using the photodiode system, the obtained data were specific for wider wavelength range (light was passing through the red filter providing the "red light" which was absorbed by blue Resazurin). This represents the main difference in the recorded data.

For a better comparison of the new optimized measuring method with the classical spectrometric one, the graph showing the dependency of $-log(I/I_0)$ on time t was plotted. However, it is important to mention that in this case, the y axis does not express absorbance.

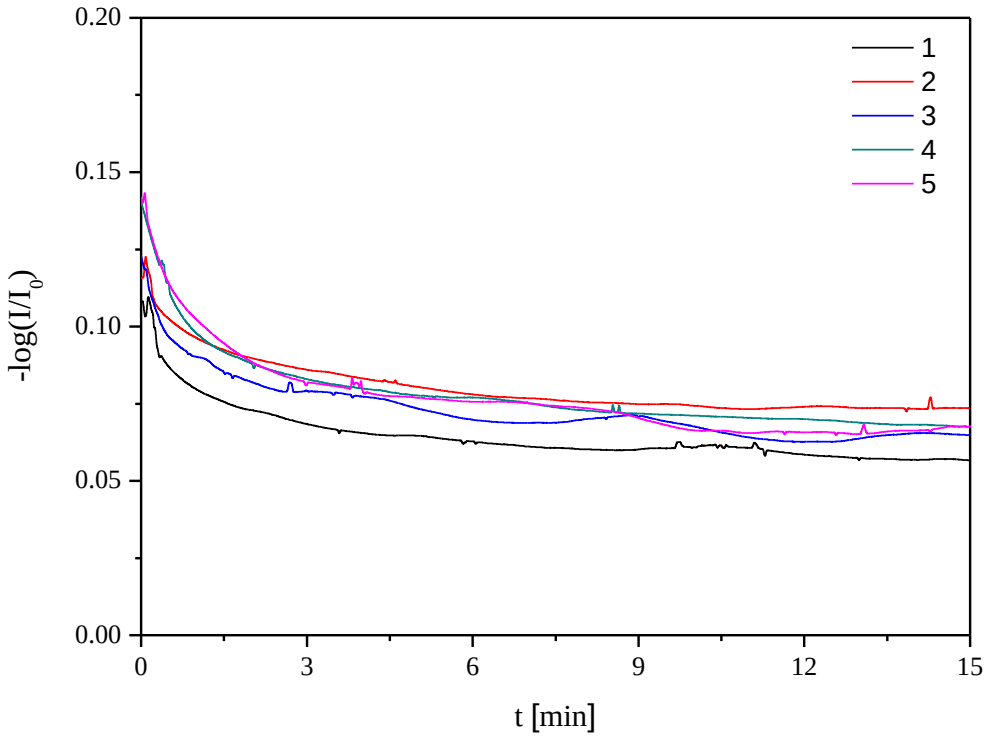

Figure 76 *–log(I/I$_0$)as a function of time.*

7 CONCLUSION

At the beginning of my experimental section, I focused on the suitable indicator ink selection. I started with so called "drop experiments" to find out which dye underwent the degradation under UV illumination fast enough to be employed as an indicator ink. From the dyes tested in the "drop experiments", I chose the most appropriate for further testing – for printed experiments. From those, the most suitable were chosen for the optimization part, where I focused on improving the quality of the printed layers by changing the printing conditions. I also performed the stability tests for two selected indicator inks – Resazurin and Methylene Blue. Furthermore, I applied the optimized procedure to print indicator ink on a different titania sample set – E5-B. Finally, I probed whether I can evaluate the photocatalytic activity by other methods than spectrophotometry.

From the drop experiments, three dyes were selected dyes: Direct Blue 10, Methylene Blue and Resazurin. These were then used for experiments with printed indicator inks. In the case of Direct Blue 10, the printed experiments results for 1-3 layers of the dye were not adequate, as all the values which were supposed to be used for average initial rate assessment differed from each other quite a lot. Therefore, Methylene Blue and Resazurin were chosen for further kinetic evaluation and optimization.

When evaluating the photocatalytic activity of E5-A sample set, I came to following conclusions:

- Although the final absorbance values for Methylene Blue exhibited significant deviations, the initial rate values were quite similar and only a little deviation was observed.
- Resazurin experiment revealed that 1 layer of printed indicator ink had the fastest average initial degradation rate. However, when observing the overall reaction time (15 minutes), the biggest absorbance drop can be seen for 3 layers of Resazurin.
- When comparing Methylene Blue to Resazurin, it can be seen that the initial rate values differ more in the case of Resazurin, and the average initial degradation rate is higher for Methylene Blue in all of the experiments conducted with 1-3 layers of the tested ink. On the other hand, Resazurin has bigger absorbance drop in time at the end of the experiment (15 min). Such behaviour can be explained by the existence of the reduced MB's form leuco Methylene Blue which is sensitive to oxygen and provokes the reversible reaction back to Methylene Blue. Consequently, the lower absorbance values for MB cannot be reached. [44]

As a consequence of damaged E5-A samples, I had to choose another sample set with the same composition but with different number of titania layers. This represented a great chance to evaluate of samples with different photocatalytic activities. In the case of PCA assessment for E5-B sample set, influence of different number of titania layers was tested, while the indicator ink layer was kept 1. The following conclusions can be drawn:

- Methylene Blue experiments for 1 and 2 layers of titania had the initial rate significantly slow. Moreover, the values from 5 experiments carried out for each number of layers, differed a lot from each other. As a consequence, I did not evaluate their kinetics. On the other hand, 3 layers of titania seemed appropriate for initial rate degradation testing. The average initial rate for 3 TiO_2 layers was

higher than for 4. This was probably the reason for damaged structure in the case of 4 TiO_2 layers.

- As far as Resazurin is concerned, with the increasing number of titania layers, the average initial rate increased as well. I would like to point out that the difference between 3 and 4 layers of titania was not that significant as in the case of 2 and 3 layers. The damaged structure was observed again in the case of 4 TiO_2 layers.
- When comparing the 2 dyes, I came to the same conclusions as in previous sample series E5-A – again, the evaluated average initial rates were generally higher for Methylene Blue. If I take into account the final absorbance value after the first 15 min of experiments, Resazurin exhibits generally lower absorbance values. Moreover, in the experiments for 1 and 2 layers of titania, MB testing did not reveal any significant change. In this case, more photocatalytic layers are necessary for noticeable degradation to take place.

The last part of my experimental thesis was to conduct the apparatus optimization experiment. I replaced the spectrophotometer system with other detection parts – photodiode and multimeter. I proved that the response corresponded to the photocatalytic degradation – the degradation of dye grew in time which was detected by the response to increasing amount of light passing through the sample. I am sure that this experimental set-up provides a great possibility of cheaper PCA testing (when compared with the spectrophotometer and photodiode cost). However, further experiments with other dyes and film forming agents need to be carried out in order to validate the method.

8 REFERENCES

[1] Photoactive Energy and Materials. *Northwestern University* [online]. 2012 [cit. 2015-04-03]. Available from: http://www.civil.northwestern.edu/EHE/HTML_KAG/Kimweb/Research.html

[2] HAGEN, Jens. *Industrial catalysis: a practical approach*. 2nd, completely rev. and extended ed. Weinheim: Wiley-VCH, c2006, xviii, 507 p. ISBN 9783527311446.

[3] CHORKENDORFF, I a J NIEMANTSVERDRIET. *Concepts of modern catalysis and kinetics.* 2nd ed. Weinheim: Wiley-VCH, c2007, xvii, 457 p. ISBN 9783527316724-.

[4] HERRMANN, Jean-Marie. Titania-based true heterogeneous photocatalysis. *Environmental Science and Pollution Research*[online]. 2012, vol. 19, issue 9, p. 3655-3665 [cit. 2015-03-12]. DOI: 10.1007/s11356-011-0697-8. Available from:http://link.springer.com/10.1007/s11356-011-0697-8

[5] SHIBATA, H, H SAKAI, P RANGSUNVIGIT, T HIRANO a M ABE. Preparation and photocatalytic activity of titania particulate film with silica as binder. *Surface Coatings International Part B: Coatings Transactions* [online]. 2003, vol. 86, issue 2, p. 125-130 [cit. 2015-02-19]. DOI: 10.1007/BF02699623. Available from: http://link.springer.com/10.1007/BF02699623

[6] ŠTANGAR, U Lavrenčič, M KETE, a ŠULIGOJ a M TASBIHI. Solution-derived photocatalytic films for environmental cleaning applications. *IOP Conference Series: Materials Science and Engineering* [online]. 2012-02-15, vol. 30, p. 012001- [cit. 2015-03-20]. DOI: 10.1088/1757-899X/30/1/012001. Available from: http://stacks.iop.org/1757-899X/30/i=1/a=012001?key=crossref.f97271ca7e3b9946576ec68053adc5c2

[7] FUJISHIMA, A, X ZHANG a D TRYK. TiO2 photocatalysis and related surface phenomena. *Surface Science Reports* [online]. 2008-12-15, vol. 63, issue 12, p. 515-582 [cit. 2014-11-23]. DOI: 10.1016/j.surfrep.2008.10.001. Available from:http://linkinghub.elsevier.com/retrieve/pii/S0167572908000757

[8] MEILERT, K.T., D. LAUB a J. KIWI. Photocatalytic self-cleaning of modified cotton textiles by TiO2 clusters attached by chemical spacers. *Journal of Molecular Catalysis A: Chemical* [online]. 2005, vol. 237, 1-2, p. 101-108 [cit. 2014-11-23]. DOI: 10.1016/j.molcata.2005.03.040. Available from:http://linkinghub.elsevier.com/retrieve/pii/S1381116905002001

[9] BENNANI, Julien, Ralf DILLERT, Thorsten M. GESING a Detlef BAHNEMANN. Physical properties, stability, and photocatalytic activity of transparent TiO2/SiO2 films. *Separation and Purification Technology* [online]. 2009, vol. 67, issue 2, p. 173-179 [cit. 2015-03-16]. DOI: 10.1016/j.seppur.2009.03.019. Available from: http://linkinghub.elsevier.com/retrieve/pii/S1383586609000902

[10] FUJISHIMA, Akira. *TiO2: Photocatalysis. Fundamentals and Applications*. Tokyo: Bkc, Inc., 1999, 176 p. ISBN 49-390-5103-X.

[11] GREENWOOD, N a Alan EARNSHAW. *Chemie prvků: Photocatalysis. Fundamentals and Applications*. 1st eddition. Praha: Informatorium, 1993, p.794-1635. ISBN 80-854-2738-9.

[12] OPPENLAENDER, Thomas. *Photochemical purification of water and air: Principles, Reaction, Mechanisms, ReactorConcepts*. Weinheim: Wiley-VCH, 2003, 368 s. ISBN 35-273-0563-7.

[13] Anatase: *AmethystGalleries': MineralGallery* [online]. 2012 [cit. 2013-02-06]. Available from: http://www.galleries.com/Anatase

[14] FUJISHIMA, AKIRA a KENICHI HONDA. Electrochemical Photolysis of Water at a Semiconductor Electrode. *Nature* [online]. 1972-7-7, vol. 238, issue 5358, p. 37-38 [cit. 2015-03-26]. DOI: 10.1038/238037a0. Available from: http://www.nature.com/doifinder/10.1038/238037a0

[15] Brookit. *Amethyst Galleries': MineralGallery* [online]. 2012 [cit. 2013-02-06]. Available from: http://www.galleries.com/Brookite

[16] Rutile. *Amethyst Galleries': Mineral Gallery* [online]. 2012 [cit. 2013-02-06]. Available from: http://www.galleries.com/Rutile

[17] TiO_2 Structures. *University of Colorado: Mineral Structure Data* [online]. 2011 [cit. 2013-02-06]. Available from: http://ruby.colorado.edu/~smyth/min/tio2.html

[18] OHNO, Teruhisa, Koji SARUKAWA, Kojiro TOKIEDA a Michio MATSUMURA. *Journal of Catalysis* [online]. 2001, vol. 203, issue 1, p. 82-86 [cit. 2015-02-15]. DOI: 10.1006/jcat.2001.3316. Available from: http://linkinghub.elsevier.com/retrieve/pii/S0021951701933160

[19] GAŽO, Ján. *Všeobecná a anorganická chémia*. 2nd eddition Bratislava: ALFA, 1978.

[20] Semiconductor Doping. *PowerGuru* [online]. 2012 [cit. 2013-04-20]. Available from: http://www.powerguru.org/semiconductor-doping/

[21] SHANG, Xili, Bin LI, Tianyong ZHANG, Changhai LI a Xiao WANG. Photocatalytic Degradation of Methyl Orange with Commercial Organic Pigment Sensitized TiO2. *Procedia Environmental Sciences* [online]. 2013, vol. 18, p. 478-485 [cit. 2015-02-15]. DOI: 10.1016/j.proenv.2013.04.064. Available from:http://linkinghub.elsevier.com/retrieve/pii/S1878029613001965

[22] PORTELA, Raquel, Benigno SÁNCHEZ, Juan M. CORONADO, Roberto CANDAL a Silvia SUÁREZ. Selection of TiO2-support: UV-transparent alternatives and long-term use limitations for H2S removal. *Catalysis Today* [online]. 2007, vol. 129, 1-2, p. 223-230 [cit. 2015-04-03]. DOI: 10.1016/j.cattod.2007.08.005. Available from: http://linkinghub.elsevier.com/retrieve/pii/S0920586107005007

[23] MOROZOVA, M., P. KLUSON, J. KRYSA, P. DZIK, M. VESELY a O. SOLCOVA. Thin TiO2 films prepared by inkjet printing of the reverse micelles sol–gel composition. *Sensors and Actuators B: Chemical* [online]. 2011, vol. 160, issue 1, p. 371-378 [cit. 2015-04-13]. DOI: 10.1016/j.snb.2011.07.063. Available from: http://linkinghub.elsevier.com/retrieve/pii/S0925400511007179

[24] SubsTech: Substances & Technologies. KOPELIOVICH, Dmitri. *Sol-Gel process* [online]. 2012 [cit. 2013-02-25]. Dostupnéz: http://www.substech.com/dokuwiki/doku.php?id=sol-gel_process

[25] ČÁSTKOVÁ, Klára. Konvenční syntézy keramických částic. [lecture]. Brno: VUT, 2013

[26] MILLS, Andrew, Claire HILL a Peter K.J. ROBERTSON. Overview of the current ISO tests for photocatalytic materials. *Journal of Photochemistry and Photobiology A: Chemistry* [online]. 2012, vol. 237, p. 7-23 [cit. 2015-04-13]. DOI: 10.1016/j.jphotochem.2012.02.024. Available from:http://linkinghub.elsevier.com/retrieve/pii/S1010603012001748

[27] ZITA, Jiří, Josef KRÝSA a Andrew MILLS. Correlation of oxidative and reductive dye bleaching on TiO2 photocatalyst films. *Journal of Photochemistry and Photobiology A: Chemistry* [online]. 2009, vol. 203, 2-3, p. 119-124 [cit. 2015-04-07]. DOI: 10.1016/j.jphotochem.2008.12.029. Available from: http://linkinghub.elsevier.com/retrieve/pii/S1010603009000021

[28] MILLS, Andrew. an overview of the methylene blue ISO test for assessing the activities of photocatalytic films. *Applied Catalysis B: Environmental* [online]. 2012, vol. 128, p. 144-149 [cit. 2015-04-07]. DOI: 10.1016/j.apcatb.2012.01.019. Available from: http://linkinghub.elsevier.com/retrieve/pii/S0926337312000203

[29] Information on contact angle. *Contact angle goniometers and tensiometers* [online]. 2014 [cit. 2014-12-19]. Available from:http://www.ramehart.com/contactangle.htm

[30] *Biolin Scientific* [online]. 2014 [cit. 2014-12-19]. Available from: http://www.biolinscientific.com/

[31] HIEMENZ, Paul C. *Principles of Colloid and Surface Chemistry*. 3rd rev. and exp.Ed. New York: Marcel Dekker, Inc., 1997, 650 s. ISBN 08-247-9397-8.

[32] LAVRENČIČ ŠTANGAR, Urška, Marko KETE, Urh ČERNIGOJ a Vilma DUCMAN. Testing of Photocatalytic Activity of Self-Cleaning Surfaces. *Advances in Science and Technology* [online]. 2010, vol. 68, p. 126-134 [cit. 2015-03-16]. DOI: 10.4028/www.scientific.net/AST.68.126. Available from: http://www.scientific.net/AST.68.126

[33] MILLS, Andrew a Michael MCFARLANE. Current and possible future methods of assessing the activities of photocatalyst films. *Catalysis Today* [online]. 2007, vol. 129, 1-2, p. 22-28 [cit. 2015-03-16]. DOI: 10.1016/j.cattod.2007.06.046. Available from: http://linkinghub.elsevier.com/retrieve/pii/S0920586107004026

[34] ČERNIGOJ, Urh, Marko KETE a Urška Lavrenčič ŠTANGAR. Development of a fluorescence-based method for evaluation of self-cleaning properties of photocatalytic layers. *Catalysis Today* [online]. 2010, vol. 151, 1-2, p. 46-52 [cit. 2015-03-16]. DOI: 10.1016/j.cattod.2010.03.043. Available from: http://linkinghub.elsevier.com/retrieve/pii/S0920586110002105

[35] AKPAN, U.G. a B.H. HAMEED. Parameters affecting the photocatalytic degradation of dyes using TiO2-based photocatalysts: a review. *Journal of Hazardous Materials* [online]. 2009-10-30, vol. 170, 2-3, p. 520-529 [cit. 2014-11-12]. DOI: 10.1016/j.jhazmat.2009.05.039. Available from: http://linkinghub.elsevier.com/retrieve/pii/S0304389409007699

[36] FERNANDO, Eustace, Taj KESHAVARZ a Godfrey KYAZZE. Enhanced bio-decolourisation of acid orange 7 by Shewanella oneidensis through co-metabolism in a microbial fuel cell. *International Biodeterioration* [online]. 2012, vol. 72, p. 1-9 [cit. 2015-04-07]. DOI: 10.1016/j.ibiod.2012.04.010. Available from: http://linkinghub.elsevier.com/retrieve/pii/S0964830512000960

[37] KLOUDA, Pavel. *Moderní analytické metody*. 2., upr. a dopl. vyd. Ostrava: Pavel Klouda, 2003, 132 s. ISBN 80-863-6907-2.

[38] USB-650 Red Tide Spectrometer. *OceanOptics* [online]. 2008 [cit. 2015-03-20]. Available from: http://oceanoptics.com/product/usb-650-red-tide-spectrometers/

[39] NanoScience Instruments. *Stylus Profilometry* [online]. 2015 [cit. 2015-03-20]. Available from: http://www.nanoscience.com/products/optical-profilometry/technology-overview/stylus-profilometry/

[40] BRUKER. *DektaXT Stylus Profiler User Manual* [online]. 2011 [cit. 2015-03-20].

[41] Industrial Inkjet Printing. *Xennia: Industrial inkjet solutions* [online]. 2013 [cit. 2013-03-23]. Available from: http://www.xennia.com/knowledgecentre/industrial-inkjet-printing.asp

[42] Inkjet. *Digital Print Preservation Portal: Research into the long-term care of digitally printed materials* [online]. 2012 [cit. 2013-03-23]. Available from: http://www.dp3project.org/technologies/digital-printing/inkjet

[43] FUJIFILM DimatixMaterials Printer DMP-2800 Series User Manual. *Manuallib* [online]. 2012 [cit. 2013-04-20]. Available from: http://www.manuallib.com/file/2593305

[44] MILLS, Andrew a Mark MCGRADY. A study of new photocatalyst indicator inks. *Journal of Photochemistry and Photobiology A: Chemistry* [online]. 2008, vol. 193, 2-3, s. 228-236 [cit. 2015-04-12]. DOI: 10.1016/j.jphotochem.2007.06.029. Available from: http://linkinghub.elsevier.com/retrieve/pii/S1010603007003449

9 LIST OF ABBREVIATIONS

A	acceptor
AO	atom orbital
AR1	Acid Red 1
BLB	Beer-Lambert-Bouguer
cb	conduction band
CS	continuous printing
D	donor
DB10	Direct Blue 10
DCIP	2,6-dichlorindofenol
DOD	drop-on-demand printing
ER	Eley-Rideal kinetics
FtCn	Ftalocyanin
GLY	glycerol
h	Planck constant
H_2O	water
HTPA	hydroxyterephtalic acid
I	indicator ink
IPA	isopropanol
ISO	Intenational Standards Organization
L	layer
LH	Langmuir-Hinschelwood kinetics
LMB	leuco form of Methylene Blue
MB	Methylene Blue
MO	molecular orbital
$NaHCO_3$	sodium bicarbonate
P	product
PCA	photocatalytic activity
PET	polyethylentereftalate
PVP	polyvinylpyrrolidon
PrEt	2-propoxyethanol
RB	Reactive Blue
RES	Resazurin
SD	standard deviation
SV11	Solvent Violet 11
T	titania
TiO_2	titania
TPA	terephtalic acid
TTIP	titanium tetraisopropoxide
UV	ultraviolet light
vb	valence band
VIS	visible light spectra